Bioactive Materials 27 (2023) 505–545

Contents lists available at ScienceDirect

Bioactive Materials

journal homepage: www.keaipublishing.com/en/journals/bioactive-materials

Review article

Multiphasic scaffolds for the repair of osteochondral defects: Outcomes of preclinical studies

Rouyan Chen [a,b], Jasmine Sarah Pye [c], Jiarong Li [a,c], Christopher B. Little [a,**], Jiao Jiao Li [a,c,*]

[a] Kolling Institute, Faculty of Medicine and Health, The University of Sydney, NSW, 2065, Australia
[b] School of Electrical and Mechanical Engineering, Faculty of Sciences, Engineering and Technology, The University of Adelaide, SA, 5005, Australia
[c] School of Biomedical Engineering, Faculty of Engineering and IT, University of Technology Sydney, NSW, 2007, Australia

ARTICLE INFO

Keywords:
Osteochondral defects
Tissue engineering
Multiphasic scaffolds
Biomaterials
Animal models

ABSTRACT

Osteochondral defects are caused by injury to both the articular cartilage and subchondral bone within skeletal joints. They can lead to irreversible joint damage and increase the risk of progression to osteoarthritis. Current treatments for osteochondral injuries are not curative and only target symptoms, highlighting the need for a tissue engineering solution. Scaffold-based approaches can be used to assist osteochondral tissue regeneration, where biomaterials tailored to the properties of cartilage and bone are used to restore the defect and minimise the risk of further joint degeneration. This review captures original research studies published since 2015, on multiphasic scaffolds used to treat osteochondral defects in animal models. These studies used an extensive range of biomaterials for scaffold fabrication, consisting mainly of natural and synthetic polymers. Different methods were used to create multiphasic scaffold designs, including by integrating or fabricating multiple layers, creating gradients, or through the addition of factors such as minerals, growth factors, and cells. The studies used a variety of animals to model osteochondral defects, where rabbits were the most commonly chosen and the vast majority of studies reported small rather than large animal models. The few available clinical studies reporting cell-free scaffolds have shown promising early-stage results in osteochondral repair, but long-term follow-up is necessary to demonstrate consistency in defect restoration. Overall, preclinical studies of multiphasic scaffolds show favourable results in simultaneously regenerating cartilage and bone in animal models of osteochondral defects, suggesting that biomaterials-based tissue engineering strategies may be a promising solution.

1. Introduction

Osteochondral defects are joint injuries involving both the articular cartilage and the underlying subchondral bone. They can be caused by acute traumatic injury, such as sports-related trauma or falls, or diseases such as osteochondritis dissecans. Osteochondral defects most commonly occur in the knee and ankle, but are also found in other sites such as the hands and spine [1]. The repair of damaged osteochondral tissue is challenging due to the generally avascular nature of the joint microenvironment leading to a restricted supply of nutrients and progenitor cells, as well as the limited self-regeneration capabilities of articular cartilage [2]. When injured cartilage is left untreated or suboptimally treated, the joint may irreversibly deteriorate which significantly increases the risk of progression to osteoarthritis, causing significant chronic pain and disability. Hence, osteochondral injuries have potentially severe impacts on quality of life in a significant portion of people globally, in particular juveniles and young to middle-aged adults who have an active lifestyle, and the need for effective treatment is vital. For instance, up to 45% of ankle fractures can result in an osteochondral lesion [3]. Such injuries can result in post-traumatic osteoarthritis which accounts for at least 12% of all cases of symptomatic osteoarthritis [4]. Current clinical methods of osteochondral repair are associated with numerous drawbacks, often resulting in limited applicability or suboptimal long-term outcomes, necessitating the development of emerging tissue engineering strategies based on multiphasic scaffolds to improve repair outcomes.

Peer review under responsibility of KeAi Communications Co., Ltd.
* Corresponding author. School of Biomedical Engineering, Faculty of Engineering and IT, University of Technology Sydney, NSW, 2007, Australia.
** Corresponding author. Raymond Purves Bone and Joint Research Lab, Kolling Institute, School of Medical Sciences, Faculty of Medicine and Health, University of Sydney, Royal North Shore Hospital, St Leonards, NSW, 2065, Australia.
E-mail addresses: christopher.little@sydney.edu.au (C.B. Little), jiaojiao.li@uts.edu.au (J.J. Li).

https://doi.org/10.1016/j.bioactmat.2023.04.016
Received 3 January 2023; Received in revised form 18 March 2023; Accepted 17 April 2023

1.1. Clinical methods of osteochondral repair

Numerous clinical strategies have been used to treat osteochondral defects, with variations in their advantages and disadvantages, and reported long-term outcomes. Surgical strategies are a standard approach, many of which involve autologous osteochondral transplantation or osteochondral autograft transplantation. The former, also known as autograft mosaicplasty, involves filling the cartilage defect with multiple small cylindrical plugs harvested from a non-weight bearing site of the patient's healthy joint, resembling a mosaic pattern [5], while the latter typically uses a single large plug. While both procedures use the patient's healthy tissue to repair the damaged joint tissue, the difference lies in the size and shape of the transplant. Systematic reviews and meta-analyses of clinical studies have reported promising long-term outcomes for these surgical approaches with respect to pain relief, function, and radiographic outcomes, while also noting a low risk of complications and revision surgery. The long-term survival rates of both procedures ranged from 76% to 97% with a 10 to 20-year follow-up period [6–8], with variations due to parameters such as patient age and comorbidities, size and location of the defect, and surgical techniques used. Nevertheless, a failure rate of 51% at an average of 8.4 years after surgery has been noted, although the cartilage survival rate was over 80% for the first 7 years and reduced to just over 60% after 15 years [9]. The application of both techniques is constrained by limited supply of autologous donor tissue, the potential for graft hypertrophy or subsidence, and the risk of chondrocyte damage during transplantation. Additionally, donor site morbidity is an issue with occurrence rates of up to 50%, which does not appear to correlate with patient age or weight, or number or size of grafts [10–12].

To avoid these problems, other tissue sources can be used for transplantation such as osteochondral allografts, which are harvested from a different human donor. However, there are obvious limitations arising from allograft processing prior to transplantation. Insufficient decellularisation may lead to immune rejection [13], transfer of diseases, and bacterial or viral infections [14]. Otherwise, the extensive removal of biological materials reduces the bioactivity of the graft, which can lead to graft destabilisation and loosening after implantation, failure of integration into the defect site, or failure to restore the osteochondral surface congruency [14], all of which result in poor repair outcomes. Retrospective studies have reported comparable survival rates for osteochondral allografts compared to autografts, usually 70–91% at 10–20 years post-operation [15–17]. A study in patients with large tibial osteochondral defects reported allograft survival to be 90% after 5 years, which reduced to 79%, 64% and 47% after 10, 15 and 20 years respectively [18]. However, complications included infection and hardware-related knee pain combined with 42% of patients having conversions to arthroplasty or another procedure. Another study on patients with femoral osteochondral defects reported similar graft survival rates, although 23% of grafts failed after 8.6 years and 43% of patients required further operations [19]. Other studies have reported reoperation rates of 22% and 36% following allograft transplantation, in which 68–70% of failures underwent total knee arthroplasty (TKA) and 23–28% underwent graft removal [15,17]. Interestingly, the reoperation rate of patellofemoral lesions (83%) was remarkably higher than lesions at the tibial plateau or the femoral condyles [15]. Contributing factors for TKA and graft removal after osteochondral allograft transplantation include infection, persistent pain, and graft-host size mismatch which can lead to mechanical stress and ultimate failure [16,20].

Another commonly used surgical procedure for osteochondral repair is arthroscopic debridement and microfracture, which involves removing loose cartilage and drilling multiple small holes in the exposed bone beneath the chondral injury [21]. This procedure allows bone marrow to infiltrate the damaged area, with the intention of introducing stem cells that can differentiate into new cartilage tissue and also facilitate better vascularisation at the injury site. However, this method generally leads to the formation of fibrocartilage instead of the desired articular cartilage, containing largely collagen type I rather than type II, and with reduced proteoglycan content [2]. This fibrocartilage has inferior biological functions and properties, which may lead to unsatisfactory long-term outcomes due to limited capability for load-bearing and wear-resistance [22]. Microfracture can produce good outcomes in patients with defect sizes less than 4 cm^2, but larger defects have worse outcomes at 18–36 months post-surgery [22]. Other reports have suggested that microfracture has no further benefit over debridement alone, and may even result in significant destruction of the subchondral bone [23]. Moreover, studies have demonstrated that osteochondral autologous transplantation is superior to microfracture in failure rate and clinical outcome scores, allowing faster return to pre-injury activity levels [24–27]. The failure rate of microfracture was 32–38% compared to <15% for mosaicplasty at 5–10 years follow-up [24,26], while another study has reported failure rate of 66% with average time to failure at 4 years [9].

Autologous chondrocyte implantation (ACI) is a cell therapy for osteochondral repair, first reported in 1994 and developed to address the drawbacks of other surgical techniques [28]. It uses arthroscopy to harvest cartilage from non-loadbearing sites of the joint, from which chondrocytes are isolated and cultured *in vitro* to increase cell number, and then the cells are re-implanted underneath a natural or synthetic membrane patch at the defect site. A 20-year follow-up study [29] has shown satisfactory long-term outcomes of ACI for the treatment of cartilage defects, where 93% of patients rated their knee-specific outcome as good or excellent, and 79% of patients still had their knee (s) that received ACI and were satisfied. Of the 24 patients included in this study, 5 required a revision ACI after an average of 1.7 years and 4 required an arthroplasty after 5.9 years. Larger studies have reported failure rate of 26% at 5.7 years after ACI in 104 patients [30], as well as 18% failure rate and 37% reoperation rate at 11.4 years follow-up in 771 patients [31]. Over the past 20 years, this procedure has evolved to its third generation, matrix-autologous chondrocyte implantation (MACI), where the expanded chondrocytes are suspended in a hydrated scaffold before insertion into the defect [28]. MACI offers advantages of removing the need for a membrane patch, more controlled cell distribution, and ability to manage more extensive defects. Clinical outcomes have shown greater success than ACI, as reflected by reports of good knee functionality and reduced pain and swelling, with a failure rate of 10.7% after 7 years [32] compared to 33% with ACI [29]. Despite promising results, ACI and MACI still have some limitations. There have been large variations in the number of chondrocytes used in ACI/MACI procedures, and the optimal cell concentration to fill the cartilage defect and give rise to consistent long-term outcomes is not yet determined [28]. Furthermore, chondrocytes typically undergo dedifferentiation during *in vitro* expansion, exhibiting increased formation of stress fibres and losing their chondrogenic phenotype if the number of cell doublings is not controlled [33]. The effectiveness of ACI and MACI in producing hyaline cartilage therefore depends on tight control of chondrocyte expansion, which can only be performed a limited number of times. Additionally, some complications are associated with ACI including graft hypertrophy, delamination, and periosteal hypertrophy [34], with the use of lower quality cells resulting in higher complication rate and poor clinical outcomes [35].

Current clinical treatments are only palliative as they do not 'cure' the defect or restore the native structure and function of osteochondral tissue [36]. New treatment approaches are necessary to provide permanent joint repair and return the damaged osteochondral tissue to its native functional state.

1.2. Emerging tissue engineering solutions for osteochondral repair

Osteochondral tissue engineering is a promising solution to address the current therapeutic limitations. As an interfacial tissue, osteochondral tissue has a complex structure involving integrated cartilage and

bone components, which has a unique set of requirements for regeneration that is unlikely to be satisfied using cell therapy alone. Osteochondral tissue engineering has evolved to focus on the fabrication of biomaterial scaffolds that mimic the physiological properties of native tissue [37], often with the addition of cells and/or growth factors to prompt cell differentiation and regeneration of cartilage and bone. In this review, we focus on biomaterials-based osteochondral tissue engineering strategies, whereby a multiphasic scaffold is constructed to simultaneously regenerate the articular cartilage, cartilage-bone interface, and subchondral bone [38], which may also feature a gradient transition among different phases [37], to restore the joint to its native state.

Different biomaterials, additional components, and fabrication methods can be used to compose an osteochondral scaffold. The most common material choices are natural and synthetic biocompatible polymers, as many of them are accessible at low cost, and can be fabricated to mimic the structure and properties of cartilage/bone extracellular matrix (ECM), as well as aid stem cell recruitment, infiltration and differentiation [39]. An ideal osteochondral scaffold design needs to account for the different regeneration requirements of cartilage and bone. Multiphasic or gradient scaffold designs are therefore more advantageous than monophasic homogenous scaffolds [36]. Fabrication methods need to be devised such that the scaffold shape and dimensions can precisely match the osteochondral defect, to allow for optimal integration with the surrounding tissue. Moreover, the internal geometry of the scaffold needs to be designed such that the pore architecture allows for cell penetration and the transfer of nutrients and waste products, while adjusting for pore sizes in the cartilage and bone components since they have different requirements for vascularisation [40]. Since the osteochondral defect often occurs in load-bearing locations, the scaffold needs to mimic the biomechanical properties of native tissue and withstand physiological forces experienced on the joint, at least in the short-term before complete tissue regeneration occurs. For instance, native human articular cartilage has compressive modulus of 240–1000 kPa depending on location within the body [39]. Biologically, the scaffold should enhance cellular responses, including to kick-start and/or maintain tissue repair processes, as well as ideally direct progenitor cell differentiation into chondrogenic and osteogenic lineages in respective scaffold components corresponding to native osteochondral anatomy.

The main design strategies for osteochondral scaffolds include monolayer (homogeneous), bilayer, multiple (more than two) layers, and gradient scaffolds [41] (Fig. 1). Monolayer scaffolds have a homogeneous composition and structure, which are often designed to mimic either the cartilage or bone portion of osteochondral tissue, and experience challenges in simultaneously regenerating the entire osteochondral unit. More complex scaffold designs have then evolved to more faithfully replicate the native osteochondral structure and composition, comprising superficial, transition, and deep cartilage zones as well as calcified cartilage and subchondral bone, with varying abundance of proteoglycans, collagen types I and II, and water content. Bilayer scaffolds consist of two layers, a cartilage layer typically composed of polymer(s) and a bone layer that may contain various combinations of polymers and/or ceramic materials. Scaffolds with more than two layers have recently emerged to better represent the spatial, compositional, and functional variation of native osteochondral tissue, and are believed to facilitate better *in vivo* repair although they may involve complex fabrication processes. Moreover, gradient osteochondral scaffolds have

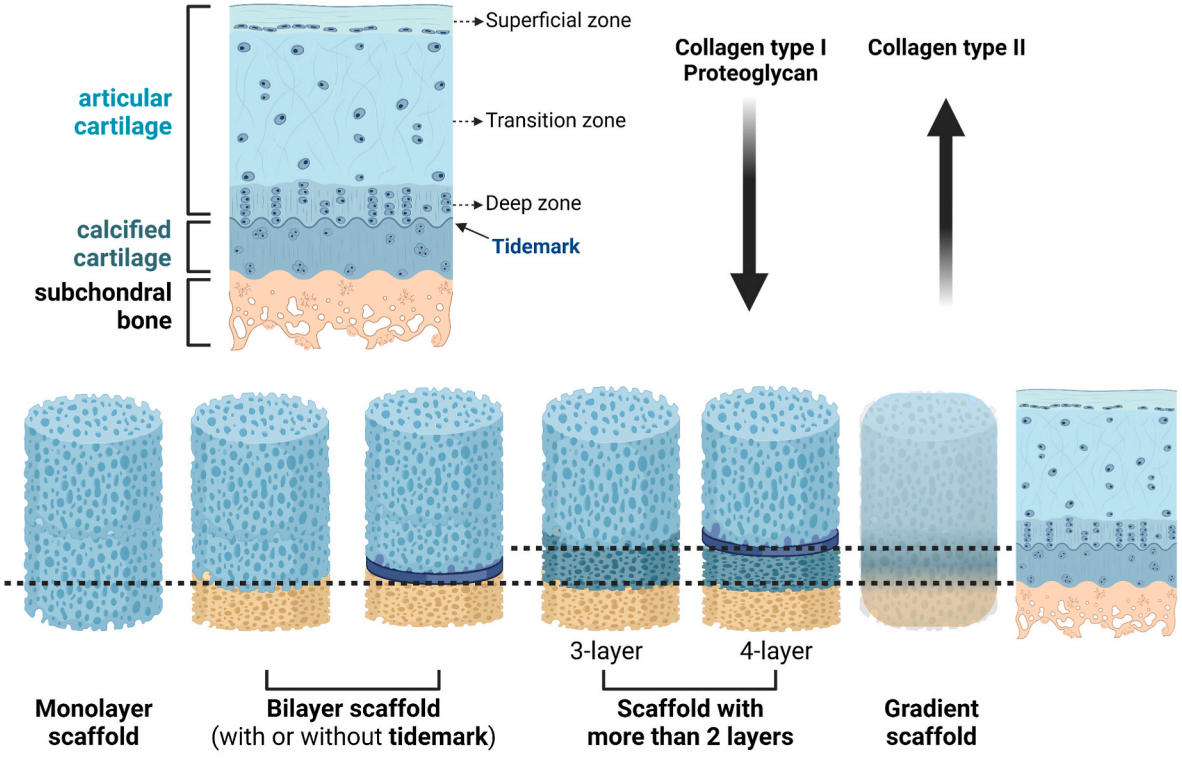

Fig. 1. Main design strategies for osteochondral scaffolds and common biomaterial selections. PLGA: poly(lactic-co-glycolic acid), PLA: poly(lactic acid), PCL: polycaprolactone, PEG: poly(ethylene glycol). Figure generated in BioRender (BioRender.com).

been constructed with continuous spatial transition in scaffold properties, often involving hierarchical stratification in the loading of cells or bioactive molecules. In this review, we focus on multiphasic osteochondral scaffold designs categorised as multilayer (two or more layers) or gradient scaffolds.

Biomaterial selections for osteochondral scaffolds typically comprise a combination of natural and synthetic polymers [38]. As discussed later in this review, the most commonly used natural materials include collagen, alginate, chitosan, gelatin, and silk fibroin, while a wide range of synthetic polymers have been applied such as poly(lactic-co-glycolic acid) (PLGA), poly(lactic acid) (PLA), polycaprolactone (PCL), and poly(ethylene glycol) (PEG). Natural polymers usually contain naturally-derived bioactive factors that promote cell adhesion, proliferation, and differentiation, and are favoured choices for the cartilage layer of multilayered scaffolds. However, their natural origin may give rise to batch-to-batch variability and risk of transfer of immunogenic material, and also restrict the degree of physicochemical modulation during scaffold synthesis. Moreover, natural polymers tend to have weak mechanical properties, making them less ideal for use as the bone layer to support weight-bearing. Comparatively, synthetic polymers have consistent and tailorable properties, with strength and stiffness mostly exceeding natural polymers, and can be processed using a wide variety of fabrication techniques. However, they are usually bioinert and require additional modification to actively interact with cells. Ceramics may be used to reinforce both natural and synthetic polymers to form the bone phase of osteochondral scaffolds, or fabricated as a bulk scaffold to provide load-bearing support. The most commonly chosen ceramics for incorporation into osteochondral scaffolds include hydroxyapatite (HA), tricalcium phosphate (TCP), and bioactive glass.

Fabrication techniques play a crucial role in scaffold construction for osteochondral repair, providing synergistic effects with biomaterials selection and architectural design. Although not the focus of this review, the method of scaffold fabrication can have profound influences on repair outcomes by modulating biological responses through control of pore structure, mechanical properties, spatial distribution of materials and/or additives such as cells and growth factors, and biodegradation. Common fabrication techniques employed for osteochondral scaffolds to realise multilayer or gradient designs include electrospinning, lyophilisation, freeze casting, gas foaming, microfluidic foaming, sol-gel process, melt moulding, compression moulding, particulate leaching, phase separation, and additive manufacturing [38].

Multiphasic scaffold designs for osteochondral repair have been captured in a number of recent reviews, some of which featured extensive discussions on fabrication techniques [38] including 3D printing [42], while others presented an in-depth analysis of specific scaffold architectures such as gradient scaffolds [37]. These reviews discussed *in vitro* as well as *in vivo* studies with a specific focus on scaffold design. Our review chose to include only preclinical studies, as scaffold testing in animal models of osteochondral injury is a fundamental step toward the development of clinically relevant repair strategies. Other recent reviews have concentrated on the evaluation of animal models for osteochondral repair studies involving biomaterials, one of which focused on large animals and specifically in the knee joint [43]. Another two reviews respectively focused on the characteristics of different animal models for osteochondral repair [44], and specific evaluation methods used in animal studies [45].

Complementing the current literature and offering an update to our previous work [46], this review provides a new perspective on tissue-engineered multiphasic scaffolds for osteochondral repair. We surveyed original research studies published in English between 2015 and 2021, reporting scaffold designs that were tested in animal models to evaluate their effects for treating osteochondral injury, which contained multiple scaffold phases and/or two or more types of biomaterials (Table 1, Table 2). We discuss scaffold materials and design to realise the multiphasic structure, including the incorporation of additional elements such as cells and growth factors, and summarise the main findings from animal experiments. We also provide a critical discussion of different animal models of osteochondral injury used to test multiphasic scaffolds, and comment on their translational validity with consideration given to the anatomical structure, biochemical composition, and weight-bearing properties of osteochondral tissue compared to humans (Table 3). We conclude with a summary of current progress in clinical studies using commercially available osteochondral scaffolds (Table 4), as well as our perspectives on future developments in this exciting field of research.

2. Multiphasic scaffold biomaterials

Biomaterials to construct multiphasic osteochondral scaffolds are generally used to make a mineral-containing layer for bone regeneration and a polymer layer for cartilage regeneration. Among studies discussed in this review, the most common minerals incorporated into multiphasic scaffolds to assist bone regeneration included hydroxyapatite (HA) or nano-HA [47–67], tricalcium phosphate (TCP) [51,68–71], bioactive glass [72,73], and other specific formulations such as aragonite [74] and wollastonite [75]. Two studies also incorporated titanium alloy in the bone phase [76,77]. Natural and synthetic polymers have been used in both cartilage and bone phases of multiphasic scaffold designs. Commonly used natural polymers included collagen [56,57,65,68,77–80], alginate [48,58,81,82], chitosan [52,59,61,65,82–86], and silk fibroin [47,61,87]. Many types of synthetic polymers were used, where the most popular were poly(lactic-co-glycolic acid) (PLGA) [49,83,86,88–93], poly(lactic acid) (PLA) [73,77,89], polycaprolactone (PCL) [50,52,64,66,70,79,94–97], and poly(ethylene glycol) (PEG) [52,63,72,98,99]. A few studies included microspheres in the scaffold design, fabricated from PLGA for growth factor delivery [47,60,100], and several studies used additive manufacturing for scaffold fabrication such as by 3D printing [71,76,85,88] or bioprinting [79,95,101].

2.1. Mineral materials in osteochondral scaffolds

Bioactive ceramics are frequently used to aid bone regeneration due to their compositional similarity to natural bone mineral. In multiphasic osteochondral scaffolds, calcium phosphate minerals were the most commonly used for doping into the bone phase, due to their osteoconductive and osteoinductive properties that help induce new bone formation [46]. The majority of studies that included a ceramic in the scaffolding materials used HA in various forms, such as a bulk scaffold layer [102], nano-HA particles incorporated into a polymer matrix [61], or nano-HA containing microspheres [60]. Synthetic HA has the same chemical composition as the HA mineral component of bone, justifying its extensive use in bone tissue engineering [103,104]. HA increases the local concentration of calcium ions, which activates osteoblast proliferation and promotes the growth and differentiation of mesenchymal stem cells (MSCs) [105], leading to new bone formation [106]. The osteoconductive properties of HA can help restore subchondral bone in osteochondral injuries, as multiphasic scaffolds containing HA in the bone layer showed better integration between the host tissue and newly formed bone [52,59], as well as improved vascularisation [50,60]. In a 3D bioprinted osteochondral scaffold, HA was also reported to improve the mechanical properties of the polymer matrix composed of alginate and gelatin to better match native bone [101]. However, a drawback of using HA is its low biodegradability, as noted in studies which showed very limited [50] or slow [48] degradation in both small and large animal models.

Other types of calcium phosphates have been incorporated into the bone layer of multiphasic osteochondral scaffolds, such as TCP where β-TCP is the most commonly used form due to its rhombohedral crystallised structure. β-TCP is less stable than HA, giving it higher solubility with faster degradation rates [106]. When incorporated into osteochondral scaffolds, β-TCP has been found to increase subchondral bone volume [107], enhance bone regeneration [69,70,88], improve

Table 1
Summary of preclinical studies which tested multilayer scaffold designs in animal models to evaluate osteochondral repair.

Multilayer scaffolds						
Study	Biomaterial(s) for bone phase (s)	Biomaterial(s) for cartilage phase(s)	Additives (e.g., cells, growth factors)	Animal model, defect size, time point(s)	Experimental groups	Main findings
Bilayer scaffolds made from polymeric materials						
Critchley et al. (2020) [94]	3D printed PCL fibre network	Alginate or agarose hydrogel, or self-assembled scaffold-free cartilage layer	Fat pad-derived stem cells + chondrocytes in cartilage layer, bone marrow-derived stem cells in bone layer for all scaffolds	Mouse: 6 weeks Subcutaneous Goat: 6 months Knee – medial condyle 6 mm diameter, 6 mm thickness	Mouse: single phase (PCL), bi-phasic alginate, bi-phasic agarose, bi-phasic self-assembly (same cells on a PCL fibre mesh for cartilage layer); implantation after 5 weeks *in vitro* priming Goat: bi-phasic self-assembly scaffold, control scaffold (MaioRegen® from a different study using same animal model); implantation after 4 weeks *in vitro* priming	Mouse model showed bi-phasic scaffolds induced cartilage-like and bone-like tissue formation in respective layers, with higher vascularisation in the bone layer. Goat model showed evidence of endochondral ossification in the bone layer of the bi-phasic scaffold. One case had a collapsed defect. Bi-phasic scaffold had higher amount of cartilage formation in the cartilage layer compared to bone layer, and significantly higher cartilage layer matrix staining compared to control group.
Korthagen et al. (2019) [123]	Polyetherketoneketone (PEKK)	Elastomer comprising polycarbonate-based aliphatic polymer containing cartilage-derived peptides RGD and GFOGER	None	Horse (Shetland pony) Knee – medial trochlear ridge of femur (2 defects, one proximal & one distal) 6 mm diameter, 7 mm thickness 12 weeks	2 groups: Control (empty), scaffold	After 12 weeks, the proximal defect was partially filled (~70%) and distal defect was almost completely covered with stiff and smooth repair tissues (~98%). Repair tissue was stiff and fibrous, presenting nearly flush surface with surrounding cartilage. However, repair tissue contained a negligible amount of collagen type II and GAG, and no hyaline cartilage-like tissue was formed on the implant.
Liao et al. (2017) [125]	Bone layer: acryloyl chloride (AC)-PCL-PEG-PCL-AC (PECDA), -poly (ε-caprolactone)-poly (ethylene glycol)-poly (ε-caprolactone)-acryloyl chloride (PECDA), AAm, PEGDA (Average pore size 112.6 μm, modulus 0.261 MPa) Intermediate layer: calcium gluconate and alginate cross-linking	Cartilage layer: methacrylated Chondroitin sulfate (CSMA), NIPAm (Average pore size 187.4 μm, modulus 0.065 MPa)	None	Rat: 1, 2, 4, 8 weeks Subcutaneous 1 cm diameter Rabbit: 6, 12, 18 weeks Knee – patellar groove 5 mm diameter, 4 mm thickness	Rat: 1 group; scaffold Rabbit: 2 groups; control (empty), scaffold	Rat model showed hydrogels degraded gradually and remained integrated 4 weeks after implantation, and did not completely disappear after 8 weeks. Acute inflammatory response observed in the first week which gradually subsided over 4 weeks. Rabbit model showed new translucent cartilage and repaired subchondral bone for scaffold group at 18 weeks. Regenerated cartilage was grown uniformly throughout the tissue, and bone volume increased from 65% to 91% from 12 to 18 weeks. Repaired cartilage had significantly higher load value than the control, and its reduced modulus was 75% of normal cartilage.
Mancini et al. (2020) [96]	3D printed PCL scaffold	Thiol-ene cross-linkable hyaluronic acid/poly (glycidol) hybrid hydrogel	Articular cartilage progenitor cells (from native cartilage) in	Horse (Shetland pony) Knee – medial trochlear ridge	2 groups: Zonal scaffold (cartilage progenitor cells in top hydrogel	Significant bone growth into the bone layer after 6 months, with similar bone volume percentage for

(*continued on next page*)

Table 1 (*continued*)

Multilayer scaffolds						
Study	Biomaterial(s) for bone phase (s)	Biomaterial(s) for cartilage phase(s)	Additives (e.g., cells, growth factors)	Animal model, defect size, time point(s)	Experimental groups	Main findings
			cartilage layer, MSCs in cartilage and bone layer	6 mm diameter, 7.5 mm thickness 6 months	layer with MSCs in lower hydrogel layers of cartilage layer), non-zonal scaffold (only MSCs in cartilage layer)	both zonal and non-zonal scaffolds. However, there was limited production of cartilage-like tissue for both scaffold groups, with no differences in histological scoring although repair tissue was stiffer in defects with zonal scaffolds. The repair tissue lacked GAG and collagen type II, but was abundant in collagen type I. The study considered this may be due to early loss of implanted cells, or inappropriate degradation rate of the hydrogel, as hydrogel fragments were observed at 6 months.
Nie et al. (2019) [90]	PLGA sintered microsphere scaffolds + alginate hydrogel (for cell encapsulation)	ECM secreted by chondrocytes (chondrocytes contained in alginate hydrogel for ECM production were either kept or decellularised)	Porcine chondrocytes	Rabbit Knee – condyles 3 mm diameter, 3 mm thickness 50, 100 days	2 groups: Scaffold with chondrocyte-laden cartilage layer or decellularised cartilage layer	Cell-laden scaffold achieved superior repair efficacy at 100 days compared to decellularised scaffold. There was better formation of hyaline cartilage-like tissue with strong staining for GAG and collagen type II, as well as higher Young's modulus. A fibrotic intermediate layer was formed at the interface. New tissue in the bone layer was mineralised and ossified.
Shim et al. (2016) [79]	3D printed PCL filled with atelocollagen	3D printed PCL filled with cucurbit [6]uril (CB [6])-conjugated hyaluronic acid and 1,6-diaminohexane (DAH)-conjugated hyaluronic acid	Human turbinate-derived MSCs in bone and cartilage layers, BMP-2 in bone layer and TGF-β in cartilage layer	Rabbit Knee – femoral patellar groove 5 mm diameter, 5 mm thickness 8 weeks	4 groups: 1: Control (empty). 2: single layer PCL scaffold with cells. 3: bilayer PCL scaffold with alginate hydrogel and cells in both layers, TGF-β in cartilage layer and BMP-2 in bone layer. 4: bilayer PCL scaffold with collagen hydrogel & BMP-2 in bone layer and CB [6]/DAH-conjugated hyaluronic acid hydrogel & TGF-β in cartilage layer, cells in both layers	No noticeable inflammatory response in all groups. Group 1: poor regeneration with fibrous tissue formation. Group 2: PCL exposed to cartilage surface was partially covered by neo-tissue showing distinct boundary with native tissue, and fibrous tissue at the periphery. Few matured osteoid islands found. Group 3: poor regeneration, defect incompletely covered by neo-tissue which appeared to be fibrous tissue. No ingrowth of native bone from surrounding tissue. Thought to be due to slow degradation of alginate hindering cell infiltration. Group 4: significant osteochondral regeneration, defect fully covered with neo-tissue exhibiting smooth surface and cartilage-like appearance, and stained for GAG and collagen type II. New bone formation

(*continued on next page*)

Table 1 (*continued*)

Multilayer scaffolds						
Study	Biomaterial(s) for bone phase (s)	Biomaterial(s) for cartilage phase(s)	Additives (e.g., cells, growth factors)	Animal model, defect size, time point(s)	Experimental groups	Main findings
						was observed and scaffold was densely filled with infiltrated bone.
Sun et al. (2020) [114]	Demineralised and decellularised allograft bone	Collagen type I scaffold (lyophilised hydrogel attached to bone layer)	Bone marrow MSCs transfected to overexpress BMP-7	Beagle dogs Knee – patellar groove 6 mm diameter, 8 mm thickness 8, 12 weeks	4 groups: Control (empty), cell-free scaffold, scaffold with untransfected cells, scaffold with transfected cells overexpressing BMP-7	Scaffold with cells overexpressing BMP-7 showed the best osteochondral repair. Defect was fully filled with new tissue, comprising hyaline-like cartilage and significant bone formation. For cell free scaffolds and scaffolds with untransfected cells, the repair tissue was mainly fibrocartilage. Transfected cells can overcome the short half-life of BMP-7 to enhance osteochondral repair, allowing sustained release of growth factor for more than 28 days. Collagen hydrogel underwent gradual degradation.
Zheng et al. (2019) [89]	PLA/PLGA/PCL nanofibrous scaffold	Gelatin, silk fibroin, oxidised dextran hydrogel	BMP-2 derived peptides (P24 peptides) in bone layer, kartogenin in cartilage layer	Rabbit Knee – distal femur tracheal groove 5 mm diameter, 4 mm thickness 4, 12 weeks	3 groups: Control (empty), drug-free scaffold, drug-containing scaffold	Drug elution lasted for more than 28 days. Drug-free scaffold group formed translucent tissue connecting to the native tissue, but the defect was not completely filled. Drug-containing group accelerated osteochondral regeneration. Defect was filled with translucent tissue with similar histological appearance to surrounding native tissue, with no obvious boundaries.
Bilayer scaffolds made from polymeric and mineral materials						
Barbeck et al. (2017) [73]	3D printed PLA/bioglass G5	3D printed PLA	None	Mouse Subcutaneous 4 mm diameter, 4 mm thickness (scaffold) 3, 10, 15, 30 days	4 groups: Control (empty), three different scaffolds (PLA, PLA/G5, bi-layer)	Both scaffold parts kept their structural integrity. Mechanical properties decreased with progressive degradation, and PLA/G5 scaffolds showed higher compressive modulus than PLA scaffolds. The tissue reaction to PLA included low numbers of biomaterial-associated multinucleated giant cell (BMGC) and minimal implant bed vascularisation, while PLA/G5 had higher numbers of BMGC and higher implant bed vascularisation. Each layer in the bi-layer scaffold showed similar tissue response as PLA and PLA/G5 layers implanted separately.
Cai et al. (2019) [124]	BCP ceramic	Collagen type I gel (gelation on the ceramic	Chondrocytes encapsulated in collagen gel	Rabbit Knee – trochlear ridge	4 groups: Control (empty), collagen gel with	No inflammation or moving of scaffold from the defect area.

(*continued on next page*)

Table 1 (*continued*)

Multilayer scaffolds						
Study	Biomaterial(s) for bone phase (s)	Biomaterial(s) for cartilage phase(s)	Additives (e.g., cells, growth factors)	Animal model, defect size, time point(s)	Experimental groups	Main findings
		layer then frozen and lyophilised)		4 mm diameter, 4 mm thickness 2, 4 weeks	chondrocytes, BCP ceramic, bi-layer scaffold with chondrocytes in collagen gel layer	For bone repair, BCP and bi-layer groups showed new bone at 2 weeks, with increased bone formation containing osteocytes and new bone trabeculae at 4 weeks, as well as well-developed blood vessels at the bone formation site. For cartilage repair, all groups showed weak staining for GAG and collagen type II at 2 weeks, and the collagen gel group collapsed due to absence of subchondral bone support. At 4 weeks, the collagen gel group still showed weak GAG and collagen type II staining, which were stronger in the BCP group and most intense in the bi-layer group. The bi-layer group showed bone and cartilage layers that were seamlessly connected with each other.
Coluccino et al. (2016) [58]	Alginate scaffold with HA granules	Alginate scaffold with TGF-β1	TGF-β1 in cartilage layer, MSCs for implanted scaffold	Rat Subcutaneous 2 weeks	1 group: Scaffold with MSCs	No significant evidence of inflammatory response or foreign body reaction. Various cell types entered the scaffold and initiated formation of new connective tissue, including fibroblasts, monocytes and lymphocytes.
Dong et al. (2020) [47]	Silk fibroin with nHA and PLGA microspheres	Porcine cartilage ECM and silk fibroin with PLGA microspheres	TGF-β3 in cartilage layer, BMP-2 in bone layer Either absorbed or encapsulated in PLGA microspheres	Rabbit Knee – centre of trochlear groove 5 mm diameter, 3 mm thickness 8, 16 weeks	5 groups: Control (empty), scaffold without microspheres or growth factors, scaffold with blank microspheres, scaffold with absorbed TGF-β3 & BMP-2, scaffold with TGF-β3 & BMP-2 encapsulated in microspheres	Scaffolds with sustained growth factor release through microspheres significantly accelerated osteochondral repair compared to other groups, with higher GAG content and collagen type II in the cartilage layer and better subchondral bone formation in the bone layer. Burst release of growth factors in absorbed scaffold group, which achieved some repair worse than microsphere growth factor group but better than scaffold with blank microspheres.
Filardo et al. (2018) [48]	1.25% alginate and 4% HA	1% alginate and 0.5% hyaluronic acid	None	Rabbit & sheep Rabbit: 8 weeks Bilaterally in the distal femoral epiphysis 6 mm diameter, 8 mm thickness Sheep: 6 months Lateral femoral condyles 7 mm diameter, 5 mm thickness	Rabbit: commercial collagen-HA scaffold (Regenoss™, Finceramica), alginate-HA scaffold (bone layer scaffold) Sheep: untreated, biphasic scaffold	Good biocompatibility profile with no inflammatory cells around the implant. Lower bone formation compared with commercial scaffold in the rabbit model, slow bioresorption. Evidence of repair and implant integration in cartilage layer but incomplete regeneration in bone layer in the sheep

(*continued on next page*)

Table 1 (*continued*)

Multilayer scaffolds						
Study	Biomaterial(s) for bone phase (s)	Biomaterial(s) for cartilage phase(s)	Additives (e.g., cells, growth factors)	Animal model, defect size, time point(s)	Experimental groups	Main findings
						model, slow bioresorption.
Giannoni et al. (2015) [50]	PCL scaffold with HA granules	PCL scaffold	Articular chondrocytes in cartilage layer, MSCs in bone layer	Mouse Subcutaneous 3 mm × 3 mm x 5 mm (scaffold) 9 weeks	1 group: Scaffold with cells	Scaffold with cells resulted in high deposition of bone matrix surrounding the HA granules in the bone layer, and cartilage matrix formation in the cartilage layer. Vascularisation was mostly observed in the bone layer, with significantly higher blood vessel density and mean area compared to cartilage layer. Poor scaffold degradability.
Gong et al. (2020) [64]	Porous 3D printed PCL-HA scaffold	3D printed radially oriented GelMA scaffold	IL-4 in cartilage layer	Rabbit Knee – patellar groove 5 mm diameter, 5 mm thickness 8, 16 weeks	3 groups: Non-treated, scaffold, scaffold + IL-4	Scaffold with IL-4 obtained the highest histological score. At 8 weeks, scaffold group contained both fibrous and cartilage-like tissues, while scaffold + IL-4 group contained a large amount of hyaline cartilage-like tissue. No significant differences between two scaffold groups in subchondral bone repair. At 16 weeks, scaffold + IL-4 group achieved the best histological repair of both cartilage and bone, where repair tissue covered the entire defect area, and also had the highest compressive modulus compared to the other two groups.
Hsieh et al. (2017) [99]	3D printed methoxy PEG-block-PCL (mPEG-PCL) scaffold with HA	Glycidyl methacrylate hyaluronic acid hydrogel with TGF-β1 For *in vivo* study, bone scaffold was implanted first followed by *in situ* hydrogel cross-linking	TGF-β1 in cartilage layer	Rabbit Knee – medial femoral condyle 3 mm diameter, 8 mm thickness 3 months	2 groups: Control (empty), scaffold	Scaffold repaired both cartilage and bone in osteochondral defect, while control showed only bone formation.
Hsieh et al. (2018) [63]	3D printed methoxy PEG-block-PCL (mPEG-PCL) scaffold with HA	Glycidyl methacrylate hyaluronic acid hydrogel with TGF-β1 For *in vivo* study, bone scaffold was implanted first followed by *in situ* hydrogel cross-linking	TGF-β1 in cartilage layer	Mini pigs Knee – medial femoral condyle 10 mm diameter, 10 mm thickness 1 year	2 groups: Control (empty), scaffold Total 2 animals	Control defects remained mostly empty, filled with hypertrophic cartilage-like soft tissue and some overgrowth into the subchondral area. Scaffold showed regeneration of hyaline-like cartilage (not fully differentiated) and bone, and a clear tidemark between calcified and uncalcified cartilage. Non-degraded scaffold was present in the deep bone layer after 1 year, surrounded by regenerated fibrotic tissue and bone tissue.
Jia et al. (2018) [88]	Bone layer: porous 3D printed PLGA/TCP scaffold Intermediate: compact interfacial layer (PLGA/TCP)	Bovine articular cartilage ECM Bonded to bone layer through thermal-	None	Goat Knee – medial femoral condyle 6 mm diameter, 8	3 groups: Multilayered scaffold, bilayered scaffold,	Multilayered scaffold helped to form hyaline cartilage and subchondral bone over 48 weeks.

(*continued on next page*)

Table 1 (*continued*)

Multilayer scaffolds						
Study	Biomaterial(s) for bone phase (s)	Biomaterial(s) for cartilage phase(s)	Additives (e.g., cells, growth factors)	Animal model, defect size, time point(s)	Experimental groups	Main findings
		induced phase separation (TIPS)		mm thickness 12, 24, 48 weeks	negative control (empty)	Interfacial layer in the multilayered scaffold significantly improved biomechanical and biochemical properties (GAG The interfacial layer in the MLS significantly improved the biomechanical and biochemical properties (GAG & collagen II increased more quickly in the initial phase <24 weeks) of the new tissue. Multilayered scaffold formed a smooth interface with integrated tidemark, well organised cell structure with columnar distribution, and orientation of collagen fibres in cartilage layer with increased compressive modulus.
Kim et al. (2015) [69]	PLGA/β-TCP scaffold	Poly (lactide-co-caprolactone) scaffold	Bone marrow MSCs in bone layer, chondrocytes in cartilage layer	Mouse Subcutaneous 6 mm diameter, 11 mm thickness (scaffold) 6 weeks	1 group: Scaffold Cultured in osteogenic medium for 3 days before implantation	Top layer formed mature and well-developed cartilaginous tissue, with chondrocytes within lacunae. Bottom layer had presence of calcium phosphates indicative of osteogenic ECM produced by MSCs. Implanted chondrocytes (tagged) remained in the cartilage layer over 6 weeks and did not move into the bone layer.
Kon et al. (2015) [74]	Aragonite	Hyaluronate	None	Goat Knee – load-bearing medial femoral condyle 6 mm diameter, 10 mm thickness 6, 12 months	2 groups: Control (empty, filled with blood clot), scaffold implant (press-fit)	Defects in the scaffold group were mostly reconstructed – 5/7 at 6 months, and 6/7 at 12 months. Defects were filled with hyaline cartilage and normal bone. Results improved at 12 compared to 6 months, suggesting a continuous maturation process. Few defects in the control group were fully repaired – 1/3 at 6 months, and 0/3 at 12 months. Defects were filled with fibrous tissue.
Kumai et al. (2019) [67]	HA block or HA powder coated onto the bottom of the cartilage layer scaffold	Aggrecan, hyaluronic acid, and type II collagen complex	None	Rat Knee – femoral condyle 2 mm diameter, 2 mm thickness 4, 8 weeks	3 groups: Cartilage layer complex only, bi-layer scaffold with HA block, bi-layer scaffold with HA-coated portion of cartilage scaffold	Bi-layered scaffolds could induce cartilage and subchondral bone regeneration, with presence of chondrocytes although no visible amount of GAG. Bi-layered scaffolds containing HA as a block or as HA coating produced better repair compared to single-layer scaffold. Single-layer scaffold alone was not sufficient for repairing subchondral bone.

(*continued on next page*)

Table 1 (*continued*)

Multilayer scaffolds						
Study	Biomaterial(s) for bone phase (s)	Biomaterial(s) for cartilage phase(s)	Additives (e.g., cells, growth factors)	Animal model, defect size, time point(s)	Experimental groups	Main findings
Kumbhar et al. (2017) [136]	Bacterial cellulose (BC) scaffold with HA	BC scaffold with GAG Scaffolds press fitted on each other	BMP-2, TGF-β3	Rat Knee – patellar groove 1 mm diameter, 3 mm thickness 1, 3 months	4 groups: Control (empty), BC scaffold, bilayer scaffold, bilayer scaffold with growth factors	Histological scores for bilayer groups were significantly better than other two groups at 1 and 3 months. At 3 months, control defect was completely filled with fibrous tissue, while BC group had a mixture of fibrocartilage and cartilage-like tissue in the defect, and some small bony islands. Bilayer groups with or without growth factors showed complete formation of new cartilage and bone in the defect, with full integration to surrounding tissue. Bilayer group left a small portion of the scaffold at 3 months while bilayer with growth factors group was completely resorbed.
Li et al. (2015) [54]	nHA, polyamide-6	PVA, gelatin, vanillin	Bone marrow stromal cells	Rabbit Knee – patellar groove 4 mm diameter, 6 mm thickness 6, 12 weeks	3 groups: Control (empty), bilayer scaffold, bilayer scaffold with cells	Scaffold with cells resulted in faster chondrogenesis and osteogenesis at 6 weeks. At 12 weeks, scaffold-only group showed well-repaired smooth surface, but new cartilage was thinner than surrounding cartilage. Scaffold with cells had similar contour of repair tissue compared to normal cartilage. Both scaffold groups showed direct bonding to native cartilage and bone with indistinguishable interface. Increased expression of collagen type I in both scaffold groups, but higher expression of collagen type II in scaffold with cells group. Cells were responsible for repairing the defect for at least 4 weeks after implantation (shown by cell tracker).
Liang et al. (2018) [49]	PLGA-HA	PLGA (85 PLA:15 PGA) Glued to bone layer using Ch_2Cl_2	Bone marrow MSCs	Rabbit Knee – medial femoral condyle 4 mm diameter, 5 mm thickness 8, 16 weeks	3 groups: Control (empty), scaffold only, scaffold with MSCs	Bilayer scaffolds with or without cells showed osteochondral repair. Scaffold with MSCs showed favourable osteochondral regeneration through biomechanical testing, micro-CT, western blot, and histology. The time for the study was too short to determine the final effects of the scaffold without cells, since it showed poorer repair compared to scaffold with cells.

(*continued on next page*)

Table 1 (*continued*)

Multilayer scaffolds						
Study	Biomaterial(s) for bone phase (s)	Biomaterial(s) for cartilage phase(s)	Additives (e.g., cells, growth factors)	Animal model, defect size, time point(s)	Experimental groups	Main findings
Lin et al. (2020) [72]	Mesoporous bioactive glass (MBG) Prepared by sol-gel and polyurethane foam templating process	PEGS=PEG/PGS With controllable crosslinking degree and hierarchical macro/microporosities	None	Rabbit Knee – anterior articular surface of the distal femur 6.5 mm diameter, 4 mm thickness 12 weeks	4 groups: Control (empty), PEGS, MBG, PEGS/MBG	Bilayer scaffold had hierarchical porosity and successfully reconstructed hyaline cartilage and bone in 12 weeks. The subchondral bone formed in the bilayer scaffold group had the highest bone volume percentage and trabecular thickness. Blank control and single-layer PEGS had low bone volume percentage. The centre of the defect of PEGS group had a depression. Single-layer MBG achieved good bone regeneration but fragmented cartilage formation. The bilayer group promoted cartilage regeneration which smoothly integrated with native cartilage tissue.
Liu et al. (2015) [126]	Porous β-TCP scaffold	Electrospun PLA-co-PCL/collagen type I yarn or freeze-dried collagen type I/HA sponge	Bone marrow MSCs in cartilage layer	Rabbit Knee – patellar groove 5 mm diameter, 6 mm thickness 12 weeks	6 groups: Biphasic scaffold with yarn layer & biphasic scaffold with sponge layer, with differentiated or undifferentiated cells, osteochondral autograft, control (empty)	Scaffold with yarn layer resulted in better osteochondral repair than scaffold with sponge layer, showing superior cartilage formation that had higher compressive modulus and GAG deposition. Yarn scaffold showed defect bridging while sponge scaffold showed fibrocartilage formation with differentiated cells. Undifferentiated cells led to defect filling with rough tissue, which had higher fibrocartilage formation, lower collagen type II deposition, and GAG depletion.
Liu et al. (2019) [53]	Bone: 30%/3% GelMA/nHA hydrogel Intermediate: 20%/3% GelMA/nHA hydrogel	GelMA hydrogel 3D printed in all three layers	None	Rabbit Knee – centre of trochlear groove 3.5 mm diameter, 3 mm thickness 12 weeks	3 groups: Control (empty), monophasic scaffold, tri-layer scaffold	Neo-tissues in defects for all three groups integrated with surrounding tissues. Tri-layer scaffold showed >60% of the defect filled with neo-cartilage, smoother joint interface, more cartilage ECM and collagen type II, and faster repair rate. Neo-tissue for monophasic scaffold had distinct differences compared to native cartilage.
Liu B et al. (2020) [85]	Double-network (DN) hydrogel reinforced with bioactive glass particles	DN hydrogel composed of glycol chitosan and dibenzaldhyde functionalized poly (ethylene oxide) network, and sodium alginate and calcium chloride network	TGF-β1	Rabbit Knee – trochlear groove 3 mm diameter, 4 mm thickness 4, 12, 24 weeks	6 groups: Control (empty), microfracture, bioactive glass scaffold, DN gel, bi-layer scaffold, bi-layer scaffold with TGF-β1 in cartilage layer	Bioactive glass and DN hydrogel scaffolds respectively showed only cartilage and bone repair. Bioactive glass scaffold showed only a thin fibrocartilage layer. DN gel showed fine cartilage regeneration that integrated with surrounding cartilage, but less bone formation. Bi-

(*continued on next page*)

Table 1 (*continued*)

Multilayer scaffolds						
Study	Biomaterial(s) for bone phase (s)	Biomaterial(s) for cartilage phase(s)	Additives (e.g., cells, growth factors)	Animal model, defect size, time point(s)	Experimental groups	Main findings
						layer scaffold with or without TGF-β1 repaired cartilage and bone at the same time, with positive staining for toluidine blue and collagen type II in the cartilage layer and dense trabecular bone integrating with surrounding native tissue. TGF-β1 did not significantly change the repair outcomes.
Liu X et al. (2020) [128]	3D printed hydroxyapatite scaffold to release alendronate	Hyaluronic acid hydrogel to release KGN	KGN to induce chondrogenic differentiation of MSCs Alendronate to induce osteogenic differentiation of MSCs Bone marrow MSCs	Rat Subcutaneous 6 mm diameter, 3 mm thickness (scaffold) 2 months	2 groups: Drug free scaffold, alendronate & KGN scaffold	Addition of drugs showed strong ability of scaffold to promote cartilage and bone regeneration in their respective layers, through histology and gene expression. Scaffold could anchor the two layers for two months without separation.
Liu et al. (2021) [95]	Bottom layer: PCL/β-TCP porous scaffold	Top layer: diclofenac sodium (DC)-loaded matrix metalloproteinase (MMP)-sensitive methacrylated hyaluronic acid (MeHA) hydrogel Middle layer: MeHA hydrogel and PCL	Bone marrow MSCs in middle layer, DC in top layer, KGN in bottom layer	Rat Knee – femoral trochlear groove 2.3 mm diameter, 3 mm thickness 12 weeks	6 groups: Blank control, scaffold only control, scaffold with DC/KGN, scaffold with DC/KGN/cells, scaffold with KGN/cells, scaffold with KGN	Scaffold treatments were effective in helping functional recovery of the joint through osteochondral repair and inflammatory modulation. Treated animals showed significant improvements in ground support force, paw grip force, and walk gait parameters. Each of the additives had beneficial effect. Cell-laden scaffolds showed less cartilage degradation, increased collagen II expression, and decreased IL-1β expression compared with blank and scaffold control groups, and may also help to relieve inflammation and joint swelling. DC helps to further reduce inflammation. KGN helps to improve bone regeneration including increased trabecular thickness.
Lv & Yu (2015) [68]	Mineralised collagen type I/β-TCP scaffold	Non-mineralised collagen type II/β-TCP scaffold	Bone marrow MSCs	Dog Knee – femoral trochlea 6 mm diameter, 4 mm thickness 12, 24 weeks	2 groups: Control (empty), scaffold + MSCs	Slight elevation of newly formed tissue at defect site. New repair tissue was semi-translucent and integrated with surrounding tissue. Scaffold was degraded and absorbed after 24 weeks. Did not evaluate cartilage markers in the repair tissue.
Nordberg et al. (2021) [70]	3D printed scaffold with 80% PCL and 20% TCP	3D printed scaffold with 100% PCL With or without a tidemark layer of electrospun PCL disk	Adipose derived stem cells	Mini pig Knee – trochlear groove 8 mm diameter, 6 mm thickness 4 months	5 groups: Control (empty), autologous explant, acellular scaffold with no tidemark, acellular scaffold with tidemark, cell-seeded scaffold	Cell-seeded scaffolds healed defects with closest resemblance to autologous explant. Acellular scaffolds allowed subchondral bone repair mimicking native bone structure, but

(*continued on next page*)

Table 1 (*continued*)

Multilayer scaffolds						
Study	Biomaterial(s) for bone phase (s)	Biomaterial(s) for cartilage phase(s)	Additives (e.g., cells, growth factors)	Animal model, defect size, time point(s)	Experimental groups	Main findings
						showed little cartilage repair with no apparent cartilage matrix staining. Acellular scaffold without tidemark showed significantly more volumetric filling compared to other scaffold groups, suggesting that the tidemark limited cell infiltration into the cartilage layer.
Ruan et al. (2017) [61]	Silk fibroin/chitosan/nHA scaffold	Silk fibroin/chitosan scaffold	Bone marrow MSCs	Rabbit Knee – patella groove 4 mm diameter, 3 mm thickness 4, 8, 12 weeks	4 groups: Control (empty), cartilage layer scaffold, bone layer scaffold, bilayer scaffold with cells	Bilayer scaffold showed sufficient repair in both chondral and subchondral layers with no holes in the centre, while significant holes were seen in the control and cartilage layer scaffolds, or surface defects in the bone layer scaffolds. Cartilage layer scaffold expressed less collagen type I than type II while bone layer scaffold was the opposite. Bilayer scaffold expressed high levels of both collagen type I and II.
Seol et al. (2015) [55]	3D printed HA/TCP scaffold	Alginate hydrogel	TGF-β and articular chondrocytes in cartilage layer	Rabbit Knee – femoral patellar groove 4 mm diameter, 6 mm thickness (blank & hybrid) or 2 mm thickness (hydrogel) 12 weeks	3 groups: Control (empty), hydrogel (cartilage layer only), hybrid (bilayer scaffold)	Hybrid scaffold produced cartilage repair tissue that was morphologically similar compared to native cartilage and had smooth connection to surrounding tissue, with evidence of GAG staining. However, the repair tissue did not resemble mature cartilage. Control and hydrogel groups showed defects filled with fibrous tissue.
Seong et al. (2017) [127]	β-TCP scaffold Formed through sequential coextrusion	Collagen scaffold Formed through unidirectional freezing followed by lyophilisation to connect it to the bone phase with aligned internal pores	None	Rabbit Knee – patellar groove 6 mm diameter, 6 mm thickness 6, 12 weeks	4 groups: Randomly structured porous scaffold (R-270), and aligned channel scaffolds with different channel sizes (A-620, A-270, A-140); numbers indicate channel diameter in μm	Aligned pore scaffolds had better mechanical properties than random pore scaffold. Smaller channel diameter led to greater compressive strength. Aligned pore scaffolds regenerated superior osteochondral tissue compared to random pore scaffold. Diameter of the channel greatly affected tissue regeneration, with 270 μm diameter channels providing the best regeneration, for both subchondral bone and hyaline cartilage. R-270 scaffold produced fibrous tissue that did not differentiate into cartilage. A-620 scaffold had fibrocartilage around the defect edges and fibrous tissue in the centre. A-140 scaffold also formed hyaline cartilage,

(*continued on next page*)

Table 1 (*continued*)

Multilayer scaffolds						
Study	Biomaterial(s) for bone phase (s)	Biomaterial(s) for cartilage phase(s)	Additives (e.g., cells, growth factors)	Animal model, defect size, time point(s)	Experimental groups	Main findings
						but with non-uniform distribution of chondrocytes and lower cell density compared to A-270.
Shalumon et al. (2016) [60]	Microsphere sintered scaffold with PLGA/nHA (15% nHA) microspheres	Microsphere sintered scaffold with PLGA microspheres	Bone marrow MSCs in bone part, chondrocytes in cartilage part	Mouse Subcutaneous 6 mm diameter, 2 mm thickness (scaffold) 4, 8, 12 weeks	2 groups: Acellular scaffold, cell-seeded scaffold	Acellular scaffold collapsed at 12 weeks with no sign of regeneration. Cell-seeded scaffold showed cell proliferation and tissue development, with progressively more positive staining for collagen type II in the cartilage layer, and OCN and mineralisation in the bone layer. Vascularisation found in both cartilage and bone layers. Microspheres were partially/completely degraded by 12 weeks.
Shen et al. (2018) [75]	3D printed wollastonite scaffold containing 8% $MgSiO_3$	Fibrin scaffold	Bone marrow MSCs	Rabbit Knee – patellar groove 4 mm diameter, 4 mm thickness 18 weeks	2 groups: Scaffold with or without cells	Scaffold induced significant regeneration of cartilage and subchondral bone, with or without incorporating cells. Better cartilage repair in the group implanted with cells as the regenerated cartilage was smoother, better integrated with surrounding tissue, and showed tidemark formation, although hyaline cartilage-specific markers were not evaluated. Scaffolds with or without cells did not show much difference in bone formation, or gene expression in both phases.
Shimomura et al. (2017) [51]	HA or β-TCP scaffold	MSC-based scaffold-free tissue-engineered construct (TEC)	Synovial MSCs	Rabbit Knee – femoral groove 5 mm diameter, 6 mm thickness 1, 2, 6 months	2 groups: Scaffold with HA or β-TCP as the bone layer	At 1 months, defects in both groups were uniformly covered by repair tissue. At 2 months, defects were fully covered by repair tissue. At 6 months, repair tissues were continuous with surrounding cartilage and complete defect repair was observed. Both groups had similar macroscopic scores. β-TCP group showed more fibrous cartilage-like repair tissue, while HA group showed hyaline cartilage-like repair tissue with better cell morphology and stronger toluidine blue staining. β-TCP group showed better bone repair, by bone infiltration and cell morphology. The bone layer was fully resorbed at 6 months in the β-TCP group. HA group showed better mechanical

(*continued on next page*)

Table 1 (*continued*)

Multilayer scaffolds						
Study	Biomaterial(s) for bone phase (s)	Biomaterial(s) for cartilage phase(s)	Additives (e.g., cells, growth factors)	Animal model, defect size, time point(s)	Experimental groups	Main findings
						properties and stiffness value reaching 73% of natural osteochondral tissue, which was significantly higher than the β-TCP group.
Sosio et al. (2015) [102]	HA scaffold	Collagen scaffold (equine collagen type I)	Autologous chondrocytes in cartilage layer	Pig Knee – medial and lateral aspects of patellar groove 8 mm diameter, 9 mm thickness 3 months	3 groups: Control (empty), scaffold only, scaffold with cells	Scaffold with or without cells promoted tissue regeneration in the defect, and implants integrated with surrounding tissues. Scaffolds with cells were not more advantageous than scaffolds without cells. Scaffold without cells had higher cartilage repair score. Scaffold with cells showed repair tissue with high cellularity but low GAG production, while scaffold without cells showed repair tissue with low cellularity but higher and uniform GAG distribution. Mechanical properties of both scaffold groups were similar to empty control and significantly lower than native cartilage.
Stuckensen et al. (2018) [130]	Subchondral zone: 50% collagen I, 50% brushite	Chondral zone: 40% collagen I, 60% collagen II, 10% collagenous dry weight of chondroitin sulfate	Human MSCs (hMSCs)	Mouse Subcutaneous 4 mm diameter, 2 mm thickness (scaffold) 6 weeks	4 groups: Control (untreated), scaffold, scaffold + hMSCs, scaffold + hMSCs and maintained in a bioreactor for 3 weeks Osteochondral biopsies were taken from swine joints, and defects created in biopsy tissue to create all groups. Groups were then implanted (biopsy ± scaffold) in mouse subcutaneous model.	Scaffold created by unidirectional freezing to create consecutive pores, which propagate perpendicular to the chondral surface and resemble collagen fibre arrangement in native osteochondral tissue. After 6 weeks subcutaneous implantation, scaffolds induced collagen type 2 expression and aggrecan formation without the need to add growth factors.
Wang et al. (2017) [62]	3D printed PCL/HA scaffold	Cartilage cell sheet (cell sheet group) PGA/PLA (biphasic group)	Bone marrow MSCs in bone layer, auricular chondrocytes as cell sheet (cell sheet group) or seeded in scaffold (biphasic group)	Mouse Subcutaneous 12 weeks	2 groups: Cell sheet, biphasic	Study was focused on generating osteochondral tissue for mandibular condyle repair. Both groups formed mature cartilage-like tissues, with typical lacunae and abundant cartilage-specific ECM. Bone layer was filled with bone tissue in both groups and an interface formed between the cartilage and bone layers. Cell sheet group had higher (but not significant) score for cartilage regeneration, and both groups had similar bone formation. Few PGA fibres remained in the cartilage layer of the biphasic group.

(*continued on next page*)

Table 1 (*continued*)

Multilayer scaffolds						
Study	Biomaterial(s) for bone phase (s)	Biomaterial(s) for cartilage phase(s)	Additives (e.g., cells, growth factors)	Animal model, defect size, time point(s)	Experimental groups	Main findings
Wei et al. (2019) [113]	Porous tantalum	Collagen membrane attached by fibrin glue	Autologous bone marrow MSCs in bone layer, chondrocytes in cartilage layer	Goat Knee – femoral head 10 mm diameter, 12 mm thickness 16 weeks	3 groups: Control (empty), cell-free scaffold, scaffold with cells in each layer	At 16 weeks, almost half of the defects treated with cell-containing scaffolds were repaired. Cartilage layer with cells led to better repair than without cells. In cell-free group, the repair tissue as mainly fibrous tissue, while in the cell-containing group the repair tissue was hyaline-like cartilage with lacunae and stained for collagen type II. Bone layer with cells accelerated new bone formation in the pores of the tantalum scaffold, with trabecular-looking structure.
Xu et al. (2021) [107]	Chitosan/β-TCP	Chitosan	None	Rat Knee – femoral trochlear groove 1.5 mm diameter, 3 mm thickness 6, 12 weeks	3 groups: Control (empty), chitosan scaffold, bilayer scaffold	Bilayer scaffold almost completely repaired the defect at 12 weeks, showing good integration with surrounding tissue. There was new bone tissue and a limited amount of cartilaginous tissue with expression of collagen type II. Chitosan scaffold showed incomplete defect repair and filling with fibrous tissue, and almost no expression of collagen type II.
Yan et al. (2015) [87]	Silk fibroin/nano-calcium phosphate	Silk fibroin	None	Rabbit Knee – one defect between lateral & medial condyle, one in the opposite site of the patella 4.5 mm diameter, 5 mm thickness 4 weeks	2 groups: Control (empty), scaffold	Scaffold compressive modulus was 0.4 MPa in wet state, approaching natural cartilage. No acute inflammation or defect collapse for scaffold-implanted group. Cartilage layer showed new cartilage formation which stained positive for collagen type II and GAG. Bone layer showed new subchondral bone growth which stained positive for an angiogenesis marker, indicating endothelial cell colonisation, and bone infiltration was limited to the bone layer.
Yang et al. (2019) [101]	Sodium alginate, gelatin and hydroxyapatite	Sodium alginate and gelatin	Osteogenic and chondrogenic induced bone marrow MSCs	Rabbits Knee – femoral trochlea 4 mm diameter, 7 mm thickness 3, 6 months	3 groups: Control (empty), cell-free scaffold, cell seeded scaffold (cultured for 3 days before implantation)	3D bioprinted scaffold was produced with chondrogenic and osteogenic MSCs respectively embedded in the cartilage and bone layers. Scaffold integrated with the subchondral bone and formed hyaline cartilage-like tissue, achieving almost complete repair of the injured site after 6 months. Quality of repaired cartilage was similar to surrounding native tissue. Improved mechanical properties after 3 and 6 months

(*continued on next page*)

Table 1 (*continued*)

Multilayer scaffolds						
Study	Biomaterial(s) for bone phase (s)	Biomaterial(s) for cartilage phase(s)	Additives (e.g., cells, growth factors)	Animal model, defect size, time point(s)	Experimental groups	Main findings
						compared to initial scaffold construct, but still significantly lower (~20%) of native articular cartilage.
Yang et al. (2021) [76]	3D printed titanium alloy scaffold	Freeze dried collagen sponge reinforced with PLGA	None	Rabbit Knee – distal femoral trochlea 4 mm diameter, 6 mm thickness 4, 12, 24 weeks	3 groups: Control (empty), monolayer collagen-PLGA scaffold, bilayer scaffold	Bilayer scaffold showed osteochondral tissue regeneration which integrated to the surrounding native tissue, with similar chondrocyte morphology and arrangement. Titanium bone layer provided mechanical support which greatly increased bone formation and was important for cartilage repair. The collagen-PLGA scaffold had completely degraded by 12 weeks.
Zhang et al. (2016) [59]	Poly (l-glutamic acid) (PLGluA) and chitosan polyelectrolyte complex containing PLGluA-grafted HA composite nanoparticles	PLGluA/chitosan hydrogel	BMP-2 in bone layer, adipose-derived stem cell spheroids cultured within cartilage layer in presence of TGF-β1 and IGF-1 for 1 week before implantation	Rabbit @ 6 weeks and 12 weeks Diameter = 4 mm, depth = 6 mm (n = 42)	3 groups: Scaffold with BMP-2 in bone layer and induced cell spheroids in cartilage layer, cell-free scaffold with BMP-2 in bone layer, scaffold only with no cells or growth factor	Scaffold with cells and BMP-2 showed regeneration of both cartilage and subchondral bone. Cartilage repair tissue integrated with native cartilage and showed zonal organisation, with positive staining for collagen type II and GAG. Subchondral region showed mature trabecular bone ingrowth, as well as tidemark formation. Scaffold with BMP-2 showed subchondral bone regeneration but cartilage was not repaired. Chondral region at 6 weeks had a thin and irregular layer of tissue that integrated poorly with underlying tissue, which degraded at 12 weeks and was replaced by fibrous tissue that did not stain for collagen type II and GAG. Bone regeneration was observed with thin trabecular bone. Scaffold only group showed limited cartilage and bone regeneration. Significant fibrous tissue in chondral region and poor bone restoration in the subchondral region.
Zhao et al. (2019) [137]	Hydroxyapatite	Silk fibroin + calcified cartilage layer (CCL)	Adipose derived stem cells (ADSCs)	Rabbit Knee – femoral intercondylar fossa 5 mm diameter, 5.5 mm thickness 4, 8, 12 weeks	4 groups: Untreated, CCL scaffold, non-CCL scaffold + ADSCs, CCL scaffold + ADSCs	Scaffold with CCL between cartilage and bone layers had a dense structure. CCL + ADSCs group showed the best surface roughness and integrity, highest GAG and collagen type II in the regenerated cartilage, and smooth subchondral bone regeneration. Presence of CCL enhanced

(*continued on next page*)

Table 1 (*continued*)

Multilayer scaffolds						
Study	Biomaterial(s) for bone phase (s)	Biomaterial(s) for cartilage phase(s)	Additives (e.g., cells, growth factors)	Animal model, defect size, time point(s)	Experimental groups	Main findings
						osteochondral repair but did not affect bone strength or quality. Incorporation of ADSCs helped with repair.
Zhou et al. (2020) [78]	HA-incorporated fish collagen scaffold with larger pores (~326 μm)	Chondroitin sulfate-incorporated fish collagen scaffold with smaller pores (~128 μm)	None	Rabbit Knee – patellar groove 4 mm diameter, 4 mm thickness 6, 12 weeks	2 groups: Control (empty), scaffold	Promoted simultaneous regeneration of cartilage and bone layers compared to control, confirmed by gross, histological, and μ-CT images. No obvious long-term inflammatory response.
Scaffolds with more than two distinct layers						
Algul et al. (2016) [82]	Bone layer: 30% CA/PEC, 70% β-TCP Intermediate: 60% CA/PEC, 40% β-TCP	Chitosan and alginate polyelectrolyte complex (CA/PEC)	None	Rat Knee – trochlea 2 mm diameter, 2 mm thickness 6 weeks	4 groups: Control (empty), placebo (defect filled with cartilaginous layer), trilayer (trilayer scaffold), reference (MaioRegen® commercial scaffold)	Good tissue biocompatibility and degradation rate, no signs of foreign body reaction, vascularisation observed in the scaffold pores. Scaffold showed better healing compared to commercial product, with significant improvement in osteogenesis at 6 weeks, and significant matrix formation. There was a correlation between scaffold degradation and new tissue formation.
Chen et al. (2018) [52]	Layer C: PCL/PEG electrospun fibre membrane (tidemark) Layer D: Porous alginate hydrogel/nHA/BMP-2 loaded short fibres	Layer A: Oxidised sodium alginate & N-succinyl chitosan (OSA/NSC) hydrogel Layer B: Composite hydrogel of OSA/NSC/micro-HA (calcified cartilage layer)	Layer A: FGF-2, BMP-2, TGF-β1 Layer B: wnt/β-catenin, micro-HA Layer 3: None Layer D: nHA, BMP-2 Low intensity pulsed ultrasound (LIPUS)	Rabbit Knee – trochlear groove 5 mm diameter, 5 mm thickness 12 weeks	4 groups: Control (empty), 3 experimental groups with LIPUS, growth factors, and both growth factors and LIPUS	Inclusion of growth factors and LIPUS stimulation in scaffolds achieved good overall integration between the scaffold and host tissue, and the newly formed subchondral bone and cartilage. Thickness of regenerated cartilage was in line with surrounding native cartilage, and contained cartilage lacunae. Potential vascularisation enhancement. Scaffold degraded after 12 weeks.
Flaherty et al. (2021) [77]	Scaffold 1: HA-collagen (30% collagen & 70% HA in bone layer, 60% collagen & 40% HA in middle layer) Scaffold 2: Ti-collagen (Porous Ti matrix in bone layer, PLA in middle layer)	Scaffold 1: HA-collagen (100% collagen top layer) Scaffold 2: Ti-collagen (Collagen-PLGA top layer)	Bone marrow concentrate	Sheep Knee – medial femoral condyle 8 mm diameter, 10 mm thickness 6 months	4 groups: HA-collagen and Ti-collagen scaffolds with or without bone marrow concentrate	Micro-CT analysis showed that both scaffolds could induce bone regeneration, while cartilage regeneration was not evaluated. Scaffold composition and addition of bone marrow concentrate did not significantly affect bone regeneration in osteochondral defects after 6 months. HA-collagen scaffold degraded after 6 months.
Gao et al. (2018) [71]	Poly (N-acryloyl glycinamide) (PNAGA) N-acryloyl glycinamide-co-N-[tris (hydroxymethyl) methyl] acrylamide (THMMA) copolymer hydrogel = PNT hydrogel Produced by 3D bioprinting in	PNT hydrogel produced by 3D bioprinting with TGF-β1 in top layers	TGF-β1 in cartilage part	Rat Knee – trochlear groove 2.5 mm diameter, 3.3 mm thickness 12 weeks	3 groups: Control (empty), pure hydrogel scaffold, biohybrid hydrogel scaffold	Biohybrid scaffold promotes simultaneous cartilage and bone formation, and better osteochondral repair compared to pure scaffold. At 12 weeks, biohybrid scaffold formed

(*continued on next page*)

Table 1 (*continued*)

Multilayer scaffolds						
Study	Biomaterial(s) for bone phase (s)	Biomaterial(s) for cartilage phase(s)	Additives (e.g., cells, growth factors)	Animal model, defect size, time point(s)	Experimental groups	Main findings
	sequential layers with β-TCP embedded in bottom layers					a uniform and smooth layer of new cartilage with thickness similar to adjacent cartilage, and strong staining for GAG and collagen type II. Good subchondral bone repair was indicated by micro-CT and staining for OCN and collagen type I. The pure scaffold exhibited weaker staining in both layers.
Kang et al. (2018) [129]	Bone layer: biomineralised macroporous PEGDA + N-acryloyl 6-aminocaproic acid (A6ACA) = PEGDA-*co*-A6ACA cryogel	Middle layer: PEGDA-*co*-A6ACA cryogel with columnar pores Cartilage layer: PEGDA hydrogel	hMSCs & bovine chondrocytes in middle layer, hMSC aggregates in cartilage layer	Mouse Subcutaneous 8 mm diameter, 5 mm thickness (scaffold) 4, 8 weeks	2 groups: Positive control (osteochondral tissue), scaffold with cells Scaffold implanted after 1 week *in vitro* chondrogenic induction	Scaffold showed formation of osteochondral tissue with a lubricin-rich cartilage surface. Suggestion that cells within the scaffold underwent continuous differentiation to form cartilage-like tissue, and recruited endogenous cells through the bottom mineralised layer to form bone tissue.
Korpayev et al. (2020) [65]	Bone layer: chitosan, collagen type I, nHA Formed by freeze-drying	Intermediate layer: chitosan, collagen type II, nHA Cartilage layer: chitosan, collagen type II Both formed by thermal gelation	MC3T3-E1 cells in bone layer, ATDC5 cells in intermediate and cartilage layers First cultured in respective layers for 7 days, then co-cultured within integrated layers for 21 days	Mouse Subcutaneous 14 days	1 group: Scaffold	Subcutaneous implantation showed inflammatory response towards the scaffold and infiltration of inflammatory cells. Osteochondral repair was not evaluated.
Levingstone & Ramesh et al. (2016) [57]	Bone layer: collagen type I, HA Intermediate layer: collagen type I, hyaluronic acid Freeze-dried	Cartilage layer: collagen type I, collagen type II, hyaluronic acid Freeze-dried	None	Goat Knee – 2 sites; trochlear ridge, medial femoral condyle 6 mm diameter, 6 mm thickness 3, 6, 12 months	3 groups: Control (empty), multilayer scaffold, commercial bilayer scaffold (Trufit®)	Multilayer scaffold was more effective at inducing osteochondral repair than other two groups at 12 months, with significantly better histological scores. Radiological analysis showed better subchondral bone formation in both defect sites at 3 months, with complete bone regeneration at 12 months. Multilayer scaffold showed tidemark and evidence of neovascularisation at 6 months but fibrocartilage formation, with more hyaline cartilage-like tissue at 12 months. Multilayer scaffold also showed better maturation of cartilaginous tissue over 12 months and better integration with surrounding cartilage compared to other two groups.
Levingstone & Thompson et al. (2016) [56]	Bone layer: collagen type I, HA Intermediate layer: collagen type I and type II, HA	Cartilage layer: collagen type I and type II, hyaluronic acid	None	Rabbit Knee – medial femoral condyle 3 mm diameter, 5 mm thickness 12 weeks	2 groups: Control (empty), scaffold	Scaffold showed better macroscopic appearance of repair tissue compared to the control. Scaffold enabled native cell infiltration and subchondral bone repair,

(*continued on next page*)

Table 1 (*continued*)

Multilayer scaffolds						
Study	Biomaterial(s) for bone phase (s)	Biomaterial(s) for cartilage phase(s)	Additives (e.g., cells, growth factors)	Animal model, defect size, time point(s)	Experimental groups	Main findings
						as well as formation of overlying cartilaginous layer containing GAGs and an intermediate tidemark. Calcification and vascularisation were mostly limited to the bone layer.
Yucekul et al. (2017) [80]	Bone layer: porous PLLA/PCL scaffold coated with collagen type I and β-TCP microparticles Middle layer: PLLA mixed with a colorant (solvent blue) to form tidemark	Cartilage layer: nonwoven PGA felt	Coated with collagen I and β-TCP	Sheep Knee – lateral condyles 8 mm diameter, 10 mm thickness 3, 6 months	3 groups: Control (empty), scaffold, scaffold with hyaluronic acid gel	At 3 months, scaffold groups achieved 50–80% defect coverage with new tissue, and scaffold with hyaluronic acid showed 65–80% reduction of the defect area. At 6 months, repair was seen in both scaffold groups, showing full defect coverage with new tissue that had positive staining for collagen type II and aggrecan. However, the majority of repair tissue was fibrous connective tissue in both groups.
Zhai et al. (2018) [84]	Bone layer: β-TCP scaffold Intermediate layer: high-concentration chitosan/gelatin (2%)	Cartilage layer: low-concentration chitosan/gelatin (0.5%) Scaffold integrated by freeze-drying	Autologous chondrocytes in cartilage layer	Goat Knee – medial femoral condyle 6 mm diameter, 9 mm thickness 3, 6 months	5 groups: Control (empty), mosaicplasty, bilayer scaffold, trilayer scaffold, cell-free scaffold	Cell-free scaffold: No obvious repair, noticeable depressions in the centre. Bilayer scaffold: Cartilage downgrowth into subchondral bone in some samples. Less collagen type II and GAG accumulation compared to trilayer and mosaicplasty groups. Fibrosis seen in central cartilage, with uneven new cancellous bone and no interface between layers. Lower Young's modulus compared to trilayer and mosaicplasty, which was 65% of normal cartilage at 6 months. Trilayer scaffold: No cartilage downgrowth into subchondral bone. Repair tissue achieved good integration with native tissue and showed collagen type II and GAG accumulation matching mosaicplasty. Cartilage repair tissue showed lacunae and clear tidemark formation. Young's modulus reached 90% of normal cartilage at 6 months.
Zhang T et al. (2017) [83]	Bone layer: 3D printed PLGA/β-TCP-collagen scaffold Compact layer: PLGA/TCP	Cartilage layer: cartilage ECM/chitosan	Autologous bone marrow MSCs	Goat Knee – femoral condyle 6 mm diameter, 8 mm thickness 12, 24 weeks	2 groups: Control (empty), scaffold with cells	At 24 weeks, scaffold group showed relatively flat femoral condyle surface but with a small amount of sinking. Defect was filled with cartilage-like tissue although boundaries were seen with surrounding cartilage. Cell morphology was similar

(*continued on next page*)

Table 1 (*continued*)

Multilayer scaffolds						
Study	Biomaterial(s) for bone phase (s)	Biomaterial(s) for cartilage phase(s)	Additives (e.g., cells, growth factors)	Animal model, defect size, time point(s)	Experimental groups	Main findings
						to chondrocytes. Trabecular bone regeneration occurred, although looked slightly different from surrounding normal tissue. Young's modulus of repair tissue in the scaffold group reached 0.35 MPa at 12 weeks and 0.55 MPa at 24 weeks, which was within the range of healthy human articular cartilage.

vascularisation in the scaffold pores [82], as well as display good tissue biocompatibility and degradation rate with no signs of foreign body reaction in most studies. One study compared the use of HA and β-TCP as the bone phase of an osteochondral scaffold [51]. The results showed improved bone infiltration and cell morphology in the β-TCP group at 1 month post-implantation in a rabbit model, but similar repair outcomes between the two groups at 2 months. Interestingly, the HA group showed better mechanical properties with stiffness values reaching 73% of natural osteochondral tissue, which was significantly higher than the β-TCP group.

Bioactive glass is an amorphous mineral which is gaining increasing popularity as a type of bone phase material for osteochondral scaffolds. They contain network modifiers that can trigger a cascade of events to form a bioactive hydroxyapatite-like surface layer, enhancing bone cell adhesion and subsequent new bone formation, as well as repair of surrounding soft tissue [108]. Osteochondral scaffolds containing bioactive glass have shown improved vascularisation and higher compressive modulus after subcutaneous implantation in a mouse model [73], as well as successful reconstruction of bone and hyaline cartilage with hierarchical porosity after 12 weeks implantation in a rabbit osteochondral defect [72]. Additionally, the incorporation of bioactive glass may help to modulate the *in vivo* scaffold biodegradation rate [73].

Other osteochondral scaffold designs have incorporated specific ceramic formulations such as aragonite and wollastonite as minerals for the bone layer. Aragonite is a calcium carbonate material derived from cockle shell [109], while wollastonite is a calcium silicate mineral [110], both of which are bioactive and help promote subchondral bone repair. An aragonite scaffold combined with hyaluronate as the cartilage phase completely regenerated an osteochondral defect in 6 of 7 animals at 12 months after implantation in a goat model, exhibiting formation of hyaline cartilage and subchondral bone with strong integration into adjacent native tissues [74]. A 3D printed wollastonite scaffold achieved subchondral bone repair after 18 weeks in a rabbit model, as shown through μ-CT and histological analyses [75]. Both acellular and cellular scaffolds were found to induce cartilage repair, although scaffolds containing bone marrow-derived MSCs led to cartilage formation with a smoother surface and better integrity than cell-free scaffolds, and clear tidemark formation was only seen in the cellular scaffolds.

Although not a mineral, two studies used titanium alloy as a hard replacement for the bone phase, which were fabricated into porous scaffolds by 3D printing [76,77]. Both studies reported successful integration of the metal scaffold into the surrounding native tissue, when implanted in a rabbit [76] or sheep [77] osteochondral defect for 6 months, where the increased mechanical support provided by the bone phase was thought to be important for encouraging cartilage repair.

2.2. Polymer materials in osteochondral scaffolds

Polymers comprise the majority of materials chosen to construct osteochondral scaffolds, particularly for the cartilage phase since they can be fabricated to mimic native cartilage ECM structure and function. Through various fabrication methods and the addition of other components such as minerals, cells, and growth factors, polymers can be used to create a range of multiphasic scaffold designs and as a matrix for both the cartilage and bone components. Both natural and synthetic polymers have been popular choices for osteochondral scaffolds discussed in this review. Natural polymers are more commonly chosen as the material(s) for the cartilage phase, since they are derived from biological systems and are more likely to be compatible with cells or provide natural cues for cell attachment and growth [111]. When used in the bone phase, natural polymers can serve as a matrix for ceramic particles [57,61,78,87,101], which may result in better subchondral bone regeneration.

Collagen is a ubiquitous component of the ECM in most tissues, including in both articular cartilage and subchondral bone [2], and is a popular material choice for fabricating osteochondral scaffolds [112]. Using collagen in the cartilage phase has been shown to enhance articular cartilage repair with better macroscopic appearance of the regenerated tissue [56]. Multilayered scaffolds with an integrated collagen layer as the cartilage phase were shown to successfully integrate with the surrounding cartilage and help with the formation of hyaline-like cartilage tissue in both rabbit [56] and goat [57] osteochondral defects. A collagen membrane as the cartilage phase joined to a porous tantalum scaffold was shown to improve cell attachment and lead to hyaline cartilage formation, where almost half of the defects in a caprine model were completely repaired after 16 weeks [113]. In a canine model, a collagen type I hydrogel was shown to facilitate cartilage formation with similar thickness to native cartilage and neat arrangement of collagen fibres [114]. Another canine study showed complete integration of their collagen scaffold into the surrounding cartilage with no clear margins, as well as complete scaffold degradation after 24 weeks with concurrent cartilage repair [68].

Alginate is a versatile biomaterial derived from brown algae, which is often used in osteochondral scaffolds as a hydrogel. Alginate is biocompatible and can be processed into a range of morphologies, but its main limitations are lack of mechanical stability and biodegradability once implanted [115], which may be improved through the addition of other polymers to create hybrid materials [52,101]. Using alginate as the base for the cartilage layer of osteochondral scaffolds has demonstrated good *in vivo* tissue biocompatibility, with no inflammatory cells surrounding the implant [48,82]. In a rat model, alginate scaffolds showed good degradation and vascularisation in the scaffold pores [82]. In rabbits and sheep, a hybrid scaffold consisting of alginate and

Table 2
Summary of preclinical studies which tested gradient scaffold designs in animal models to evaluate osteochondral repair.

Gradient scaffolds					
Study	Biomaterial(s) & scaffold design	Additives (e.g., cells, growth factors)	Animal model, defect size, time point(s)	Experimental groups	Main findings
Barron et al. (2016) [131]	PLA/PCL co-polymer (70:30) with functionally graded pore size. Pore size increases from 180 μm diameter at the top to 200 μm × 600 μm at the bottom surface, with open microtunnels through the scaffold structure	Bone marrow MSCs	Rabbit Knee – medial condyle 3 mm diameter, 1 mm thickness 4 weeks	3 groups:Control (empty), cell-free scaffold, cell-seeded scaffold	No inflammation or giant cells. Acellular scaffolds performed better than cell-seeded scaffolds, showing better lateral integration with surrounding tissue and formation of hyaline-like cartilage. Cartilaginous repair tissue for acellular scaffolds stained more strongly for collagen type II than cell-seeded scaffolds.
Du et al. (2017) [66]	Scaffold formed by microsphere sintering, with PCL microspheres at the top and HA/PCL microspheres at the bottom. 0 to 30 wt% HA content of microspheres from top to bottom, at 5% increments over 7 layers.	None	Rabbit Knee 4 mm diameter, 3 mm thickness 6, 12 weeks	3 groups: Control (empty), PCL scaffold, multiphasic scaffold	Multiphasic scaffold achieved the best osteochondral repair. New cartilage tissue showed intense cartilage-specific staining and integration with native cartilage as well as newly formed subchondral bone. PCL scaffold showed limited bone and cartilage repair with poor quality. Multiphasic group showed much stronger staining for collagen type II and aggrecan in the cartilage region, as well as collagen type I and osteocalcin in the bone region. Chondrogenic and osteogenic gene expression verified the staining results.
Duan et al. (2019) [91]	PLGA scaffold with 100–200 μm pore size in the cartilage layer and 300–450 μm pore size in the bone layer	Bone marrow MSCs in cartilage layer	Rabbit Knee – medial condyle 4 mm diameter, 5 mm thickness 12, 24 weeks	3 groups: Control (empty), scaffold with or without cells in cartilage layer	No significant inflammation. At 24 weeks, scaffold with cells showed repair tissue with higher percentage of hyaline-like cartilage and better bone regeneration than scaffold without cells, as well as visible tidemark between cartilage and bone layers. Scaffold with cells had higher Young's modulus (91.2 MPa compared to 28.9 MPa for scaffold without cells) although this was half the value of native cartilage. Scaffolds with or without cells had no significant differences in gene expression of collagen type I and II, between groups or compared to native cartilage.
Han et al. (2015) [132]	Methacrylated gelatin and carboxymethyl chitosan with different degrees of methacrylation, deep layer reinforced with octavinyl-polyhedral oligomeric silsesquioxanes Pore sizes were 115 ± 30, 94 ± 34, and 51 ± 12 μm in the superficial, transitional, and deep layers	TGF-β1	Rabbit Knee – patellar groove 5 mm diameter, 6 mm thickness 2 months	3 groups: Control (empty), scaffold with or without TGF-β1	Scaffold only group formed new cartilage matrix at 2 months which was partly integrated with adjacent native tissue, but the cartilage-like tissue was too thick or too thin compared to native cartilage. Scaffold with TGF-β1 showed new cartilage and bone regeneration in the defect with similar morphology to native tissue. No evaluation of cartilage-specific staining or markers.
Kim et al. (2018) [100]	Low to high concentration of tauroursodeoxycholic acid (TUDCA)-PLGA microspheres from bottom to top, in a glycidyl methacrylate-hyaluronic acid (MAHA) hydrogel	None	Rat Knee – trochlear groove 2 mm diameter, 2 mm thickness 10 weeks	4 groups: Sham, control (empty), scaffold with PLGA microspheres (PBS instead of TUDCA), scaffold with TUDCA-PLGA microspheres	Scaffold regenerated both cartilage and subchondral bone. Low concentration (25 μM0 TUDCA increased osteogenic differentiation and high concentration (2500 μM) increased chondrogenic differentiation. TUDCA-PLGA group showed more complete tissue repair compared to PLGA group, with formation of lacunae and tidemark although it did not provide complete tissue restoration. Collagen type II was increased in the cartilage layer, but aggrecan expression was not significantly different compared to PLGA group. TUDCA-PLGA group showed the best subchondral bone formation with higher bone volume percentage, trabecular number, and trabecular separation although collagen type I and osteocalcin expression were similar to the PLGA group.

(*continued on next page*)

Table 2 (*continued*)

Gradient scaffolds					
Study	Biomaterial(s) & scaffold design	Additives (e.g., cells, growth factors)	Animal model, defect size, time point(s)	Experimental groups	Main findings
Lu et al. (2015) [133]	Oligo (poly (ethylene glyol) fumerate) (OPF) hydrogel with gelatin microparticles (GMPs), containing IGF-1 and BMP-2 in different phases	IGF-1 in chondral layer, BMP-2 in subchondral layer	Rabbit Knee – medial femoral condyle 3 mm diameter, 3 mm thickness 6, 12 weeks	3 groups: IGF-1 only in chondral layer, BMP-2 only in subchondral layer, IGF-1 and BMP-2 respectively in chondral and subchondral layers	Analysis conducted through comparison between micro-CT and histology results for correlation between bone and cartilage repair. Moderate to strong correlation between cartilage regularity and bone formation, where better histological features of new cartilage were associated with better bone parameters measured by micro-CT. Each growth factor had different effects on osteochondral repair. It was thought that BMP-2 promotes bone formation at the early stage, while IGF-1 promotes cartilage protection during later stage.
Mohan et al. (2015) [86]	PLGA scaffold with opposing gradients of chondrogenic (chondroitin sulfate) and osteogenic (β-TCP) PLGA microspheres	TGF-β3, IGF-1	Sheep Knee – medial & lateral femoral condyles 6 mm diameter, 6 mm thickness 1 year	4 groups: Gradient scaffold only, scaffold with TGF-β3, scaffold with IGF-1, microfracture	Scaffold only group showed cells with morphology resembling hyaline cartilage. Cartilage had slight disintegration but near normal integrity compared to native cartilage. TGF-β3 group had similar repair but received highest histological score for structural integrity. IGF-1 group contained a mix of hyaline and fibrous cartilage or only fibrocartilage. Both growth factor groups had normal cellularity and moderate GAG staining. All scaffold groups had no inflammatory reaction in the subchondral bone. Microfracture produced mostly fibrous repair tissue and had scattered fissures with degenerative changes. Cartilage regenerated by scaffold groups had equal or superior mechanical properties.
Pan et al. (2015) [93]	PLGA scaffold with 77/92%, 85/85%, or 92/77% porosity in cartilage/bone phases	Bone marrow MSCs	Rabbit Knee – medial & lateral femoral condyles 4 mm diameter, 5 mm thickness 6, 12 weeks	5 groups: Control (empty), autologous osteochondral plug, 3 types of scaffolds Scaffolds implanted with or without MSCs but results not shown for all analyses	Scaffold with 92/77% porosity in the cartilage/bone layers showed best osteochondral repair compared to other porosity combinations, assessed by histological scores, and gene expression for collagen type II and aggrecan.
Parisi et al. (2020) [134]	Gradient concentration of HA/collagen type I in 4 layers: 0/100, 10/90, 30/70, 50/50 Structure formed by freeze-drying	None	Rat Subcutaneous 15 days	1 group: Scaffold	Scaffold showed no evidence of inflammatory response, and allowed infiltration of highly vascularised fibrous-looking tissue. Some evidence from immunohistochemistry to show collagen type I deposition and expression of some osteogenesis-related proteins such as osteopontin.
Park et al. (2016) [97]	PCL scaffold coated with a collagen type II layer. Two types of scaffold produced, one by 3D plotting system with 100/300 μm pore size and one by salt leaching with <100/100–250 μm pore size in the cartilage/bone phases	None	Rabbit Knee – patellar groove 5 mm diameter, 5 mm thickness 4, 8 weeks	3 groups: Control (empty), PCL scaffold groups produced by 3D plotting or salt leaching	No severe inflammatory response for both scaffolds, 3D plotting scaffold had significantly higher histological scores than salt leaching scaffold at 8 weeks. However, both scaffolds showed relatively poor cartilage staining. 3D plotting: Cell ingrowth into scaffold at 4 weeks and partial defect filling. Enhanced subchondral bone formation at 8 weeks. Salt leaching: Less than half of porous scaffold space was filled with repair tissue at 4 weeks and top area of scaffold remained empty. Empty space decreased with time but top area of scaffold was still empty at 8 weeks, and subchondral bone formation was hardly observed.
Ruvinov et al. (2019) [81]	Alginate hydrogel with TGF-β1 and BMP-4 respectively in cartilage and bone phases	TGF-β1 in cartilage phase, BMP-4 in bone phase	Mini pig Knee – medial femoral condyle 6 mm diameter, 8 mm thickness 6 months	2 groups: Scaffold with or without growth factors	Scaffold with growth factors resulted in significantly higher histological scores than scaffold without. Growth factor scaffold showed formation of a continuous cartilage layer, with chondrocyte morphology, cell density, and proteoglycan deposition similar to

(*continued on next page*)

Table 2 (*continued*)

Gradient scaffolds					
Study	Biomaterial(s) & scaffold design	Additives (e.g., cells, growth factors)	Animal model, defect size, time point(s)	Experimental groups	Main findings
					surrounding healthy cartilage. Cartilaginous ECM stained strongly for collagen type II. Scaffold without growth factors had inhomogeneous staining, with repair tissue lacking normal organisation and defect was filled mainly by fibrocartilage that stained faintly for collagen type II. Micro-CT showed incomplete bone formation in both scaffold groups, although growth factor scaffold achieved a higher degree of bone restoration.
Studle et al. (2018) [98]	PEG hydrogel with human MSCs and TGF-β3 or BMP-2 in bone layer, and human nasal chondrocytes in cartilage layer	Human bone marrow MSCs and TGF-β3 or BMP-2 in bone layer, human nasal chondrocytes in cartilage layer	Mouse Subcutaneous Hydrogel volume of 35 μL for bi-layer scaffold 2, 4, 8, 12 weeks	Experiment 1: 3 groups: MSCs in bottom layer with no TGF-β3, non-immobilised TGF-β3, or immobilised TGF-β3 Experiment 2: 2 groups: MSCs in bottom layer with or without BMP-2	Experiment 1: Whether TGF-β3 was immobilised or not, scaffolds showed significant cartilage tissue formation in both layers which stained for collagen type II and X. Tissue in the cartilage layer showed hypertrophy at 12 weeks, while tissue in the bone layer never developed into mature bone. Immobilisation or not of TGF-β3 did not affect the amount/distribution of cartilage or the efficiency of bone formation. Experiment 2: When TGF-β3 was replaced by non-immobilised BMP-2, scaffold formed a clear bi-layer configuration at 12 weeks. Non-hypertrophic cartilage tissue that stained for collagen type II and GAG but not collagen type X was seen in the cartilage layer, while the bone layer generated ossicles containing bone and marrow suggesting endochondral ossification. BMP-2 allowed the formation of phenotypically stable hyaline-like cartilage and orderly osteochondral tissue.
Zhang Y et al. (2017) [92]	PLGA scaffold with 92% porosity in cartilage and bone layers, cartilage layer has 50–100 μm pore size and 300 μm thickness, bone layer has 300–450 μm pore size and 3.4 mm thickness, joined with an adhesive layer of PLGA film with 300 μm thickness	Autologous PRP	Rabbit Knee – medial femoral condyle 4 mm diameter, 4 mm thickness 4, 12 weeks	3 groups: Control (empty), bilayer scaffold with or without PRP	Scaffold with PRP showed the highest scores for gross appearance and histology, and highest expression of collagen type II and aggrecan in the new tissue. Scaffold without PRP showed more irregular surfaces and fewer lacunae in the repair tissue. Gene expression for collagen type II and aggrecan was significantly higher in the scaffold with PRP, but similar between scaffold groups for collagen type I and X. Micro-CT showed similar amount of mineralised subchondral bone formation in both scaffold groups, which was higher than in the empty control group.

BCP: biphasic calcium phosphate; BMP: bone morphogenetic protein; ECM: extracellular matrix; FGF: fibroblast growth factor; GAG: glycosaminoglycan; GelMA: gelatin methacrylate; HA: hydroxyapatite; hMSC: human mesenchymal stem cell; kartogenin (KGN); nHA: nano-hydroxyapatite; MSC: mesenchymal stem cell; PBS: phosphate buffered saline; PCL: polycaprolactone; PEG: poly(ethylene glycol); PEGDA: poly(ethylene glycol) diacrylate; PGA: poly(glycolic acid); PGS: poly(glycerol sebacate); PLA: poly(lactic acid); PLGA: poly(lactic-co-glycolic acid); PLLA: poly(L-lactic acid); PRP: platelet rich plasma; PVA: poly(vinyl alcohol); TCP: tricalcium phosphate; TGF: transforming growth factor.

hyaluronic acid in the chondral layer showed evidence of repair and integration with host cartilage [48].

Chitosan is derived from chitin found in the shells of crustaceans, offering the advantages of biocompatibility, biodegradability, and low toxicity together with having structural similarities to glycosaminoglycans (GAGs) found in cartilage ECM [116]. It is possible to fabricate chitosan-based scaffolds with mechanical properties approaching the range of native articular cartilage in strength and modulus [117,118]. A chitosan-based cartilage layer pressed onto a compact bone layer to form an osteochondral scaffold reached compressive modulus of 0.8 MPa, which helped promote hyaline cartilage formation after 24 weeks in a goat model [83]. A bi-layer scaffold comprising chitosan in the cartilage layer and chitosan/β-TCP composite in the bone layer led to almost complete defect repair in a rat model after 12 weeks, with evidence of hyaline cartilage formation and integration of the newly formed tissue with surrounding cartilage [107].

Silk fibroin is a protein derived from silkworm cocoons, and has been used in osteochondral scaffolds for both cartilage and bone regeneration due to its higher mechanical properties compared to most other natural polymers [46]. Silk fibroin-based multilayer scaffolds have been shown

Table 3
A summary of animal models used for testing osteochondral scaffolds.

Animal model	Advantages	Disadvantages	Typical intervention time	Representative studies
Mouse/ Rat	• Lower maintenance cost •Readily available •Short study time	• Do not well replicate human osteochondral anatomy • Mainly for proof-of-concept studies	2–12 weeks	[67,71,82,95,100,136]
Rabbit	• Easy to source •Less maintenance compared to large animals •Has similar bone mineral density to humans	• Mainly for proof-of-concept studies • Cartilage thickness is too thin compared to human cartilage	4–24 weeks	[47–49,51–56,59,61,64,66,72,75,76,78,79,85,87,89–93,97,99,101,124–127,131–133,137]
Dog	• Susceptible to cartilage diseases and have limited cartilage regeneration capabilities	• Social and ethical considerations in their use as animal models	12–24 weeks	[68,114]
Sheep/ Goat	• Joint loading conditions are comparable to humans •Can adopt clinically used surgical techniques •Proportion of cartilage to subchondral bone is similar to humans •Progression of osteochondral repair is similar to humans	• Prolonged study time • High cost for maintenance • Cartilage layer is thinner compared to humans, causing defect being mostly in the subchondral bone area	3–6 months	[48,57,74,77,80,83,84,86,88,94,113]
Pig/ Minipig	• Like humans, has limited capability for osteochondral repair • Structural and weight-bearing properties of the joint similar to humans	• Prolonged study time • High cost for maintenance • Has different knee range of motion compared to humans	3 months to 1 year	[63,70,81,102]
Horse	• Higher accessibility of the joint • Similar biochemical composition and cartilage thickness compared to humans • Similar bone density compared to humans • Naturally suffer from osteochondral diseases and other joint injuries	• High costs • Source of animal model is limited • Animal undergoes immediate load-bearing post-surgery	6 months	[96,123]

to promote cell adhesion and proliferation, as well as tissue infiltration and osteochondral repair *in vivo* [47,61]. Moreover, silk scaffolds can be made with compressive modulus reaching 0.4 MPa [87], approaching the range of human articular cartilage. Satisfactory osteochondral regeneration in rabbits was observed in all studies, although one reported signs of a foreign body reaction [87].

Gelatin is another natural polymer that has been used quite frequently in osteochondral scaffolds, but either in combination with other natural polymers or in the form of gelatin methacrylate (GelMA). One example is a 3D bioprinted gelatin and alginate scaffold, which integrated well into the subchondral bone and formed hyaline cartilage similar to surrounding native tissue, achieving almost complete defect repair together with improvement in mechanical properties over 6 months in a rabbit model [101]. A gelatin and chitosan scaffold as the cartilage layer integrated to a bone layer of β-TCP seeded with MSCs demonstrated satisfactory scaffold integration with surrounding tissues at 1 month after implantation in goats, as well as better cartilage formation and increased collagen II content at 6 months compared to cell-free scaffolds and empty defects, matching the repair outcomes of gold-standard mosaicplasty [84]. Mechanical testing at 6 months also indicated Young's modulus values reaching 90% of normal tissue, which was the same outcome as mosaicplasty. A 3D printed GelMA scaffold with nano-HA doped in the bone/intermediate layers was found to form new repair tissue in all scaffold layers, with a faster repair rate in the cartilage region and higher collagen type II formation compared to monophasic scaffolds [53].

It is worth mentioning that when natural polymers are used in the bone phase of an osteochondral scaffold, they usually provide a matrix that is reinforced using ceramic particles such as HA. Natural polymers can be used to improve HA mineralisation [119] and create composite hydrogel or scaffold structures resembling the structure and composition of natural bone, which may assist in scaffold integration with the surrounding tissue after implantation. For example, one study used a combination of silk fibroin and chitosan in the cartilage phase, and the same polymers together with nano-HA in the bone phase [61]. Both chondral and subchondral layers achieved satisfactory repair in a rabbit model after 12 weeks, and better overall repair was noted for the bilayer scaffold compared to the individual layers implanted as separate scaffolds. The repair tissue in the bilayer scaffold had no holes in the centre, while visible vacancies were observed in the cartilage/bone monolayer scaffolds at 12 weeks. Moreover, the bilayer scaffold induced expression of both collagen types I and II as seen through immunofluorescence staining, while monolayer scaffolds only showed strong expression of either collagen type I (bone layer scaffold) or collagen type II (cartilage layer scaffold).

Synthetic polymers are fabricated by the polymerisation of synthetic monomer chains. Unlike natural polymers, they are less favourable for cell adhesion and are generally not bioactive. Nevertheless, synthetic polymers demonstrate better and more tailorable mechanical properties to replicate native tissue biomechanics, due to the ability to easily adjust monomer arrangements during fabrication [120], which is important considering the weight-bearing function of osteochondral tissue. Synthetic polymers also benefit from more controlled and consistent properties compared to natural polymers, which may have larger batch-to-batch variations due to their biological origin. Studies on osteochondral scaffolds have used synthetic polymers for both cartilage and bone layers, frequently with the addition of growth factors or cells to overcome their inertness and improve regeneration outcomes [91,98]. For the bone phase, synthetic polymers can be reinforced with ceramic particles to improve subchondral bone regeneration [59,69], which also indirectly helps cartilage regeneration due to enhanced scaffold mechanical strength and integration between layers.

PLGA, a copolymer of lactic acid and glycolic acid, is the most commonly chosen synthetic polymer to construct osteochondral scaffolds, due to its biocompatibility and highly tailorable properties including mechanical characteristics and biodegradability [121]. PLGA scaffolds can be constructed with varying pore geometry in the cartilage and bone layers to form bilayer osteochondral scaffolds, which have shown good repair in rabbit models [91,93]. When the cartilage layer was added with MSCs, the compressive modulus of PLGA scaffolds

Table 4
Summary of clinical studies which evaluated osteochondral repair using commercially available scaffolds.

Study	Scaffold type, implantation	Injury type & defect size	Patients, follow-up duration	Main findings
Berruto et al. (2016) [139]	MaioRegen®	Spontaneous osteonecrosis of the knee (SPONK) Mean 3.47 ± 1.75 cm^2 (range 1.5–7.5)	11 patients <65 years selected Mean age 52.1 ± 9.6 years (range 35–64) Time: 1, 2 years	At 2 years, subjective IKDC (40 ± 15.0 to 65.7 ± 14.8) and Lysholm Knee Scale (49.7 ± 17.9 to 86.6 ± 12.7) scores improved significantly from pre-operation, while VAS scores decreased (6.3 ± 2.5 to 1.6 ± 2.7). No significant differences in Tegner Activity Scale score compared to pre-operation. 9 of 11 patients had successful clinical outcome, but 2 were symptomatic at 18 months post-implantation and progressed to condylar collapse, and subsequently underwent total knee arthroplasty.
Brix et al. (2016) [140]	MaioRegen®	Single osteochondral lesion on femoral condyle, with lesion size ≥1.5 $ccmm^{22}$ aatt the surface/maximal depth of 1.5 cm Mean 2.07 cm^2 (range 1.5–3.75)	8 patients 15–55 years selected Mean age 37 years (range 15–51) Time: 6, 12, 18, 24 months	Assessed by IDKC, Tegner-Lysholm and Cincinnati scores. All three clinical outcome scores consistently improved over time without reaching statistical significance. At 18 months, 7 of 8 patients showed complete scaffold integration into the border zone, and 5 of 8 patients showed excellent or good subchondral ossification. All 8 patients had repair tissue with intact surface, but repair tissue had inhomogeneous structure in 7 of 8 patients. T2 mapping data indicated limited quality of repair cartilage.
Christensen et al. (2016) [141]	MaioRegen®	Osteochondral lesion, with lesion size <6 cm^2 6 knee lesions, 4 talus lesions Mean 3.0 ± 1.9 cm^2	10 patients 18–50 years selected Mean age 27 ± 7 years Time: 1, 2.5 years	Knee patients were evaluated using KOOS, IKDC and Tegner scores, ankle patients with AOFAS Hindfoot and Tegner scores. 2 patients were excluded from follow-up due to treatment failure and re-operation. At 2.5 years, 6 of 8 patients had no or very limited (<10%) bone formation, and 2 had 50–75% bone formation. IKDC score improved from 71.3 to 80.7, and KOOS pain subscale improved from 63.8 to 90.8. No improvements were found in the remaining KOOS subscales or other outcome scores. No improvements were seen in the talus patients. Study advised to "use the MaioRegen® scaffold with caution".
Condello et al. (2018) [142]	MaioRegen®	Cartilage lesions in early knee osteoarthritis of III or IV degree by ICRS 19 microtraumatic or degenerative, 7 post-traumatic (not acute) Size of defect/scaffold unspecified	26 patients Mean age 43.8 ± 11.2 years, mean symptoms duration 20.0 ± 14.9 months Time: mean 35 months	VAS, Lysholm, IKDC subjective score, and KOOS subscales showed significant improvement in in 69% of patients, while 31% of patients did not reach significant improvement and were considered as clinical failure. Previous surgical procedures found to be significantly correlated with worse outcome in KOOS pain, KOOS sport, KOOS quality of life, and IKDC. Complication rate was 11%, with no surgical failure but 1 case of scaffold resorption and 2 cases of joint stiffness. MOCART showed complete cartilage filling in 63.2% of lesions and complete graft integration in 47.4%, while subchondral bone appearance was considered normal in 42.1%.
Gabusi et al. (2018) [143]	MaioRegen®	Knee osteochondritis dissecans focal lesions 1.5–4 cm^2	14 patients Mean age 23.6 ± 8.6 years Time: 3 months, 1 year	Evaluated serum biomarkers of cartilage (fragments or propeptide of type II collagen: CTXII, C2C, CPII) and bone (TRAP5b, OC) turnover. Cartilage (CPII) and bone (OC) synthetic biomarkers were significantly increased at 1 year, while degradative markers (CTXII, C2C, TRAP5b) were not modulated. Higher remodelling of cartilage compared to bone tissue. IKDC score increased significantly at 1 year while Tegner score did not. Considering IKDC score >70 as clinical success, all cases with both CPII >300 pg/mL and C2C/CPII <0.35 presented clinical success.
Kon et al. (2018) [144]	MaioRegen®	Knee chondral and osteochondral lesions Mean 3.4 ± 1.5 cm^2	100 patients Mean age 34.0 ± 10.9 years Time: 6, 12, 24 months	Scaffold was compared to bone marrow stimulation. Primary measurement was IKDC subjective score at 2 years, secondary were KOOS, IKDC Knee Examination form, Tegner, and VAS pain scores. Significant improvement in all clinical scores at 2 years compared to baseline, but no significant differences between the two treatment groups.

(*continued on next page*)

Table 4 (*continued*)

Study	Scaffold type, implantation	Injury type & defect size	Patients, follow-up duration	Main findings
				Subgroups with deep osteochondral lesions and sport active patients showed significantly better IKDC subjective outcome in scaffold treatment group. Severe treatment-related adverse events in 3 patients in scaffold group and 1 in bone marrow stimulation group. MOCART score showed no significant differences between two treatment groups.
Perdisa et al. (2018) [145]	MaioRegen®	Knee osteochondritis dissecans with ICRS grade III to IV lesions Mean 3.4 ± 2.2 cm^2 (range 1.5–12)	27 patients Mean age 25.5 ± 7.7 years (range 14–42) Time: 12, 24, 36, 48, 60 months	All patients showed significant improvement in clinical scores. IKDC subjective score significantly improved from 48.4 ± 17.8 to 82.2 ± 12.2 at 2 years and then remained stable for up to 5 years post-operation. Tegner score increased from 2.4 ± 1.7 to 4.4 ± 1.6 at 2 years and reached 5.0 ± 1.7 at 5 years (almost pre-injury level). MOCART score was stable between 24 and 60 months. Subchondral bone regeneration showed significant improvement in total score between 2 and 5 years, although abnormalities persisted until the last follow-up.
Sessa et al. (2019) [146]	MaioRegen®	Knee articular defects in the femoral condyles or trochlea, ICRS grade III or IV, meeting early OA criteria Mean 3.2 ± 1.9 cm^2	22 patients (5 with multiple lesions, total 27 defects) Mean age 39.0 ± 8.2 years Time: 24, 60 months	All scores improved at 2 year follow-up and remained stable at final follow-up. IKDC subjective score improved from 42.8 ± 13.8 to 74.9 ± 20.4 at 2 years and remained stable for up to 5 years. IKDC objective score significantly increased, with 12 knees considered 'normal' or 'nearly normal' at baseline, 19 at 2 years and 20 at 5 years. Tegner score improved significantly from 3.3 ± 2.7 to 4.7 ± 2.1 at 2 years and remained stable at 5 years. However, activity level never reached pre-injury level. Complication rate was 8.3% with 2 patients undergoing re-operation. Comprehensive definition of failure (surgical and clinical criteria) identified 16.6% failed patients.
Sessa et al. (2021) [147]	MaioRegen®	Juvenile knee osteochondritis dissecans with ICRS grade III or IV Mean 3.2 ± 1.8 cm^2	20 patients ≤18 years selected Mean age 16.2 ± 1.4 years, mean symptoms duration 20.2 ± 17.9 months Time: 1, 2 and mean final follow-up at 6 years (5–7 years)	All scores showed significant improvement. IKDC subjective score improve from 50.3 ± 17.4 to 75.3 ± 14.6 at 1 year, 80.8 ± 14.6 at 2 years, and 85.0 ± 9.3 at 6 years. Tegner score improved from 2.6 ± 1.4 to 5.5 ± 2.0 at 6 years, although not to the level prior to symptom onset. Longer symptoms duration negatively influenced IKDC subjective and Tegner scores up to 2 years but did not affect final outcome. MOCART 2.0 score showed significant improvement between 1 year and final follow-up, although there were persistent MRI abnormalities at the subchondral bone level. No surgical failures, but 4 patients presented post-operative complications, with 2 cases of joint stiffness, 1 with persistent swelling, and 1 trauma. All were treated and the complication was resolved.
Verdonk et al. (2015) [148]	MaioRegen®	Knee osteochondral defects involving the femoral condyles, patella or trochlea All included defects were ICRS grade IV Mean 3.7 cm^2 (range 1–10)	38 patients 12–65 years selected Mean age 30.5 ± 11.9 years (range 15–64), mean symptoms duration 17.2 ± 22.3 months Time: 3, 6, 12, 18, 24 months	Significant improvement in all KOOS subdomains and VAS scores (at each interval) and Tegner scores (at 3 and 24 months). Significant improvement in MOCART scores during 24 months post-operation. Scaffold treatment failed in 2 (5.3%) patients, and 2 patients had persistent pain who underwent knee arthroplasty respectively at 14 and 20 months. MRI showed hypertrophic defect filling in 15 of 36 knees (41.7%) at 24 months, as well as bone marrow changes (oedema or cysts) in 33 patients (91.7%). Intralesional osteophytes were seen in 2 patients.
Dell'Osso et al. (2016) [151]	Trufit®	One or more focal osteochondral lesions of the femoral condyles Size of scaffold was 7 mm in 5 cases, 9 mm in 26 cases and 11 mm in 12 cases	30 patients reviewed, 19 received one implant and 12 received multiple implants (total 43 implants) Mean age 60.57 years (range 32–79) Time: 6, 12, 24, 48 months	One of the 31 cases was switched to knee arthroplasty. Of the other 30 cases, Lysholm Knee Scoring Scale improved from average of 50.40–76.2 at 6 months and 87.1 at 48 months. MRI showed progressive partial scaffold integration but poor integration at the scaffold centre. Integration was almost complete at longer follow-up. Integration failure was noted in one case. Lack of complete resorption at 4 years. Study suggested that longer follow-up was necessary.

(*continued on next page*)

Table 4 (*continued*)

Study	Scaffold type, implantation	Injury type & defect size	Patients, follow-up duration	Main findings
Dhollander et al. (2015) [150]	Trufit®	One focal cartilage defect involving the femoral condyle, patella, or trochlea Defects <2 cm^2 chosen Mean 0.83 cm^2 (range 0.38–1.58) 7 traumatic, 9 focal non-traumatic (focal degenerative), 4 osteochondritis dissecans	20 patients Mean age 31.65 years (range 17–53), mean symptoms duration 26.3 months (range 2–122) Time: 6, 12, 18, 24, 36, 48 months (mean 34.15 months)	Patients showed significant gradual clinical improvement but this was not confirmed by the MRI findings. VAS pain and mean total KOOS scores improved significantly at 12, 18, 24 and 36 months. Tegner activity scale score showed no significant improvement. 6 of 20 patients (30%) showed persistent or increased symptoms after scaffold implantation which did not improve over time, in whom the scaffold was subsequently removed and replaced with autologous bone graft. Another 6 patients underwent revision surgery at 9–20 months after surgery. MOCART scores significantly decreased over time, indicating significant deterioration of the repair tissue over 24 months. Complete defect filling was found in 4 cases (30.8%) and synovitis in 3 patients (23%) at 24 months. Bone marrow and subchondral lamina changes were observed in all patients. There was no evidence that the scaffold could support osteoconductive bone ingrowth.
Di Cave et al. (2017) [149]	Trufit®	One focal osteochondral lesion of the talus (OLT) Defects <15 mm diameter chosen	12 patients Mean age 38.6 years (range 22–57) Time: mean 7.5 years (range 6.5–8.7)	Mean AOFAS score improved from 47.2 ± 10.7 to 84.4 ± 8 at the last follow-up. According to post-operative AOFAS scores, 1 case obtained excellent results, 9 were good, and 2 were fair. VAS score improved from 6.9 ± 1.4 to 1.2 ± 1.1 at the last follow-up. 9 patients (75%) declared they were very satisfied, 3 patients (25%) were satisfied with reserve, and all patients would have the procedure again. MRI showed complete defect filling in 50% of cases, and complete graft integration in 71.7%. Subchondral lamina was restored in 75% of cases and intact subchondral bone was observed in 58.3%.
Krych et al. (2016) [152]	Trufit®	Focal cartilage lesions of the femur on the medial or lateral condyle, or trochlea Defects 1.5–6 cm^2 chosen Chondral lesion area averaged 320–390 mm^2 across groups, patients in each group were treated with 1–4 scaffolds	46 patients Control scaffold: 11 patients, mean age 38.4 (range 20–51) Scaffold + PRP: 23 patients, mean age 39.0 (range 19–54) Scaffold + BMAC: 12 patients, mean age 36.1 (18–49) Time: 12 months	Aim: compare the early MRI appearance, including T2 values between cartilage defects treated with scaffold vs scaffold with platelet rich plasma or bone marrow aspirate concentration Scaffold with PRP and BMAC both showed superior cartilage fill compared to the control group. T2 mapping showed that PRP group had mean T2 value (49.1 ms) similar to the control scaffold group (42.7 ms), but BMAC group showed mean T2 value (60.5 ms) closer to superficial hyaline cartilage. Scaffold integration in the bone phase evaluated by MRI did not differ significantly between groups, and patients showed similar amounts of mild subchondral oedema.
Shivji et al. (2020) [153]	Trufit®	Full-thickness chondral lesions of the knee Defect sizes unspecified; defects were mostly located in the medial femoral condyle with some in the lateral femoral condyle, trochlea, and patella	11 patients Time: mean 121 months for outcome scores (SD 12 months), mean 70 months for radiology (range 77–113)	All outcome scores (OKS, Lysholm, Tegner) improved at 1-year and latest follow-ups although there were no statistically significant improvements in any score at both time points. Radiology showed that all patients had incomplete or no evidence of scaffold incorporation, persistent chondral loss, and residual oedema or cystic changes in the latter years.
Wang et al. (2021) [154]	Trufit®	Single cartilage lesion of medial or lateral femoral condyle, or trochlea classified as Outerbridge grade III or IV Defects 1–6 cm^2 chosen Mean 3.0 ± 1.7 cm^2 in scaffold group, 2.2 ± 1.8 cm^2 in microfracture group Patients were treated with average 2.5 plugs per case	Scaffold: 66 patients, mean age 42.9 ± 12.8 years Microfracture: 66 patients, mean age 40.7 ± 11.5 years Time: 1, 2, 3, 4, 5 years	Both groups showed clinically significant improvements in knee clinical scores over 5 years. Mean SF-36 physical component summary (PCS) scores significantly improved in the scaffold group from baseline to all post-operative time points, but remained similar in the microfracture group at all post-operative time points compared to baseline. No significant differences in KOS-ADL and IKDC scores between groups for up to 5 years. Marx activity level scores in microfracture group declined over time, while scaffold group showed significant improvements over 5 years. MRI showed better tissue repair in the scaffold group. Microfracture group had significantly more bony overgrowth of cartilage repair tissue, and scaffold group showed native cartilage isointensity in the majority of cases compared to 50% in the microfracture group. Scaffold group

(*continued on next page*)

Table 4 (*continued*)

Study	Scaffold type, implantation	Injury type & defect size	Patients, follow-up duration	Main findings
				had flush cartilage surface while microfracture group had recessed cartilage surfaces in ~60% of cases. All scaffold cases at >4 years had complete cartilage fill, while microfracture cases had <33% cartilage fill at the same follow-up. In scaffold group, there was 1 failure due to persistent pain and progressive osteoarthritic change treated with knee replacement, and 2 peri-operative complications treated with reoperation. Increasing age, high body mass index, prior microfracture, and traumatic aetiology were predictors for inferior outcomes in the scaffold group.
Kon et al. (2016) [155]	Agili-C™	Focal chondral-osteochondral knee lesions of the condyle and trochlea with ICRS grade III-IV Mean 2.5 ± 1.7 cm^2	21 patients (tapered implants in this study), compared to 76 control patients (previous data with cylindrical implants) <50 years selected Mean age 31.0 ± 8.6 years Time: 6, 12 months	Tapered implants (this study) were compared to data previously obtained with cylindrical implants. Tapered implant showed significant improvements in all clinical scores, at both 6 and 12 months for IKDC subjective score and Lysholm score. Increase was also seen for all KOOS subscales. MRI in 19 of 21 patients showed 84% with >75% defect fill, 84% with complete cartilage interface, and 89% with intact subchondral bone. There was no difference between the level of improvement obtained with the two implant types in clinical or imaging evaluations. The tapered group produced a significantly lower revision rate (0%) compared to the cylindrical group (8 cases or 10.5% failure).
Kon et al. (2021) [156]	Agili-C™	Mild to moderate knee osteoarthritis according to radiographs (Kellgren-Lawrence grade 2 or 3) and up to 3 treatable joint surface lesions (chondral/osteochondral) Defects 1–7 cm^2 chosen Mean 3.0 ± 1.7 cm^2	86 patients Mean age 37.4 ± 10.0 years Time: 6, 12, 18, 24 months	Significant improvement on all KOOS subscales and IKDC subjective score from baseline to 24 months. MRI showed significant increase in defect filling to 78.7% ± 25.3% surface coverage at 24 months. Treatment failure requiring revision surgery occurred in 8 patients (9.3%).
Kanatli et al. (2017) [157]	Chondrotissue®	Talar osteochondral lesions Defects ≥1.5 cm^2 chosen Mean 2.5 ± 0.8 cm^2 defect size, 2.4 ± 1.9 cm^3 defect volume	32 patients Mean age 38 ± 12 years (range 30–70) Time: 33.8 ± 14.0 months	Significant improvement in AOFAS score from 52.8 ± 13.9 to 87.1 ± 11.1 at mean follow-up time. 84.4% of patients had good to excellent clinical scores. Mean MOCART score was 64.2 ± 12.0. Clinical scores had not significant correlation with age, lesion size, depth, or body mass index. No significant correlation between total MOCART and AOFAS scores. Significant correlation between defect filling (subgroup of MOCART score) and clinical outcomes. Some limitations were identified including lack of longer-term follow-up, as well as the patient population being mixed with accompanying treatments such as ligament reconstruction or bone grafting.

AOFAS: American Orthopedic Foot and Ankle Society; BMAC: bone marrow aspirate concentrate; ICRS: International Cartilage Repair Society; IKDC: International Knee Documentation Committee; KOOS: Knee Injury and Osteoarthritis Outcome Score; KOS-ADL: Activities of Daily Living of the Knee Outcome Survey; MRI: magnetic resonance imaging; MOCART: Magnetic Resonance Observation of Cartilage Repair Tissue; OA: osteoarthritis; OC: osteocalcin; OKS: Oxford Knee Score; PRP: platelet rich plasma; TRAP: tartrate-resistant acid phosphatase; VAS: Visual Analog Scale.

reached half of that of normal cartilage at 24 weeks after implantation [91]. Other types of design variations include incorporating ceramic particles into a PLGA matrix [49,88,92], integrating PLGA with an underlying titanium scaffold [76,77], and PLGA microspheres for biomolecule delivery [47,60,86].

PCL is a polyester frequently employed for tissue engineering due to its affordability and ease of modification [122]. PCL can be used to produce highly porous bilayer scaffolds that permit greater vascularisation in the bone layer compared to the cartilage layer, mimicking the native structure of osteochondral tissue [50]. PCL scaffolds have shown satisfactory repair in murine osteochondral models [50,70], with evidence of inflammatory modulation [95]. Interestingly, a study in minipigs noted greater bone regeneration with limited cartilage repair [70]. Some studies have also noted poor degradability [50]. The internal geometry and composition of PCL-based scaffolds can be modulated using a variety of additive manufacturing techniques to create multiphasic scaffolds for osteochondral repair [64,66,79,94,96].

Other types of synthetic polymers used more sparingly for osteochondral scaffolds included PEG, which was often combined with other polymers such as PCL [52,63,99], or a bioactive ceramic scaffold base [72]. Otherwise, PEG could be incorporated with cells and growth factors to form different phases, which respectively modulate cartilage and bone formation [98]. A scaffold involving poly(vinyl alcohol) (PVA) in the cartilage layer and polyamide-6 in the bone layer has demonstrated chondrogenesis and osteogenesis in the respective layers, as well as integration with native cartilage and bone, although the scaffold alone achieved limited bone formation compared to scaffolds containing MSCs [54]. In a study involving an equine model, the osteochondral scaffold

was composed of polyetherketoneketone (PEKK) for the bone layer and a polyurethane elastomer for the cartilage layer [123]. The scaffold was well tolerated at 12 weeks and defects were mostly filled with stiff and smooth repair tissue, although the new tissue did not resemble the composition of hyaline cartilage.

3. Multiphasic scaffold design

Designs for osteochondral scaffolds that involve more than one phase or biomaterial for supporting cartilage and bone regeneration can be broadly classified into 1) multilayer scaffolds, which have distinct but integrated layers that may differ in material composition and scaffold geometry (Fig. 1), and 2) gradient scaffolds which are generally composed of homogeneous material(s) but separated into continuous layers by different sized pores or additional components such as mineral particles, growth factors, or cells (Fig. 2).

3.1. Multilayer osteochondral scaffolds

Multilayer scaffolds were by far the most popular design for osteochondral repair, with most studies adopting a bilayer structure for cartilage and bone, while some used a tri- or even four-layer structure that also included intermediate layer(s) for calcified cartilage (Fig. 3). A wide variety of fabrication methods were used to create multilayer scaffold structures, many of which were tailored to the specific combination of materials used in the scaffold, since natural and synthetic polymers, and ceramic materials require different sets of processing techniques. A popular strategy used to create bilayer osteochondral scaffolds was to fabricate the cartilage and bone layers through relatively separate processes, and then integrate them together through various techniques such as gluing or creating an interfacial binding layer [49,54,63,67,83,124–126]. This strategy allows relatively easy creation of biphasic scaffolds with a wider range of material choices and morphologies for the cartilage and bone components, which may help to better satisfy the regeneration requirements of different tissues. However, the two phases are relatively separate and not connected through an intermediate phase. Depending on the strength of the interfacial bonding, delamination of layers may be an issue following *in vivo* implantation. This problem may similarly affect scaffold designs comprising a separately fabricated ceramic scaffold [51,72,74,75,102,127] or 3D printed scaffold [62,64,88,94,96,128] as the bone phase, with a different construct usually containing some biological components such as growth factors or cells for the cartilage phase. These designs focus on regenerating the subchondral bone, based on the idea that cartilage restoration will follow from successful bone repair. Other strategies featuring a more limited set of material choices but better ability to create indistinct, integrated phases for bilayer scaffolds include solvent casting and particular leaching [50,87], sequential freeze drying [61,78,107], and 3D printing [53,70] or bioprinting [79,101] to deposit connected layers. More adventurous studies have created tri-layer [56,57,65,129,130] or four-layer [52] osteochondral scaffolds, each involving customised and multi-step fabrication processes that were tailored for the types of materials used.

Studies testing bilayer scaffolds have generally shown that their design can induce osteochondral repair in various animal models and restore the defect to a normal state. For instance, a biphasic scaffold incorporating natural and synthetic polymers as well as ceramic particles and growth factors in different phases led to successful regeneration of hyaline cartilage and subchondral bone in a minipig model after 1 year, compared to the empty defect control which regenerated non-continuous cartilage and overgrowth into the subchondral area [63]. Another study showed that a biphasic design comprising hydrogels with different composition in the two layers was better at simultaneously repairing cartilage and bone, producing more hyaline cartilage-like tissue that stained for collagen type II and overall showing better integration with the native tissue, compared to a monophasic hydrogel that only formed a thin fibrocartilage layer [85]. A biphasic scaffold comprising a 3D printed PCL network for the bone phase and alginate

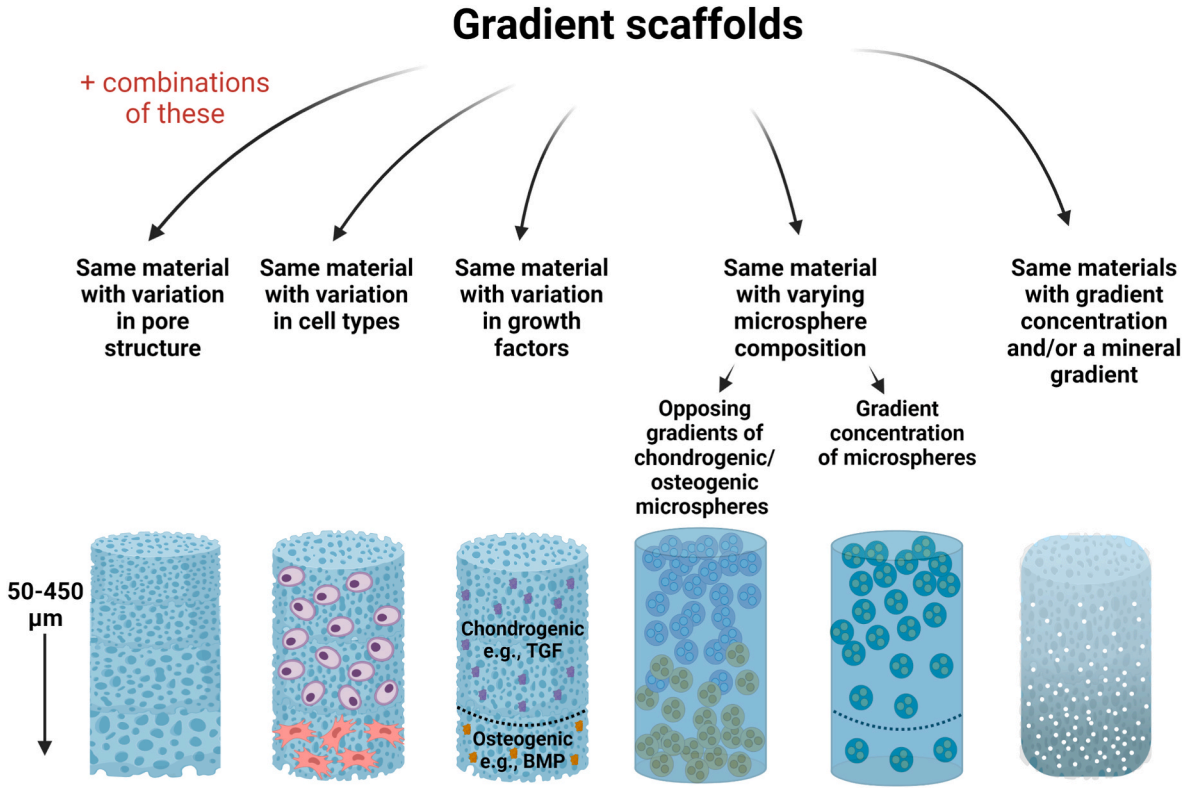

Fig. 2. Different design strategies for gradient osteochondral scaffolds. TGF: transforming growth factor, BMP: bone morphogenetic protein. Figure generated in BioRender (BioRender.com).

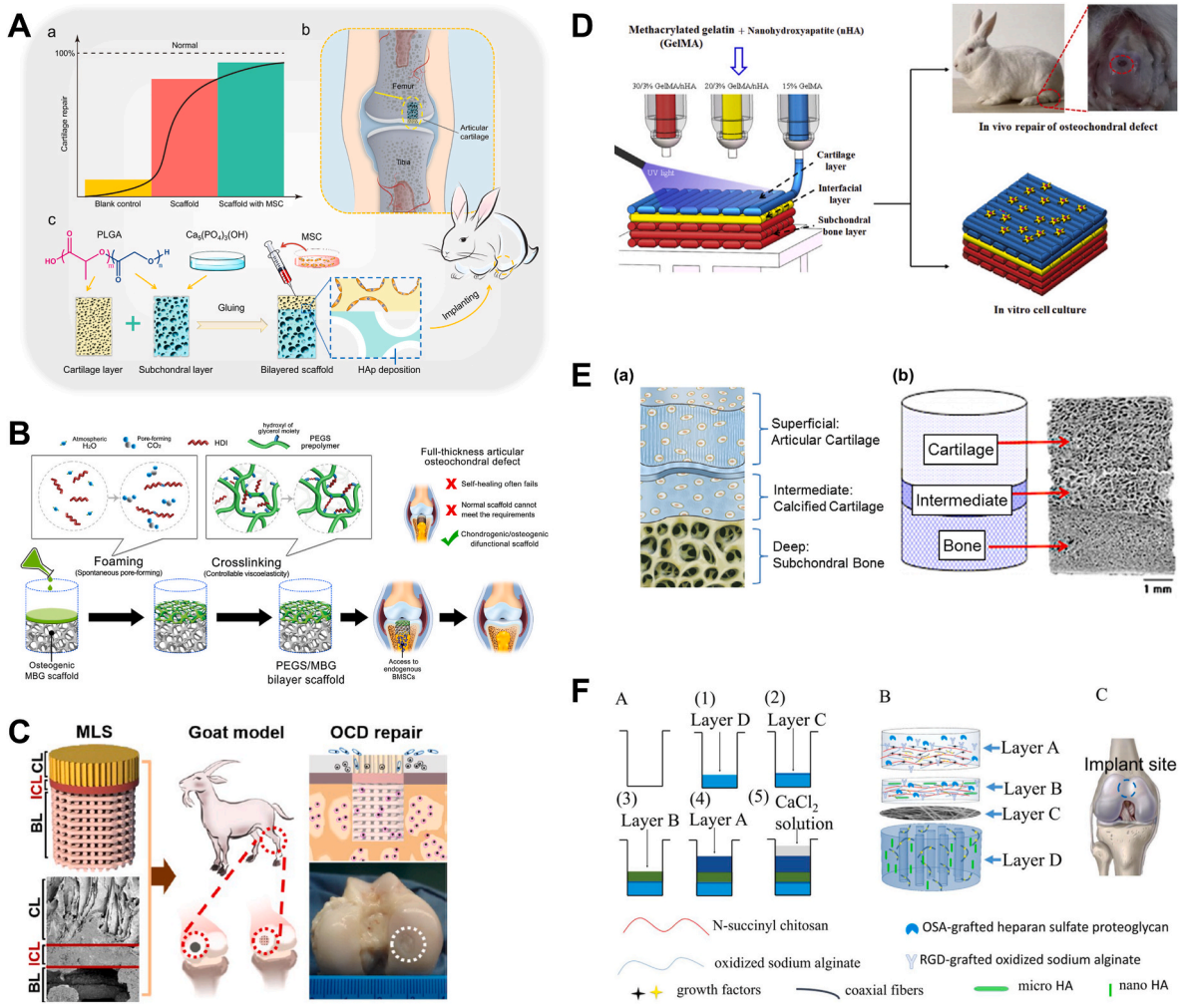

Fig. 3. Examples of multilayer scaffold designs for osteochondral tissue repair. **(A)** A bilayer PLGA-based scaffold glued together at the interface. Reproduced with permission [49]. Copyright 2018, American Chemical Society. **(B)** A bilayer scaffold with a separately fabricated mesoporous bioactive glass (MBG) scaffold as the bone phase and PEGylated poly(glycerol sebacate) (PEGS) as the cartilage phase. Reproduced with permission [72]. Copyright 2020, Elsevier **(C)** Multilayered scaffold (MLS) with a 3D printed bone layer (BL), interfacial compact layer (ICL), and chondral layer (CL) for osteochondral defect (OCD) repair. Reproduced with permission [88]. Copyright 2018, American Chemical Society. **(D)** Scaffold with connected subchondral bone, interfacial, and cartilage hydrogel layers deposited by 3D printing. Reproduced with permission [53]. Copyright 2019, Elsevier. **(E)** Tri-layer scaffold with varying amounts of collagen type I and II, HA, and hyaluronic acid in the superficial, intermediate, and deep layers. Reproduced with permission [56]. Copyright 2015, Elsevier. **(F)** Four-layer scaffold comprising various hydrogels containing HA and short polymer fibres in different phases, joined by an electrospun fibre membrane. Reproduced with permission [52]. Copyright 2018, Elsevier.

hydrogel containing cells for the cartilage phase was tested in both mice and goats, with both models showing better hyaline cartilage formation and bone vascularisation for the biphasic design compared to the single-phase control [94].

Introducing more layers into the osteochondral scaffold design is becoming an increasingly popular strategy to closely mimic the complex anatomy of native tissue. A third or fourth layer between the cartilage and subchondral bone layers can assist in the formation of a tidemark, mimicking the native interface that separates calcified cartilage from uncalcified cartilage. This may have a critical role in providing stability to the newly formed osteochondral tissue, as well as prevent subchondral bone overgrowth into the cartilage region which is linked to degenerative joint changes [57]. An interesting tri-layer scaffold design that was tested in both rabbit [56] and goat [57] osteochondral defects comprised a top layer of type I and type II collagen and hyaluronic acid, intermediate layer of type I and type II collagen and hydroxyapatite, and bottom layer of type I collagen and hydroxyapatite, with the intention of replicating the native transition in biochemical composition within the osteochondral unit. In rabbits, the scaffold group showed nearly normal cartilage repair after 12 weeks, with infiltration of native cells and the formation of an intermediate tidemark which limited calcification and vascularisation to occur in the bone rather than cartilage layer [56]. In goats, the same scaffold produced hyaline cartilage and complete regeneration of the subchondral bone after 12 months, with the intermediate layer also leading to restoration of the anatomical tidemark [57]. The findings also suggested more effective bone regeneration using this tri-layer scaffold compared to the commercially available Trufit®, a bilayer synthetic polymer scaffold. One study reported a complex four-layer design comprising hydrogels made from combinations of natural polymers, doped with HA particles and various growth factors to create the cartilage, calcified cartilage, and bone phases, with the bone phase separated from the other two using an electrospun membrane as the fourth phase [52]. This scaffold showed satisfactory osteochondral repair in rabbits after 12 weeks, with good overall integration between the scaffold and host tissue in the cartilage and bone compartments, and thickness of regenerated cartilage matching host tissue. The scaffold design was thought to enhance vascularisation and provide better conditions for overall osteochondral repair.

3.2. Gradient osteochondral scaffolds

Gradient scaffolds can be created using a variety of methods such as 3D printing, sequential hydrogel deposition, and addition of microspheres or biological components to create a continuous structure, composed of the same material(s) but with transitional differences between phases to enable osteochondral regeneration. For instance, gradient scaffolds composed of the same material but with variations in porosity/pore size [91–93,97,131,132], cell types [91,98], growth factors [81,98,133], or microsphere composition [86,100] to facilitate simultaneous cartilage and bone regeneration have been reported. Other gradient designs have used the same material combination but in different percentages throughout the scaffold, such as increasing HA concentration from top to bottom in a polymer matrix [66,134]. Gradient scaffolds can benefit from having a continuous structure that allows cellular communication between layers and possibly better *in vivo* integration with native tissue. However, fabrication processes may be complex or require better control for consistency, and the mechanical properties of hydrogel-based scaffolds may be insufficient for immediate weight-bearing.

Studies reporting osteochondral scaffolds with a porosity/pore size gradient were generally missing control scaffolds with homogenous pore structure, making it difficult to determine whether porosity/pore size variations alone can be sufficient for directing cartilage and bone regeneration in respective compartments. The closest study produced different combinations of pore structure in the cartilage and bone phases, concluding that a porosity of 92% in the cartilage phase combined with porosity of 77% in the bone phase provided the best osteochondral regeneration in rabbits compared to other combinations [93]. This porosity combination gave rise to the best cell morphology, matrix staining, surface regularity, cartilage thickness, integration with adjacent cartilage, and the highest expression of aggrecan and collagen types I and II. The other two porosity combinations tested were 85% in both layers and 77%/92% in the cartilage/bone layers. Other studies have adopted the formula of designing smaller pores of 100–200 μm for the cartilage part and larger pores of 300–600 μm for the bone part, with the justification that this should control the amount of vascularisation in different areas of the scaffold to respectively modulate cartilage and bone regeneration [91,92,131]. Interestingly, the pore size variation alone did not have a significant effect [131], while biological additives such as platelet-rich plasma (PRP) appeared to have much greater influence on the outcome of osteochondral regeneration [92]. Two studies also reported suboptimal repair using synthetic polymer scaffolds with pore size gradient alone and no additional factors, where the defect was filled with fibrous tissue [131] or there was no obvious cartilage repair [97].

Hydrogel scaffolds containing a growth factor gradient have generally shown good ability to simultaneously encourage cartilage and bone regeneration in small and large animal models [81,98,133]. Commonly chosen growth factors from the transforming growth factor (TGF) and bone morphogenetic protein (BMP) families were observed to have differing but also overlapping effects on osteochondral regeneration. For studies that employed a HA mineral gradient in a PCL [66] or collagen [134] matrix, the scaffolds have shown potential ability to differentially modulate chondrogenesis and osteogenesis, with osteogenesis becoming more likely in layers with higher HA concentration. Other scaffolds have used a gradient concentration of PLGA-based microspheres [100] or microspheres with a gradient of chondrogenic/osteogenic induction factors [86]. The latter has demonstrated better cartilage repair in sheep compared to the microfracture group after 1 year. Defects filled with the scaffold group showed cartilage lacunae and stable ECM similar to the appearance of native hyaline cartilage, visualised by haematoxylin-eosin and Safranin O staining, while the microfracture group contained only fibrous tissue.

4. Addition of biological factors in multiphasic scaffolds

Biological additives such as growth factors and cells are often incorporated into osteochondral scaffolds, to help create a multiphasic structure as well as to enhance differential cartilage and bone regeneration in respective layers (Fig. 4). The vast majority of studies incorporating biological additives reported better osteochondral repair compared to scaffold-only implants.

4.1. Growth factors in osteochondral scaffolds

Growth factors can be doped into osteochondral scaffolds to promote cell proliferation and differentiation as well as ECM synthesis, leading to better tissue repair [135]. Studies incorporating growth factors as part of the scaffold design have primarily concentrated on the TGF [52,55,58,62,63,71,79,81,98,99,132,136] and BMP [47,52,59,79,81,98,114,133,136] families to respectively induce chondrogenesis and osteogenesis. Other biomolecules such as insulin-like growth factor(IGF)-1 [62,133], fibroblast growth factor(FGF)-2 [52], interleukin(IL)-4 [64], and kartogenin [89,128] have been used. TGF-β is a popular choice due to its potent action in chondrogenic induction, by stimulating chondrogenic differentiation and cartilage ECM synthesis in progenitor cells, and decreasing the activity of catabolic factors such as IL-1 and matrix metalloproteinases (MMPs) [135]. TGF-β1 incorporated in the cartilage layer of a biphasic scaffold was shown to aid the repair of both cartilage and subchondral bone while preventing fibrous tissue formation [63]. TGF-β3 supplementation in a gradient scaffold containing human chondrocytes in the cartilage part and MSCs in the bone part was shown to induce strong chondrogenic differentiation and reduce the tendency of chondrocytes to undergo hypertrophy, as well as induce subchondral bone formation by MSCs [98]. The same study replaced TGF-β3 with BMP-2, which interestingly led to hyaline cartilage formation in the cartilage part with high concentration of GAGs and collagen type II, and similar subchondral bone formation in the bone part. BMP-2 is frequently employed to induce osteogenesis, although a comparison between IGF-1 and BMP-2 in a gradient scaffold showed their differential effects in osteochondral repair, where BMP-2 prompted bone formation in the early stages while IGF-1 assisted cartilage protection in the later stages [133]. A study that simultaneously incorporated TGF-β1, BMP-2 and FGF-2 in different scaffold phases and supplemented the treatment with Low-Intensity Pulsed Ultrasound (LIPUS) stimulation found that the inclusion of growth factors accelerated cartilage and bone repair while also enhancing vascularisation [52].

4.2. Cells in osteochondral scaffolds

A large portion of studies incorporated cells into the osteochondral scaffold to promote tissue repair. In studies which tested scaffolds in orthotopic defects, MSCs from various tissue sources were by far the most commonly chosen cell type [49,51,54,59,61,68,70,75,79,83,91,95,114,126,131,137], which were mostly derived from the bone marrow with the few alternate sources being adipose tissue and umbilical cord. Other studies have incorporated chondrocytes into the cartilage layer, either by themselves [55,90,102,124] or at the same time as having MSCs in the bone layer [94,96,113]. A few studies have not used isolated cells but rather PRP [92] or bone marrow concentrate [77]. The incorporation of cells or cell-containing substances into osteochondral scaffolds was generally shown to improve the outcome of repair in various animal models.

MSCs are a natural choice for inclusion into osteochondral scaffolds due to their ability to differentiate into both cartilage and bone, and are much easier to source as well as grow *in vitro* compared to primary cells such as chondrocytes and osteoblasts [113]. In one study, bone marrow-derived MSCs subjected to chondrogenic and osteogenic differentiation were respectively incorporated into the bone and cartilage layers of a biphasic scaffold, and found to be involved in osteochondral

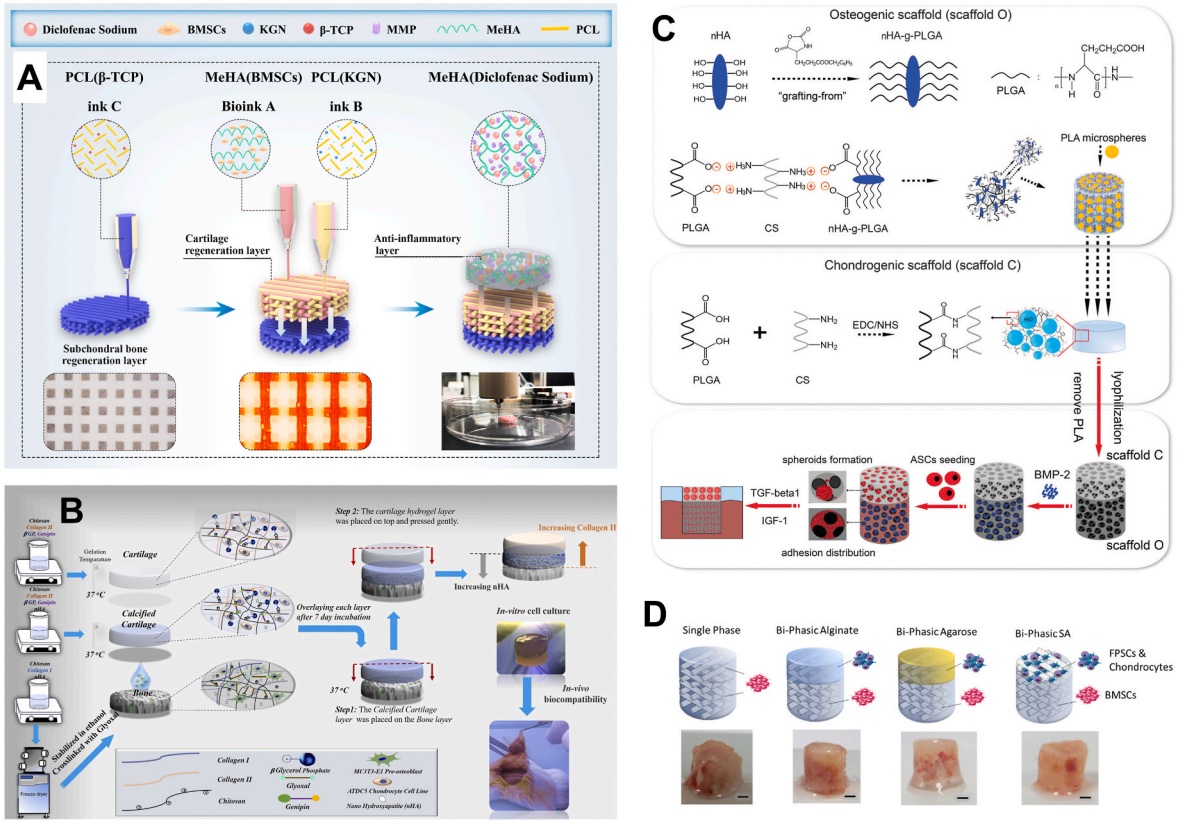

Fig. 4. Examples of scaffold designs incorporating growth factors and/or cells in different layers for osteochondral tissue repair. **(A)** Multilayered scaffold containing kartogenin (KGN), bone marrow MSCs (BMSCs), and diclofenac sodium-loaded matrix metalloproteinase (MMP)-sensitive methacrylated hyaluronic acid (MeHA) hydrogel as well as PCL matrix in different layers to confer anti-inflammatory as well as chondrogenic and osteogenic effects. Adapted with permission [95]. Copyright 2021, Elsevier. **(B)** Multilayered scaffold with different material compositions and cell types (MT3T3-E1 cells in bone layer, ATDC5 cells in intermediate and cartilage layers) in various layers. Reproduced with permission [65]. Copyright 2020, Elsevier. **(C)** Bilayer hydrogel scaffold with BMP-2 in bone layer and adipose-derived stem cell (ASC) spheroids in cartilage layer (cultured in presence of TGF-β1 and IGF-1 for 1 week before implantation). Reproduced with permission [59]. Copyright 2016, The Royal Society of Chemistry. **(D)** Bilayer scaffold with fat pad-derived stem cells (FPSCs) and chondrocytes embedded in various cartilage layer designs and bone marrow-derived stem cells (BMSCs) in the bone layer, together with representative macroscopic images post-implantation in nude mice. Adapted with permission [94]. Copyright 2020, Elsevier.

repair in rabbits for a minimum of 4 weeks after scaffold implantation [54]. The MSCs were thought to enhance the efficiency of bone and cartilage regeneration in the early stages of tissue repair. Other studies have similarly shown that scaffolds incorporating cells possessed better regenerative capability compared to those without [49,113], while one that included both chondrocytes and MSCs showed that the chondrocytes maintained phenotype in the cartilage layer while the MSCs differentiated into osteogenic cells in the bone layer [107]. Interestingly, a few studies have noted little difference in regenerative response between cell-seeded and unseeded scaffolds. A study using MSC-incorporated scaffolds showed little specificity in the repair tissue [131], while another using autologous chondrocytes did not show higher GAG formation compared to an unseeded scaffold [102]. Despite potential advantages in providing better regeneration, the incorporation of cells into osteochondral scaffolds requires higher maintenance and preparation, as well as higher demand for post-manufacture processes and handling. In addition, a large number of cells is often required to produce a significant therapeutic response, all of which are associated with higher costs and may not be desirable from a practical perspective [2].

A number of studies have investigated the simultaneous inclusion of cells and growth factors in the osteochondral scaffold. For instance, a biphasic scaffold inserted in a rat subcutaneous implantation model, comprising HA scaffold releasing alendronate in the bone layer and hyaluronic acid hydrogel containing kartogenin in the cartilage layer was found to strongly promote respective cartilage and bone regeneration, as verified by histology and differentiation-specific gene expression [128]. A study in rabbits subjected adipose-derived stem cells to chondrogenic differentiation by IGF-1 and TGF-β1 prior to incorporation into the cartilage layer of the scaffold, which was implanted with supplementation of BMP-2 in the bone layer [59]. This achieved significant subchondral bone formation at 6 weeks, with complete cartilage and bone regeneration at 12 weeks. Other studies in rabbits showed complete osteochondral regeneration at 8–12 weeks with cartilage and bone formation in respective compartments, using biphasic scaffolds containing chondrocytes and TGF-β in the cartilage layer [55], or MSCs with TGF-β in the cartilage layer and BMP-2 in the bone layer [79].

5. Animal model selection for testing osteochondral scaffolds

An ideal animal species for modelling human osteochondral repair to provide the greatest relevance to clinical translation should mimic human injury progression and have similar biological properties such as biochemical composition and tissue thickness. Among the studies discussed in this review, osteochondral scaffolds were tested in a variety of quadrupedal mammals and the progression of repair was studied over different timeframes. Due to large variations in the modelling method among studies, even within the same species, it is not clear which model provides the best predictive utility for scaffold-based osteochondral repair. A range of factors should be considered when choosing the most appropriate model for the study, including anatomical/physiological similarity to humans, accessibility, cost, and ethical implications

(Table 3).

Small animal models including mice and rats [67,71,82,95,100,136], and rabbits [47–49,51–56,59,61,64,66,72,75,76,78,79,85,87,89–93,97,99,101,124–127,131–133,137] are generally more accessible, being easily sourced and readily available. They are easier to handle and maintain than larger animals and have shorter healing time, with the time of intervention for rabbit studies usually falling within 4–24 weeks. Shorter study time and lower maintenance requirements also result in lower cost. However, the results obtained using these models may be less relevant for clinical translation due to anatomical differences compared to humans, as small animals have small joints, a thin cartilage layer and intrinsic self-repair capacity after injury, as well as vastly different joint biomechanics. For these reasons, small animal models are typically used for proof-of-concept studies. It should be noted that although studies reporting subcutaneous implantation of osteochondral scaffolds into mice were included in our review, which can provide information on the scaffold's biocompatibility and ability to promote tissue infiltration and vascularisation, this is an ectopic implantation model and does not provide direct indication of the scaffold's ability to achieve osteochondral repair.

Larger animal models such as dogs [68,114], sheep/goats [48,57,74,77,80,83,84,86,88,94,113], pigs [63,70,81,102], and horses [96,123] have been used to model osteochondral injuries. These species provide larger-sized joints, thicker cartilage, and heavier body weight, therefore providing results with greater clinical relevance since the articular cartilage structure, progression of osteochondral repair and loads experienced by the joint are more similar to what is observed in humans [44]. However, the use of large animal models is limited by practical considerations, as these species have higher maintenance requirements and therefore higher cost for animal husbandry. Certain species such as dogs and horses commonly serve other purposes such as companion animals or for recreational activities, and sourcing them for preclinical testing is restricted by availability and ethical considerations. Due to the longer healing time in large animals spanning several months to a year, similar to that observed in humans, prolonged study endpoints are needed to achieve meaningful osteochondral repair, creating practical challenges for study execution and cost consideration. For example, sheep/goat and pig models typically require an intervention period of 6–12 months. Long-term studies in large animals provide clinically relevant evidence for translating the osteochondral solution, such as long-term *in vivo* scaffold degradation, continuous formation of new cartilage and bone and restoration of native tissue anatomy, and durability of the repair tissue when subjected to prolonged physiological loading [138].

The majority of preclinical studies testing osteochondral scaffolds utilised a rabbit model. This is likely because the rabbit provides a good compromise where it better represents a human joint compared to smaller rodents, while being more easily sourced, easily maintained, and cost-effective compared to larger animals. Only two studies reported scaffold testing in both small and large animal models. Mice and goats were used in one study [94], although the mouse was a subcutaneous model and the scaffold was implanted together with cells, which resulted in the formation of some hyaline cartilage-like tissue. The same biphasic scaffold in the goat model showed some ability to induce spatially-relevant osteochondral repair, whereby a significantly higher amount of cartilage was observed in the chondral as opposed to the osseous region, although the quality of the tissue in the osseous region was quite variable and one animal also showed a collapsed defect. The other study showed some consistency in results using both a rabbit and sheep model [48]. In the rabbit, the scaffold showed lower bone formation compared with a commercial product at 8 weeks, while in the sheep, the scaffold showed evidence of repair and tissue integration in the cartilage layer but incomplete regeneration in the bone layer at 6 months. The scaffold showed slow resorption in both models.

Among studies which used large animal models, only 5 had an endpoint of longer than one year. Although shorter-term studies all reported evidence of osteochondral repair in a range of large animals, the extent of repair was often incomplete and the outcomes of these studies might not provide a good indication for long-term structural repair of the joint. Where possible, longer studies should be designed to demonstrate the durability and effectiveness of osteochondral repair using scaffold-based approaches, with the intention of establishing clinical relevance and predictability of the research outcomes in humans. Where possible, an adequate sample size should be used when testing osteochondral scaffolds in large animals, as current studies are typically limited to a small number of animals (<10 across all groups) for models using dogs, sheep, pigs and horses, Additionally, there is a need for better standardisation of methods to create osteochondral defects and assess repair outcomes for studies using the same animal species, to enable better comparability of results across different scaffold designs. On this topic, trends in the selection of animal models to assess osteochondral repair using biomaterials [44] and evaluation methods [45] have been discussed in recent reviews. Analysis of studies in the last 10 years suggests that small animals are typically used for testing degradation, biocompatibility, and biomaterial interactions with host tissues in non-load bearing regions such as the femoral groove, while large animals tend to have defects created in load bearing regions such as the medial femoral condyle for testing durability and repair outcomes of biomaterials [44]. Evaluation methods used are dominated by histological/histomorphometric and biomechanical analyses [45]. However, significant heterogeneity exists among studies regarding animal characteristics (breed, age, sex, size), surgical protocols, osteochondral defect location and dimensions, timepoints of outcome evaluation, and choice of evaluation methods for the same type of animal model.

6. Current outcomes of osteochondral scaffolds in clinical studies

Currently, four types of commercially available scaffolds have been reported in clinical studies published between 2015 and 2021 (Table 4). These include MaioRegen® from Finceramica Italy [139–148], Trufit® from Smith & Nephew USA [149–154], Agili-C™ from CartiHeal Israel [155,156], and Chondrotissue® from BioTissue Switzerland [157]. The MaioRegen® is a tri-layer scaffold, while Trufit® and Agili-C™ are bi-layer scaffolds, and Chondrotissue® is a single layer scaffold. All scaffolds were designed for cell-free implantation and applied as such in clinical studies, except for one study using Trufit® which immersed the scaffold in PRP or bone marrow concentrate prior to implantation [152].

MaioRegen® is composed of collagen and HA arranged into layers by freeze drying. This tri-layer scaffold includes a top layer of collagen type I, intermediate layer of 60% collagen and 40% HA, and bottom layer of 30% collagen and 70% HA. Clinical studies using this scaffold have been reported since 2011, for the treatment of a variety of osteochondral lesions including most commonly the femoral condyles, tibial plateau, patella, and talus [158]. The more recent studies have investigated the use of MaioRegen® in a range of age groups, including juveniles [147], young adults [141,143,145], and middle-aged to elderly patients [139,140,142,144,146,148]. In juvenile knee osteochondritis dissecans (OCD), MaioRegen® achieved stable improvement over time with International Knee Documentation Committee (IKDC) subject score of 50.3 ± 17.4 at 1 year to 85.0 ± 9.3 at 6 years (higher score equates to better symptomatic and functional outcomes; maximum score 100), and Tegner score of 2.6 ± 1.4 pre-operation to 5.5 ± 2.0 at 6 years (higher score equates to better symptomatic and functional outcomes; maximum score 10) [147]. However, persistent abnormal magnetic resonance imaging (MRI) findings were seen at the subchondral bone level in this study. In young adults 25 ± 7 years of age, one study showed significant improvement in clinical scores for all patients treated with MaioRegen® at 5 years post-implantation [145], while another showed evidence of repair at 1 year [143]. However, a study reporting a similar age cohort but osteochondral lesions due to OCD, trauma and subchondral bone cyst, in both knee regions and the talus, suggested fewer promising

outcomes [141]. No or very limited bone formation was observed in 6 out of 8 patients, and the remaining 2 patients had 50–75% bone formation. No improvements were shown by MRI or Magnetic Resonance Observation of Cartilage Repair Tissue (MOCART) scores at any time point (1 and 2.5 years), and no improvements overall were found in the talus injury patients. Results were more promising for treating knee osteochondral lesions in middle-aged patients with mean age of 30–40 years, with most studies suggesting improved clinical scores at follow-up time points generally at 1–2 years [139,140,144,148] and up to 5 years [146]. However, one study noted 11% complication rate and 31% clinical failure due to lack of improvement, and the scaffold was only intact in 47% of the 26 patients [142].

Trufit® is a synthetic polymer scaffold with a biphasic structure, composed of poly(glycolic acid) (PGA) fibres and calcium sulfate in the bone layer and PLGA in the cartilage layer. Clinical evidence on the short- and long-term results of Trufit® in knee osteochondral lesions has been contradictory. An earlier study has shown that 30.7% of all cases had evident failing from MRI evaluation at up to 3 years, and was unable to conclude that the scaffold had osteoconductive effects [150]. Another study suggested improvements in clinical scores but poor integration of the central part of the scaffold with surrounding tissue, as well as slow scaffold resorption, and a longer study period was advised although the last follow-up was at 4 years [151]. In a more recent study, Trufit® was shown to provide significant improvements in activity level scores over 5 years compared to the microfracture group, together with better cartilage regeneration and evidence of tissue maturation over time [154]. A longer-term study over mean follow-up of 7.5 years for treating osteochondral lesions in the talus showed improvement in clinical scores for pain relief, American Orthopedic Foot and Ankle Score (AOFAS), and patient satisfaction [149]. Based on the consideration that Trufit® is a synthetic scaffold and may achieve limited regeneration as a cell-free implant, one study has tested scaffold immersion in PRP or bone marrow concentrate prior to implantation in full-thickness knee osteochondral defects [152]. At 1 year follow-up, both supplemented groups showed better cartilage filling compared to the scaffold-only group, while the bone marrow concentrate group appeared to improve cartilage maturation compared to the PRP group, although longer-term follow-up is required to confirm these findings. A recent study with long-term mean follow-up of 10 years showed no statistically significant improvements in any outcome scores following Trufit® implantation, while radiology indicated that all 11 patients had incomplete or no evidence of scaffold incorporation as well as persistent chondral loss and residual oedema or cystic changes [153]. Although it was the first osteochondral scaffold to be introduced in clinical practice, Trufit® has now been withdrawn from the market due to its high failure rate and generally poor clinical outcomes as a scaffold-only implant [159].

Agili-C™ is a bi-layer scaffold composed of coral-derived aragonite for the bone phase and hyaluronic acid for the cartilage phase, same as the scaffold tested in a goat preclinical study by the same group [74]. It has been approved for use by the Food and Drug Administration (FDA) in March 2021, and is the most recent osteochondral scaffold to reach clinical application. An earlier clinical study on this scaffold compared repair outcomes in knee osteochondral defects treated with cylindrical or tapered implants in 21 patients, which showed improvements in clinical scores for both types of implants at the 12 month follow-up, although the tapered implant group had a significantly lower (0%) revision rate [155]. A recent case series of 86 patients treated with Agili-C™ for mild to moderate knee osteoarthritis showed significant clinical improvement at the 24-month follow-up, as indicated by Knee injury and Osteoarthritis Outcome Score (KOOS) and IKDC subjective score, as well as substantial defect filling to almost 80% as evaluated by MRI [156]. However, treatment failure occurred in 9.3% of patients necessitating revision surgery.

Chondrotissue® is a single-phase scaffold composed of PGA-hyaluronan. When used to treat osteochondral defects in the talus, results from 32 patients showed good to excellent clinical scores in 84.4% of patients at mean follow-up of 33.8 months [157]. However, the follow-up period was considered too short for predicting long-term repair outcomes.

The available literature on osteochondral scaffolds reported in clinical studies supports the use of cell-free multiphasic scaffolds for treating patients with knee osteochondral defects. According to the results of a recent systematic review and meta-analysis of clinical studies on this topic [159], patients treated with MaioRegen®, Trufit®, and Agili-C™ respectively had overall failure rate of 4.8%, 9.9%, and 8.2% at mean follow-up of 28.4, 39.8, and 18.0 months. Quantitative synthesis of outcome scores for MaioRegen® and Agili-C™ demonstrated statistically significant improvements in IKDC subjective score and activity level evaluated with Tegner score at 1, 2, and $\geq$3 year follow-up compared to baseline. With the exception of Trufit® which has been withdrawn from the market, multiphasic scaffolds available for clinical use have provided promising treatment of osteochondral defects at short-to mid-term follow-up with a relatively low rate of adverse events. However, current results should be interpreted with caution as the overall quality level of available clinical studies is low, and evidence is missing from high-level trials with long-term follow-up. Moreover, comparative trials evaluating the outcomes of scaffold-based osteochondral repair with other well-established techniques such as osteochondral autografting and ACI, as well as among different scaffold types and between cell-loaded and cell-free scaffolds are needed to improve the evidence base. Future studies addressing these deficiencies may provide greater confidence to using scaffold-based therapies in the clinical treatment of osteochondral defects.

7. Conclusions and future perspectives

Clinical results on commercially available multiphasic scaffolds currently suggest a limited ability for complete restoration of osteochondral tissue. For instance, studies have indicated a poor resorption rate for Trufit® [151] and lack of subchondral bone regeneration for MaioRegen® [141]. These commercial osteochondral scaffolds are typically applied as cell-free implants, although current preclinical studies testing new scaffold designs have mostly incorporated additional factors to help with regeneration, such as stem cells or primary cells, and growth factors or other biomolecules. The inclusion of a biological supplement has generally led to improved outcomes in osteochondral regeneration, manifested as increase in GAG and collagen type II levels [88,137] and integrity of the regenerated cartilage [137], as well as shorter time required to achieve satisfactory defect repair [47,89]. The combination of different cell types and growth factors, coupled with other stimulatory methods may work synergistically to enhance osteochondral repair [52]. Different types of multiphasic designs, including multilayer and gradient scaffolds have been shown to enhance preclinical repair outcomes by better mimicking the stratified osteochondral anatomy and enabling appropriate zonation of the repair tissue [130].

Despite promising advances, an ‘ideal’ scaffold that perfectly addresses the complex and multifaceted requirements for osteochondral repair while being relevant for clinical translation is still missing. Among the studies discussed in this review, current experimental scaffold designs face a number of common challenges including limited ability to induce hyaline cartilage formation, inability to differentially facilitate cartilage and bone regeneration, inferior mechanical properties compared to native tissue, slow or unpredictable resorption time, and prolonged time required to achieve stable osteochondral repair. Advances in scaffold fabrication methods may be one strategy to help address some of these challenges. For instance, using 3D printing to create osteochondral scaffolds enables the stacking of various materials with more control over resolution and reproducibility compared to manual fabrication methods. This also enables intricate design factors to be more easily realised, such as pore geometry gradients and spatial distribution of additives including minerals and growth factors. For example, a recent study has described a biphasic 3D printed scaffold

produced from GelMA and poly(ethylene glycol) diacrylate (PEGDA) bio-ink, which incorporated nano-HA and TGF-β1 nanoparticles respectively into the lower and upper scaffold layers [160]. This design was found to separately induce *in vitro* chondrogenic and osteogenic differentiation of human bone marrow MSCs in the two layers. In another study, 3D printing was used to create customisable implants from MRI scans of a patient's osteochondral defect [161]. A CAD model was generated for a biphasic implant with the same geometrical dimensions and tissue thicknesses as the missing tissue in the defect. The implant was 3D printed using a bio-ink made from alginate-methylcellulose for the cartilage phase and calcium phosphate cement for the bone phase. This was a proof-of-concept study to show that it was possible to create a customised implant, but opened up exciting possibilities for developing personalised treatments for osteochondral injuries. To generate more anatomically similar osteochondral tissue with correct spatial distribution of cells and ECM, 3D bioprinting is being increasingly employed, although this method imposes more restrictions on material choices and fabrication conditions to ensure cell viability after printing [162].

Although not specifically discussed in this review, injectable hydrogels that can be delivered in a non-invasive manner, comply with irregularly shaped defects, and cure *in situ* may present unique advantages for treating osteochondral defects, particularly for defects with defined boundaries. It is difficult to create a multiphasic structure using injectable hydrogels, but emerging research is working towards the generation of hierarchically structured hydrogels that undergo *in situ* gelation. For example, one injectable system was developed using hyaluronic acid incorporating bone marrow-derived MSC spheroids and kartogenin-loaded short fibres within spheroids to modulate chondrogenic differentiation [163]. At the same time, the hydrogel also incorporates celecoxib-loaded short fibres for mechanical reinforcement and sustained anti-inflammatory effects. After being delivered by intra-articular injection, this hydrogel system was found to completely repair osteochondral defects in a rabbit model, with generation of hyaline cartilage-like tissue after 12 weeks. This approach provides new ideas for creating injectable multiphasic scaffold systems, potentially through sequential delivery of multiple hierarchical layers.

The introduction of cells such as MSCs into multiphasic scaffolds has been shown to improve osteochondral repair in the majority of preclinical studies discussed in this review. Despite obvious benefits, the incorporation of cells into biomaterial implants presents challenges for clinical translation, whereby the ability to source autologous cells and expand them *ex vivo* may be limited in many patients, while the use of allogeneic cells introduces risks associated with immunogenicity. An emerging approach to circumvent these challenges is to use stem cell-derived secretory products such as extracellular vesicles (EVs). Because of their roles in intercellular communication, EVs can deliver a wide range of signalling molecules including nucleic acids, proteins, and lipids to modulate the behaviour of target cells [164]. Moreover, MSC-derived EVs have been shown to capture similar anti-inflammatory and other paracrine effects as the parent cells, while offering minimal immunogenicity when delivered into preclinical *in vivo* models [165]. The use of stem cell-derived EVs in regenerative medicine has so far shown promising results in repairing joint tissue [166] and treating a range of inflammation-related conditions [165]. In an *in vitro* study, MSC-EVs were shown to promote cartilage regeneration when applied to human osteoarthritic chondrocytes, by inhibiting tumour necrosis factor (TNF)-α induced collagenase activity and therefore the adverse effects of inflammation, while stimulating the production of proteoglycans and collagen type II [167]. MSC-EVs can also be bioengineered with specific cargo such as miRNA or drugs to further assist their therapeutic effects. For example, one study investigated the use of TGF-β1 to stimulate MSCs, which resulted in upregulation of miRNA-135b expression in MSC-derived EVs, found to significantly promote cartilage repair in a rat osteoarthritis model possibly through downregulation of Sp1 (an inhibitor of chondrocyte proliferation) [168]. EVs derived from rabbit serum and subsequently loaded with miR-140 have also been found to induce chondrogenic differentiation in bone marrow MSCs [169]. Emerging research on stem cell-derived or bioengineered EVs suggests these may provide a viable and more practical alternative than the incorporation of cells into biomaterial scaffolds to enhance osteochondral repair [170].

As reflected by the studies discussed in this review, finding the best animal model to accurately represent human osteochondral defects is challenging but critical for indicating the clinical relevance of new treatment strategies. Current small animal models do not accurately mimic human joint anatomy and pathophysiology or load-bearing conditions, while the use of large animal models presents limitations of increased cost and ethical considerations, as well as the need for prolonged study time. Although unlikely to replace the use of animal models in the immediate future, recent emerging discoveries into *ex vivo* organoid systems may provide alternative options for modelling osteochondral tissue in early proof-of-concept experiments. For instance, a clinically relevant *ex vivo* osteochondral model was reported to be useful for testing hydrogel-based materials for cartilage regeneration, which remained metabolically stable for 4 weeks in a perfusion bioreactor without compromising the integrity of different tissue components [171]. Alternative methods of producing osteochondral organoids using induced pluripotent stem cells (iPSCs) have been reported [172,173]. Other technological developments relevant to *in vitro* modelling of osteochondral tissue include organ-on-a-chip systems that aim to recreate the *in vivo* cellular microenvironment on a microfluidic device [174]. For instance, joint-on-a-chip devices have been reported that incorporate synovial fibroblasts and articular chondrocytes within a hydrogel platform, which recapitulate complex multi-tissue interactions along with biochemical and mechanical cues, and can be used to evaluate new therapies for joint repair [174].

This review has explored a range of recent studies that have tested new multiphasic scaffold designs for osteochondral repair in animal models. Our discussions highlighted the types of biomaterials, scaffold designs, and additive factors used to enhance repair outcomes, as well as recent clinical progress on a few commercially available osteochondral scaffolds. We also presented factors to consider when choosing an adequate *in vivo* model for assessing the outcomes of scaffold-based osteochondral repair. Tissue engineering using multiphasic scaffolds is a promising strategy for effective clinical repair of osteochondral defects, which will benefit from cross-disciplinary integration of innovative approaches in biofabrication, micro-/nano-devices, and stem cell engineering.

Ethics approval and consent to participate

N/A.

Author contributions

Conceptualisation: J.J.L., C.B.L.; Formal analysis; all authors; Funding acquisition: J.J.L.; Investigation: R.C., J.S.P, J.L.; Methodology: J.J.L., R.C.; Writing – original draft: R.C., J.J.L.; Writing – review & editing: all authors.

Declaration of competing interest

There are no conflicts to declare.

Acknowledgements

We acknowledge funding support from the National Health and Medical Research Council (NHMRC) of Australia (GNT1120249).

References

[1] L. Zhou, V.O. Gjvm, J. Malda, M.J. Stoddart, Y. Lai, R.G. Richards, K. Ki-wai Ho, L. Qin, Innovative tissue-engineered strategies for osteochondral defect repair and regeneration: current progress and challenges, Adv. Healthc. Mater. 9 (2020), 2001008.

[2] J. Yang, Y.S. Zhang, K. Yue, A. Khademhosseini, Cell-laden hydrogels for osteochondral and cartilage tissue engineering, Acta Biomater. 57 (2017) 1–25.

[3] H.A. Martijn, K.T.A. Lambers, J. Dahmen, S.A.S. Stufkens, G.M.M.J. Kerkhoffs, High incidence of (osteo)chondral lesions in ankle fractures, Knee Surg. Sports Traumatol. Arthrosc. 29 (2021) 1523–1534.

[4] A.C. Thomas, T. Hubbard-Turner, E.A. Wikstrom, R.M. Palmieri-Smith, Epidemiology of posttraumatic osteoarthritis, J. Athl. Train. 52 (2017) 491–496.

[5] E. Solheim, J. Hegna, T. Strand, T. Harlem, E. Inderhaug, Randomized study of long-term (15-17 years) outcome after microfracture versus mosaicplasty in knee articular cartilage defects, Am. J. Sports Med. 46 (2018) 826–831.

[6] G. Filardo, E. Kon, F. Perdisa, B. Di Matteo, A. Di Martino, F. Iacono, S. Zaffagnini, F. Balboni, V. Vaccari, M. Marcacci, Osteochondral scaffold reconstruction for complex knee lesions: a comparative evaluation, Knee 20 (2013) 570–576.

[7] A.J. Krych, A. Pareek, A.H. King, N.R. Johnson, M.J. Stuart, R.J. Williams, Return to sport after the surgical management of articular cartilage lesions in the knee: a meta-analysis, Knee Surg. Sports Traumatol. Arthrosc. 25 (2017) 3186–3196.

[8] D.W. Shim, K.H. Park, J.W. Lee, Y.-j. Yang, J. Shin, S.H. Han, Primary autologous osteochondral transfer shows superior long-term outcome and survival rate compared with bone marrow stimulation for large cystic osteochondral lesion of talus, Arthroscopy 37 (2021) 989–997.

[9] E. Solheim, J. Hegna, E. Inderhaug, Long-term survival after microfracture and mosaicplasty for knee articular cartilage repair: a comparative study between two treatments cohorts, Cartilage 11 (2020) 71–76.

[10] R. Andrade, S. Vasta, R. Pereira, H. Pereira, R. Papalia, M. Karahan, J.M. Oliveira, R.L. Reis, J. Espregueira-Mendes, Knee donor-site morbidity after mosaicplasty – a systematic review, J. Exp. Orthop. 3 (2016) 31.

[11] N. de l'Escalopier, T. Amouyel, D. Mainard, R. Lopes, G. Cordier, N. Baudrier, J. Benoist, V.D. Ferrière, F. Leiber, A. Morvan, C. Maynou, G. Padiolleau, O. Barbier, Long-term outcome for repair of osteochondral lesions of the talus by osteochondral autograft: a series of 56 Mosaicplasties, Orthop. Traumatol. Surg. Res. 107 (2021), 103075.

[12] Y. Shimozono, D. Seow, Y. Yasui, K. Fields, J.G. Kennedy, Knee-to-talus donor-site morbidity following autologous osteochondral transplantation: a meta-analysis with best-case and worst-case analysis, Clin. Orthop. Relat. Res. 477 (2019) 1915.

[13] G. Meric, G.C. Gracitelli, S. Gortz, A.J. De Young, W.D. Bugbee, Fresh osteochondral allograft transplantation for bipolar reciprocal osteochondral lesions of the knee, Am. J. Sports Med. 43 (2015) 709–714.

[14] C.L. Camp, J.D. Barlow, A.J. Krych, Transplantation of a tibial osteochondral allograft to restore a large glenoid osteochondral defect, Orthopedics 38 (2015) e147–e152.

[15] A.T. Assenmacher, A. Pareek, P.J. Reardon, J.A. Macalena, M.J. Stuart, A. J. Krych, Long-term outcomes after osteochondral allograft: a systematic review at long-term follow-up of 12.3 years, Arthroscopy 32 (2016) 2160–2168.

[16] W.D. Bugbee, A.L. Pallante-Kichura, S. Görtz, D. Amiel, R. Sah, Osteochondral allograft transplantation in cartilage repair: graft storage paradigm, translational models, and clinical applications, J. Orthop. Res. 34 (2016) 31–38.

[17] G. Raz, O.A. Safir, D.J. Backstein, P.T. Lee, A.E. Gross, Distal femoral fresh osteochondral allografts: follow-up at a mean of twenty-two years, JBJS 96 (2014) 1101–1107.

[18] M. Abolghasemian, S. León, P.T.H. Lee, O. Safir, D. Backstein, A.E. Gross, P.R. T. Kuzyk, Long-term results of treating large posttraumatic tibial plateau lesions with fresh osteochondral allograft transplantation, JBJS 101 (2019) 1102–1108.

[19] S.A. León, X.Y. Mei, O.A. Safir, A.E. Gross, P.R. Kuzyk, Long-term results of fresh osteochondral allografts and realignment osteotomy for cartilage repair in the knee, Bone Joint Lett. J 101-B (2019) 46–52.

[20] S. León, X. Mei, O. Safir, A. Gross, P. Kuzyk, Long-term results of fresh osteochondral allografts and realignment osteotomy for cartilage repair in the knee, Bone Joint Lett. J 101 (2019) 46–52.

[21] D. Goyal, S. Keyhani, E.H. Lee, J.H.P. Hui, Evidence-based status of microfracture technique: a systematic review of Level I and II studies, Arthroscopy 29 (2013) 1579–1588.

[22] A.H. Gomoll, T. Minas, The quality of healing: articular cartilage, Wound Repair Regen. 22 (2014) 30–38.

[23] J.M. Bert, Abandoning microfracture of the knee: has the time come? Arthroscopy 31 (2015) 501–505.

[24] R. Gudas, A. Gudaitė, A. Pocius, A. Gudienė, E. Čekanauskas, E. Monastyreckienė, A. Baseviči̇us, Ten-year follow-up of a prospective, randomized clinical study of mosaic osteochondral autologous transplantation versus microfracture for the treatment of osteochondral defects in the knee joint of athletes, Am. J. Sports Med. 40 (2012) 2499–2508.

[25] Q.-x. Han, Y. Tong, L. Zhang, J. Sun, J. Ma, X. Liu, S. Zhang, B. Jiang, Y. Li, Comparative efficacy of osteochondral autologous transplantation and microfracture in the knee: an updated meta-analysis of randomized controlled trials, Arch. Orthop. Trauma Surg. 143 (2021) 317–328.

[26] A. Pareek, P.J. Reardon, J.A. Macalena, B.A. Levy, M.J. Stuart, R.J. Williams III, A.J. Krych, Osteochondral autograft transfer versus microfracture in the knee: a meta-analysis of prospective comparative studies at midterm, Arthroscopy 32 (2016) 2118–2130.

[27] E. Solheim, J. Hegna, E. Inderhaug, Long-term clinical follow-up of microfracture versus mosaicplasty in articular cartilage defects of medial femoral condyle, Knee 24 (2017) 1402–1407.

[28] R.L. Davies, N.J. Kuiper, Regenerative medicine: a review of the evolution of autologous chondrocyte implantation (ACI) therapy, Bioengineering 6 (2019) 22.

[29] T. Ogura, B.A. Mosier, T. Bryant, T. Minas, A 20-year follow-up after first-generation autologous chondrocyte implantation, Am. J. Sports Med. 45 (2017) 2751–2761.

[30] L.C. Biant, G. Bentley, S. Vijayan, J.A. Skinner, R.W. Carrington, Long-term results of autologous chondrocyte implantation in the knee for chronic chondral and osteochondral defects, Am. J. Sports Med. 42 (2014) 2178–2183.

[31] A. Pareek, J.L. Carey, P.J. Reardon, L. Peterson, M.J. Stuart, A.J. Krych, Long-term outcomes after autologous chondrocyte implantation: a systematic review at mean follow-up of 11.4 years, Cartilage 7 (2016) 298–308.

[32] G. Filardo, E. Kon, L. Andriolo, B. Di Matteo, F. Balboni, M. Marcacci, Clinical profiling in cartilage regeneration: prognostic factors for midterm results of matrix-assisted autologous chondrocyte transplantation, Am. J. Sports Med. 42 (2014) 898–905.

[33] S. Ghosh, A.K. Scott, B. Seelbinder, J.E. Barthold, B.M.S. Martin, S. Kaonis, S. E. Schneider, J.T. Henderson, C.P. Neu, Dedifferentiation alters chondrocyte nuclear mechanics during in vitro culture and expansion, Biophys. J. 121 (2022) 131–141.

[34] L. Peterson, H.S. Vasiliadis, M. Brittberg, A. Lindahl, Autologous chondrocyte implantation: a long-term follow-up, Am. J. Sports Med. 38 (2010) 1117–1124.

[35] P. Niemeyer, J.M. Pestka, G.M. Salzmann, N.P. Südkamp, H. Schmal, Influence of cell quality on clinical outcome after autologous chondrocyte implantation, Am. J. Sports Med. 40 (2012) 556–561.

[36] S.P. Nukavarapu, D.L. Dorcemus, Osteochondral tissue engineering: current strategies and challenges, Biotechnol. Adv. 31 (2013) 706–721.

[37] B. Zhang, J. Huang, R.J. Narayan, Gradient scaffolds for osteochondral tissue engineering and regeneration, J. Mater. Chem. B 8 (2020) 8149–8170.

[38] W. Wei, H. Dai, Articular cartilage and osteochondral tissue engineering techniques: recent advances and challenges, Bioact. Mater. 6 (2021) 4830–4855.

[39] E.C. Beck, M. Barragan, M.H. Tadros, S.H. Gehrke, M.S. Detamore, Approaching the compressive modulus of articular cartilage with a decellularized cartilage-based hydrogel, Acta Biomater. 38 (2016) 94–105.

[40] I. Gadjanski, G. Vunjak-Novakovic, Challenges in engineering osteochondral tissue grafts with hierarchical structures, Expet Opin. Biol. Ther. 15 (2015) 1583–1599.

[41] N. Yildirim, A. Amanzhanova, G. Kulzhanova, F. Mukasheva, C. Erisken, Osteochondral interface: regenerative engineering and challenges, ACS Biomater. Sci. Eng. 9 (2023) 1205–1223.

[42] S.E. Doyle, F. Snow, S. Duchi, C.D. O'Connell, C. Onofrillo, C. Di Bella, E. Pirogova, 3D printed multiphasic scaffolds for osteochondral repair: challenges and opportunities, Int. J. Mol. Sci. 22 (2021), 12420.

[43] A.G. González Vázquez, L.A. Blokpoel Ferreras, K.E. Bennett, S.M. Casey, P. A. Brama, F.J. O'Brien, Systematic comparison of biomaterials-based strategies for osteochondral and chondral repair in large animal models, Adv. Healthc. Mater. 10 (2021), 2100878.

[44] X. Meng, R. Ziadlou, S. Grad, M. Alini, C. Wen, Y. Lai, L. Qin, Y. Zhao, X. Wang, Animal models of osteochondral defect for testing biomaterials, Biochem. Res. Int. 2020 (2020), 9659412.

[45] M. Maglio, S. Brogini, S. Pagani, G. Giavaresi, M. Tschon, Current trends in the evaluation of osteochondral lesion treatments: histology, histomorphometry, and biomechanics in preclinical models, BioMed Res. Int. 2019 (2019), 4040236.

[46] J.J. Li, D.L. Kaplan, H. Zreiqat, Scaffold-based regeneration of skeletal tissues to meet clinical challenges, J. Mater. Chem. B 2 (2014) 7272–7306.

[47] Y. Dong, X. Sun, Z. Zhang, Y. Liu, L. Zhang, X. Zhang, Y. Huang, Y. Zhao, C. Qi, A. C. Midgley, S. Wang, Q. Yang, Regional and sustained dual-release of growth factors from biomimetic tri-layered scaffolds for the repair of large-scale osteochondral defects, Appl. Mater. Today 19 (2020), 100548.

[48] G. Filardo, F. Perdisa, M. Gelinsky, F. Despang, M. Fini, M. Marcacci, A.P. Parrilli, A. Roffi, F. Salamanna, M. Sartori, K. Schutz, E. Kon, Novel alginate biphasic scaffold for osteochondral regeneration: an in vivo evaluation in rabbit and sheep models, J. Mater. Sci. Mater. Med. 29 (2018) 74.

[49] X. Liang, P. Duan, J. Gao, R. Guo, Z. Qu, X. Li, Y. He, H. Yao, J. Ding, Bilayered PLGA/PLGA-HAp composite scaffold for osteochondral tissue engineering and tissue regeneration, ACS Biomater. Sci. Eng. 4 (2018) 3506–3521.

[50] P. Giannoni, E. Lazzarini, L. Ceseracciu, A.C. Barone, R. Quarto, S. Scaglione, Design and characterization of a tissue-engineered bilayer scaffold for osteochondral tissue repair, J. Tissue Eng. Regen. Med. 9 (2015) 1182–1192.

[51] K. Shimomura, Y. Moriguchi, R. Nansai, H. Fujie, W. Ando, S. Horibe, D.A. Hart, A. Gobbi, H. Yoshikawa, N. Nakamura, Comparison of 2 different formulations of artificial bone for a hybrid implant with a tissue-engineered construct derived from synovial mesenchymal stem cells: a study using a rabbit osteochondral defect model, Am. J. Sports Med. 45 (2017) 666–675.

[52] T. Chen, J. Bai, J. Tian, P. Huang, H. Zheng, J. Wang, A single integrated osteochondral in situ composite scaffold with a multi-layered functional structure, Colloids Surf. B Biointerfaces 167 (2018) 354–363.

[53] J. Liu, L. Li, H. Suo, M. Yan, J. Yin, J. Fu, 3D printing of biomimetic multi-layered GelMA/nHA scaffold for osteochondral defect repair, Mater. Des. 171 (2019), 107708.

[54] X. Li, Y. Li, Y. Zuo, D. Qu, Y. Liu, T. Chen, N. Jiang, H. Li, J. Li, Osteogenesis and chondrogenesis of biomimetic integrated porous PVA/gel/V-n-HA/pa6 scaffolds and BMSCs construct in repair of articular osteochondral defect, J. Biomed. Mater. Res. A. 103 (2015) 3226–3236.

[55] Y.J. Seol, J.Y. Park, W. Jeong, T.H. Kim, S.Y. Kim, D.W. Cho, Development of hybrid scaffolds using ceramic and hydrogel for articular cartilage tissue regeneration, J. Biomed. Mater. Res. A. 103 (2015) 1404–1413.
[56] T.J. Levingstone, E. Thompson, A. Matsiko, A. Schepens, J.P. Gleeson, F. J. O'Brien, Multi-layered collagen-based scaffolds for osteochondral defect repair in rabbits, Acta Biomater. 32 (2016) 149–160.
[57] T.J. Levingstone, A. Ramesh, R.T. Brady, P.A.J. Brama, C. Kearney, J.P. Gleeson, F.J. O'Brien, Cell-free multi-layered collagen-based scaffolds demonstrate layer specific regeneration of functional osteochondral tissue in caprine joints, Biomaterials 87 (2016) 69–81.
[58] L. Coluccino, P. Stagnaro, M. Vassalli, S. Scaglione, Bioactive TGF-beta1/HA alginate-based scaffolds for osteochondral tissue repair: design, realization and multilevel characterization, J. Appl. Biomater. 14 (2016) 42–52.
[59] K. Zhang, S. He, S. Yan, G. Li, D. Zhang, L. Cui, J. Yin, Regeneration of hyaline-like cartilage and subchondral bone simultaneously by poly(l-glutamic acid) based osteochondral scaffolds with induced autologous adipose derived stem cells, J. Mater. Chem. B 4 (2016) 2628–2645.
[60] K.T. Shalumon, C. Sheu, Y.T. Fong, H.T. Liao, J.P. Chen, Microsphere-based hierarchically juxtapositioned biphasic scaffolds prepared from poly(lactic-co-glycolic acid) and nanohydroxyapatite for osteochondral tissue engineering, Polymers 8 (2016) 429.
[61] S.Q. Ruan, L. Yan, J. Deng, W.L. Huang, D.M. Jiang, Preparation of a biphase composite scaffold and its application in tissue engineering for femoral osteochondral defects in rabbits, Int. Orthop. 41 (2017) 1899–1908.
[62] F. Wang, Y. Hu, D. He, G. Zhou, X. Yang, E. Ellis III, Regeneration of subcutaneous tissue-engineered mandibular condyle in nude mice, J. Cranio-Maxillo-Fac. Surg. 45 (2017) 855–861.
[63] Y.H. Hsieh, B.Y. Shen, Y.H. Wang, B. Lin, H.M. Lee, M.F. Hsieh, Healing of osteochondral defects implanted with biomimetic scaffolds of poly (ε-caprolactone)/hydroxyapatite and glycidyl-methacrylate-modified hyaluronic acid in a minipig, Int. J. Mol. Sci. 19 (2018) 1125.
[64] L. Gong, J. Li, J. Zhang, Z. Pan, Y. Liu, F. Zhou, Y. Hong, Y. Hu, Y. Gu, H. Ouyang, X. Zou, S. Zhang, An interleukin-4-loaded bi-layer 3D printed scaffold promotes osteochondral regeneration, Acta Biomater. 117 (2020) 246–260.
[65] S. Korpayev, G. Kaygusuz, M. Sen, K. Orhan, C. Oto, A. Karakecili, Chitosan/collagen based biomimetic osteochondral tissue constructs: a growth factor-free approach, Int. J. Biol. Macromol. 156 (2020) 681–690.
[66] Y. Du, H. Liu, Q. Yang, S. Wang, J. Wang, J. Ma, I. Noh, A.G. Mikos, S. Zhang, Selective laser sintering scaffold with hierarchical architecture and gradient composition for osteochondral repair in rabbits, Biomaterials 137 (2017) 37–48.
[67] T. Kumai, N. Yui, K. Yatabe, C. Sasaki, R. Fujii, M. Takenaga, H. Fujiya, H. Niki, K. Yudoh, A novel, self-assembled artificial cartilage-hydroxyapatite conjugate for combined articular cartilage and subchondral bone repair: histopathological analysis of cartilage tissue engineering in rat knee joints, Int. J. Nanomed. 14 (2019) 1283–1298.
[68] Y.M. Lv, Q.S. Yu, Repair of articular osteochondral defects of the knee joint using a composite lamellar scaffold, Bone Jt. Res. 4 (2015) 56–64.
[69] S.H. Kim, S.H. Kim, Y. Jung, Bi-layered PLCL/(PLGA/β-TCP) composite scaffold for osteochondral tissue engineering, J. Bioact. Compat Polym. 30 (2015) 178–187.
[70] R.C. Nordberg, P. Huebner, K.G. Schuchard, L.F. Mellor, R.A. Shirwaiker, E. G. Loboa, J.T. Spang, The evaluation of a multiphasic 3D-bioplotted scaffold seeded with adipose derived stem cells to repair osteochondral defects in a porcine model, J. Biomed. Mater. Res. B Appl. Biomater. 109 (2021) 2246–2258.
[71] F. Gao, Z. Xu, Q. Liang, B. Liu, H. Li, Y. Wu, Y. Zhang, Z. Lin, M. Wu, C. Ruan, W. Liu, Direct 3D printing of high strength biohybrid gradient hydrogel scaffolds for efficient repair of osteochondral defect, Adv. Funct. Mater. 28 (2018), 1706644.
[72] D. Lin, B. Cai, L. Wang, L. Cai, Z. Wang, J. Xie, Q.X. Lv, Y. Yuan, C. Liu, S.G. Shen, A viscoelastic PEGylated poly(glycerol sebacate)-based bilayer scaffold for cartilage regeneration in full-thickness osteochondral defect, Biomaterials 253 (2020), 120095.
[73] M. Barbeck, T. Serra, P. Booms, S. Stojanovic, S. Najman, E. Engel, R. Sader, C. J. Kirkpatrick, M. Navarro, S. Ghanaati, Analysis of the in vitro degradation and the in vivo tissue response to bi-layered 3D-printed scaffolds combining PLA and biphasic PLA/bioglass components - guidance of the inflammatory response as basis for osteochondral regeneration, Bioact. Mater. 2 (2017) 208–223.
[74] E. Kon, G. Filardo, J. Shani, N. Altschuler, A. Levy, K. Zaslav, J.E. Eisman, D. Robinson, Osteochondral regeneration with a novel aragonite-hyaluronate biphasic scaffold: up to 12-month follow-up study in a goat model, J. Orthop. Surg. Res. 10 (2015) 17.
[75] T. Shen, Y. Dai, X. Li, S. Xu, Z. Gou, C. Gao, Regeneration of the osteochondral defect by a wollastonite and macroporous fibrin biphasic scaffold, ACS Biomater. Sci. Eng. 4 (2018) 1942–1953.
[76] T. Yang, M. Tamaddon, L. Jiang, J. Wang, Z. Liu, Z. Liu, H. Meng, Y. Hu, J. Gao, X. Yang, Y. Zhao, Y. Wang, A. Wang, Q. Wu, C. Liu, J. Peng, X. Sun, Q. Xue, Bilayered scaffold with 3D printed stiff subchondral bony compartment to provide constant mechanical support for long-term cartilage regeneration, J. Orthop. Translat. 30 (2021) 112–121.
[77] T. Flaherty, M. Tamaddon, C. Liu, Micro-computed tomography analysis of subchondral bone regeneration using osteochondral scaffolds in an ovine condyle model, Appl. Sci. 11 (2021) 891–904.
[78] H. Zhou, R. Chen, J. Wang, J. Lu, T. Yu, X. Wu, S. Xu, Z. Li, C. Jie, R. Cao, Y. Yang, Y. Li, D. Meng, Biphasic fish collagen scaffold for osteochondral regeneration, Mater. Des. 195 (2020), 108947.
[79] J.H. Shim, K.M. Jang, S.K. Hahn, J.Y. Park, H. Jung, K. Oh, K.M. Park, J. Yeom, S. H. Park, S.W. Kim, J.H. Wang, K. Kim, D.W. Cho, Three-dimensional bioprinting of multilayered constructs containing human mesenchymal stromal cells for osteochondral tissue regeneration in the rabbit knee joint, Biofabrication 8 (2016), 014102.
[80] A. Yucekul, D. Ozdil, N.H. Kutlu, E. Erdemli, H.M. Aydin, M.N. Doral, Tri-layered composite plug for the repair of osteochondral defects: in vivo study in sheep, J. Tissue Eng. 8 (2017) 1–10.
[81] E. Ruvinov, T. Tavor Re'em, F. Witte, S. Cohen, Articular cartilage regeneration using acellular bioactive affinity-binding alginate hydrogel: a 6-month study in a mini-pig model of osteochondral defects, J. Orthop. Translat. 16 (2019) 40–52.
[82] D. Algul, A. Gokce, A. Onal, E. Servet, A.I. Dogan Ekici, F.G. Yener, In vitro release and in vivo biocompatibility studies of biomimetic multilayered alginate-chitosan/beta-TCP scaffold for osteochondral tissue, J. Biomater. Sci. Polym. Ed. 27 (2016) 431–440.
[83] T. Zhang, H. Zhang, L. Zhang, S. Jia, J. Liu, Z. Xiong, W. Sun, Biomimetic design and fabrication of multilayered osteochondral scaffolds by low-temperature deposition manufacturing and thermal-induced phase-separation techniques, Biofabrication 9 (2017), 025021.
[84] C. Zhai, H. Fei, J. Hu, Z. Wang, S. Xu, Q. Zuo, Z. Li, Z. Wang, W. Liang, W. Fan, Repair of articular osteochondral defects using an integrated and biomimetic trilayered scaffold, Tissue Eng. 24 (2018) 1680–1692.
[85] B. Liu, Y. Zhao, T. Zhu, S. Gao, K. Ye, F. Zhou, D. Qiu, X. Wang, Y. Tian, X. Qu, Biphasic double-network hydrogel with compartmentalized loading of bioactive glass for osteochondral defect repair, Front. Bioeng. Biotechnol. 8 (2020) 752.
[86] N. Mohan, V. Gupta, B.P. Sridharan, A.J. Mellott, J.T. Easley, R.H. Palmer, R. A. Galbraith, V.H. Key, C.J. Berkland, M.S. Detamore, Microsphere-based gradient implatns for osteochondral regeneration: a long-term study in sheep, Regen. Med. 10 (2015) 709–728.
[87] L.P. Yan, J. Silva-Correia, M.B. Oliveira, C. Vilela, H. Pereira, R.A. Sousa, J. F. Mano, A.L. Oliveira, J.M. Oliveira, R.L. Reis, Bilayered silk/silk-nanoCaP scaffolds for osteochondral tissue engineering: in vitro and in vivo assessment of biological performance, Acta Biomater. 12 (2015) 227–241.
[88] S. Jia, J. Wang, T. Zhang, W. Pan, Z. Li, X. He, C. Yang, Q. Wu, W. Sun, Z. Xiong, D. Hao, Multilayered scaffold with a compact interfacial layer enhances osteochondral defect repair, ACS Appl. Mater. Interfaces 10 (2018) 20296–20305.
[89] L. Zheng, D. Li, W. Wang, Q. Zhang, X. Zhou, D. Liu, J. Zhang, Z. You, J. Zhang, C. He, Bilayered scaffold prepared from a kartogenin-loaded hydrogel and BMP-2-derived peptide-loaded porous nanofibrous scaffold for osteochondral defect repair, ACS Biomater. Sci. Eng. 5 (2019) 4564–4573.
[90] X. Nie, Y.J. Chuah, P. He, D.A. Wang, Engineering a multiphasic, integrated graft with a biologically developed cartilage-bone interface for osteochondral defect repair, J. Mater. Chem. B 7 (2019) 6515–6525.
[91] P. Duan, Z. Pan, L. Cao, J. Gao, H. Yao, X. Liu, R. Guo, X. Liang, J. Dong, J. Ding, Restoration of osteochondral defects by implanting bilayered poly(lactide-co-glycolide) porous scaffolds in rabbit joints for 12 and 24 weeks, J. Orthop. Translat. 19 (2019) 68–80.
[92] Y.T. Zhang, J. Niu, Z. Wang, S. Liu, J. Wu, B. Yu, Repair of osteochondral defects in a rabbit model using bilayer poly(lactide-co-glycolide) scaffolds loaded with autologous platelet-rich plasma, Med. Sci. Mon. Int. Med. J. Exp. Clin. Res. 23 (2017) 5189–5201.
[93] Z. Pan, P. Duan, X. Liu, H. Wang, L. Cao, Y. He, J. Dong, J. Ding, Effect of porosities of bilayered porous scaffolds on spontaneous osteochondral repair in cartilage tissue engineering, Regen. Biomater. 2 (2015) 9–19.
[94] S. Critchley, E.J. Sheehy, G. Cunniffe, P. Diaz-Payno, S.F. Carroll, O. Jeon, E. Alsberg, P.A.J. Brama, D.J. Kelly, 3D printing of fibre-reinforced cartilaginous templates for the regeneration of osteochondral defects, Acta Biomater. 113 (2020) 130–143.
[95] Y. Liu, L. Peng, L. Li, C. Huang, K. Shi, X. Meng, P. Wang, M. Wu, L. Li, H. Cao, K. Wu, Q. Zeng, H. Pan, W.W. Lu, L. Qin, C. Ruan, X. Wang, 3D-bioprinted BMSC-laden biomimetic multiphasic scaffolds for efficient repair of osteochondral defects in an osteoarthritic rat model, Biomaterials 279 (2021), 121216.
[96] I.A.D. Mancini, S. Schmidt, H. Brommer, B. Pouran, S. Schafer, J. Tessmar, A. Mensinga, M.H.P. van Rijen, J. Groll, T. Blunk, R. Levato, J. Malda, P.R. van Weeren, A composite hydrogel-3D printed thermoplast osteochondral anchor as example for a zonal approach to cartilage repair: in vivo performance in a long-term equine model, Biofabrication 12 (2020), 035028.
[97] M.-h. Park, Y.-w. Hwang, D.-S. Jeong, G.-h. Kim, Evaluation of bilayer polycaprolactone scaffold for osteochondral regeneration in rabbits, J. Vet. Clin. 33 (2016) 332–339.
[98] C. Studle, Q. Vallmajo-Martin, A. Haumer, J. Guerrero, M. Centola, A. Mehrkens, D.J. Schaefer, M. Ehrbar, A. Barbero, I. Martin, Spatially confined induction of endochondral ossification by functionalized hydrogels for ectopic engineering of osteochondral tissues, Biomaterials 171 (2018) 219–229.
[99] Y.H. Hsieh, M.F. Hsieh, C.H. Fang, C.P. Jiang, B. Lin, H.M. Lee, Osteochondral regeneration induced by TGF-β loaded photo cross-linked hyaluronic acid hydrogel infiltrated in fused deposition-manufactured composite scaffold of hydroxyapatite and poly (ethylene glycol)-block-poly(ε-caprolactone), Polymers 9 (2017) 182.
[100] B.J. Kim, Y. Arai, B. Choi, S. Park, J. Ahn, I.-B. Han, S.-H. Lee, Restoration of articular osteochondral defects in rat by a bi-layered hyaluronic acid hydrogel plug with TUDCA-PLGA microsphere, J. Ind. Eng. Chem. 61 (2018) 295–303.
[101] Y. Yang, G. Yang, Y. Song, Y. Xu, S. Zhao, W. Zhang, 3D bioprinted integrated osteochondral scaffold-mediated repair of articular cartilage defects in the rabbit knee, J. Med. Biol. Eng. 40 (2019) 71–81.

[102] C. Sosio, A. Di Giancamillo, D. Deponti, F. Gervaso, F. Scalera, M. Melato, M. Campagnol, F. Boschetti, A. Nonis, C. Domeneghini, A. Sannino, G.M. Peretti, Osteochondral repair by a novel interconnecting collagen-hydroxyapatite substitute: a large-animal study, Tissue Eng. 21 (2015) 704–715.
[103] J. Fang, P. Li, X. Lu, L. Fang, X. Lü, F. Ren, A strong, tough, and osteoconductive hydroxyapatite mineralized polyacrylamide/dextran hydrogel for bone tissue regeneration, Acta Biomater. 88 (2019) 503–513.
[104] R. Kiyama, T. Nonoyama, S. Wada, S. Semba, N. Kitamura, T. Nakajima, T. Kurokawa, K. Yasuda, S. Tanaka, J.P. Gong, Micro patterning of hydroxyapatite by soft lithography on hydrogels for selective osteoconduction, Acta Biomater. 81 (2018) 60–69.
[105] H. Shi, Z. Zhou, W. Li, Y. Fan, Z. Li, J. Wei, Hydroxyapatite based materials for bone tissue engineering: a brief and comprehensive introduction, Crystals 11 (2021) 149.
[106] J. Jeong, J.H. Kim, J.H. Shim, N.S. Hwang, C.Y. Heo, Bioactive calcium phosphate materials and applications in bone regeneration, Biomater. Res. 23 (2019) 4.
[107] D. Xu, G. Cheng, J. Dai, Z. Li, Bi-layered composite scaffold for repair of the osteochondral defects, Adv. Wound Care 10 (2021) 401–414.
[108] E. Zeimaran, S. Pourshahrestani, A. Fathi, N.A.b.A. Razak, N.A. Kadri, A. Sheikhi, F. Baino, Advances in bioactive glass-containing injectable hydrogel biomaterials for tissue regeneration, Acta Biomater. 136 (2021) 1–36.
[109] M. Muhammad Mailafiya, K. Abubakar, A. Danmaigoro, S. Musa Chiroma, E. Bin Abdul Rahim, M. Aris Mohd Moklas, Z. Abu Bakar Zakaria, Cockle shell-derived calcium carbonate (aragonite) nanoparticles: a dynamite to nanomedicine, Appl. Sci. 9 (2019) 2897.
[110] R. Sainitya, M. Sriram, V. Kalyanaraman, S. Dhivya, S. Saravanan, M. Vairamani, T.P. Sastry, N. Selvamurugan, Scaffolds containing chitosan/carboxymethyl cellulose/mesoporous wollastonite for bone tissue engineering, Int. J. Biol. Macromol. 80 (2015) 481–488.
[111] Y.D. Taghipour, V.R. Hokmabad, D. Bakhshayesh, A. Rahmani, N. Asadi, R. Salehi, H.T. Nasrabadi, The application of hydrogels based on natural polymers for tissue engineering, Curr. Med. Chem. 27 (2020) 2658–2680.
[112] E. Lopez-Ruiz, G. Jimenez, M.A. Garcia, C. Antich, H. Boulaiz, J.A. Marchal, M. Peran, Polymers, scaffolds and bioactive molecules with therapeutic properties in osteochondral pathologies: what's new? Expert Opin. Ther. Pat. 26 (2016) 877–890.
[113] X. Wei, B. Liu, G. Liu, F. Yang, F. Cao, X. Dou, W. Yu, B. Wang, G. Zheng, L. Cheng, Z. Ma, Y. Zhang, J. Yang, Z. Wang, J. Li, D. Cui, W. Wang, H. Xie, L. Li, F. Zhang, W.C. Lineaweaver, D. Zhao, Mesenchymal stem cell-loaded porous tantalum integrated with biomimetic 3D collagen-based scaffold to repair large osteochondral defects in goats, Stem Cell Res. Ther. 10 (2019) 72.
[114] J. Sun, J. Lyu, F. Xing, R. Chen, X. Duan, Z. Xiang, A biphasic, demineralized, and Decellularized allograft bone-hydrogel scaffold with a cell-based BMP-7 delivery system for osteochondral defect regeneration, J. Biomed. Mater. Res. A. 108 (2020) 1909–1921.
[115] L.M. Shirehjini, F. Sharifi, S. Shojaei, S. Irani, Poly-caprolactone nanofibrous coated with sol-gel alginate/mesenchymal stem cells for cartilage tissue engineering, J. Drug Deliv. Sci. Technol. 74 (2022), 103488.
[116] B. Sultankulov, D. Berillo, K. Sultankulova, T. Tokay, A. Saparov, Progress in the development of chitosan-based biomaterials for tissue engineering and regenerative medicine, Biomolecules 9 (2019) 470.
[117] K. Maji, S. Dasgupta, K. Pramanik, A. Bissoyi, Preparation and characterization of gelatin-chitosan-nanoβ-TCP based scaffold for orthopaedic application, Mater. Sci. Eng., C 86 (2018) 83–94.
[118] T. Vieira, J.C. Silva, A.B. do Rego, J.P. Borges, C. Henriques, Electrospun biodegradable chitosan based-poly (urethane urea) scaffolds for soft tissue engineering, Mater. Sci. Eng., C 103 (2019), 109819.
[119] M. Suneetha, H.J. Kim, S.S. Han, Bone-like apatite formation in phosphate-crosslinked sodium alginate-based hydrogels, Mater. Lett. 328 (2022), 133141.
[120] A. Sionkowska, Current research on the blends of natural and synthetic polymers as new biomaterials: review, Prog. Polym. Sci. 36 (2011) 1254–1276.
[121] H.K. Makadia, S.J. Siegel, Poly lactic-co-glycolic acid (PLGA) as biodegradable controlled drug delivery carrier, Polymers 3 (2011) 1377–1397.
[122] E. Malikmammadov, T.E. Tanir, A. Kiziltay, V. Hasirci, N. Hasirci, PCL and PCL-based materials in biomedical applications, J. Biomater. Sci. Polym. Ed. 29 (2018) 863–893.
[123] N.M. Korthagen, H. Brommer, G. Hermsen, S.G.M. Plomp, G. Melsom, K. Coeleveld, S.C. Mastbergen, H. Weinans, W. van Buul, P.R. van Weeren, A short-term evaluation of a thermoplastic polyurethane implant for osteochondral defect repair in an equine model, Vet. J. 251 (2019), 105340.
[124] H. Cai, Y. Yao, Y. Xu, Q. Wang, W. Zou, J. Liang, Y. Sun, C. Zhou, Y. Fan, X. Zhang, A Col I and BCP ceramic bi-layer scaffold implant promotes regeneration in osteochondral defects, RSC Adv. 9 (2019) 3740–3748.
[125] J. Liao, T. Tian, S. Shi, X. Xie, Q. Ma, G. Li, Y. Lin, The fabrication of biomimetic biphasic CAN-PAC hydrogel with a seamless interfacial layer applied in osteochondral defect repair, Bone Res 5 (2017), 17018.
[126] S. Liu, J. Wu, X. Liu, D. Chen, G.L. Bowlin, L. Cao, J. Lu, F. Li, X. Mo, C. Fan, Osteochondral regeneration using an oriented nanofiber yarn-collagen type I/hyaluronate hybrid/TCP biphasic scaffold, J. Biomed. Mater. Res. A. 103 (2015) 581–592.
[127] Y.-J. Seong, I.-G. Kang, E.-H. Song, H.-E. Kim, S.-H. Jeong, Calcium phosphate–collagen scaffold with aligned pore channels for enhanced osteochondral regeneration, Adv. Healthc. Mater. 6 (2017), 1700966.
[128] X. Liu, Y. Wei, C. Xuan, L. Liu, C. Lai, M. Chai, Z. Zhang, L. Wang, X. Shi, A biomimetic biphasic osteochondral scaffold with layer-specific release of stem cell differentiation inducers for the reconstruction of osteochondral defects, Adv. Healthc. Mater. 9 (2020), 2000076.
[129] H. Kang, Y. Zeng, S. Varghese, Functionally graded multilayer scaffolds for in vivo osteochondral tissue engineering, Acta Biomater. 78 (2018) 365–377.
[130] K. Stuckensen, A. Schwab, M. Knauer, E. Muiños-López, F. Ehlicke, J. Reboredo, F. Granero-Moltó, U. Gbureck, F. Prósper, H. Walles, J. Groll, Tissue mimicry in morphology and composition promotes hierarchical matrix remodeling of invading stem cells in osteochondral and meniscus scaffolds, Adv. Mater. 30 (2018), 1706754.
[131] V. Barron, M. Neary, K.M. Mohamed, S. Ansboro, G. Shaw, G. O'Malley, N. Rooney, F. Barry, M. Murphy, Evaluation of the early in vivo response of a functionally graded macroporous scaffold in an osteochondral defect in a rabbit model, Ann. Biomed. Eng. 44 (2016) 1832–1844.
[132] F. Han, X. Yang, J. Zhao, Y. Zhao, X. Yuan, Photocrosslinked layered gelatin-chitosan hydrogel with graded compositions for osteochondral defect repair, J. Mater. Sci. Mater. Med. 26 (2015) 160.
[133] S. Lu, J. Lam, J.E. Trachtenberg, E.J. Lee, H. Seyednejad, J.J. van den Beucken, Y. Tabata, F.K. Kasper, D.W. Scott, M.E. Wong, J.A. Jansen, A.G. Mikos, Technical Report: correlation between the repair of cartilage and subchondral bone in an osteochondral defect using bilayered, biodegradable hydrogel composites, Tissue Eng. C Methods 21 (2015) 1216–1225.
[134] C. Parisi, L. Salvatore, L. Veschini, M.P. Serra, C. Hobbs, M. Madaghiele, A. Sannino, L. Di Silvio, Biomimetic gradient scaffold of collagen–hydroxyapatite for osteochondral regeneration, J. Tissue Eng. 11 (2020), 2041731419896068.
[135] L.A. Fortier, J.U. Barker, E.J. Strauss, T.M. McCarrel, B.J. Cole, The role of growth factors in cartilage repair, Clin. Orthop. Relat. Res. 469 (2011) 2706–2715.
[136] J.V. Kumbhar, S.H. Jadhav, D.S. Bodas, A. Barhanpurkar-Naik, M.R. Wani, K. M. Paknikar, J.M. Rajwade, In vitro and in vivo studies of a novel bacterial cellulose-based acellular bilayer nanocomposite scaffold for the repair of osteochondral defects, Int. J. Nanomed. 12 (2017) 6437–6459.
[137] Y. Zhao, X. Ding, Y. Dong, X. Sun, L. Wang, X. Ma, M. Zhu, B. Xu, Q. Yang, Role of the calcified cartilage layer of an integrated trilayered silk fibroin scaffold used to regenerate osteochondral defects in rabbit knees, ACS Biomater. Sci. Eng. 6 (2019) 1208–1216.
[138] M.L. Sennett, J.M. Friedman, B.S. Ashley, B.D. Stoeckl, J.M. Patel, M. Alini, M. Cucchiarini, D. Eglin, H. Madry, A. Mata, C. Semino, M.J. Stoddart, B. Johnstone, F.T. Moutos, B.T. Estes, F. Guilak, R.L. Mauck, G.R. Dodge, Long term outcomes of biomaterial-mediated repair of focal cartilage defects in a large animal model, Eur. Cell. Mater. 41 (2021) 40–51.
[139] M. Berruto, P. Ferrua, F. Uboldi, S. Pasqualotto, F. Ferrara, G. Carimati, E. Usellini, M. Delcogliano, Can a biomimetic osteochondral scaffold be a reliable alternative to prosthetic surgery in treating late-stage SPONK? Knee 23 (2016) 936–941.
[140] M. Brix, M. Kaipel, R. Kellner, M. Schreiner, S. Apprich, H. Boszotta, R. Windhager, S. Domayer, S. Trattnig, Successful osteoconduction but limited cartilage tissue quality following osteochondral repair by a cell-free multilayered nano-composite scaffold at the knee, Int. Orthop. 40 (2016) 625–632.
[141] B.B. Christensen, C.B. Foldager, J. Jensen, N.C. Jensen, M. Lind, Poor osteochondral repair by a biomimetic collagen scaffold: 1- to 3-year clinical and radiological follow-up, Knee Surg. Sports Traumatol. Arthrosc. 24 (2016) 2380–2387.
[142] V. Condello, G. Filardo, V. Madonna, L. Andriolo, D. Screpis, M. Bonomo, M. Zappia, L. Dei Giudici, C. Zorzi, Use of a biomimetic scaffold for the treatment of osteochondral lesions in early osteoarthritis, BioMed Res. Int. 2018 (2018), 7937089.
[143] E. Gabusi, F. Paolella, C. Manferdini, L. Gambari, E. Kon, G. Filardo, E. Mariani, G. Lisignoli, Cartilage and bone serum biomarkers as novel tools for monitoring knee osteochondritis dissecans treated with osteochondral scaffold, BioMed Res. Int. 2018 (2018), 9275102.
[144] E. Kon, G. Filardo, M. Brittberg, M. Busacca, V. Condello, L. Engebretsen, S. Marlovits, P. Niemeyer, P. Platzer, M. Posthumus, P. Verdonk, R. Verdonk, J. Victor, W. van der Merwe, W. Widuchowski, C. Zorzi, M. Marcacci, A multilayer biomaterial for osteochondral regeneration shows superiority vs microfractures for the treatment of osteochondral lesions in a multicentre randomized trial at 2 years, Knee Surg. Sports Traumatol. Arthrosc. 26 (2018) 2704–2715.
[145] F. Perdisa, E. Kon, A. Sessa, L. Andriolo, M. Busacca, M. Marcacci, G. Filardo, Treatment of knee osteochondritis dissecans with a cell-free biomimetic osteochondral scaffold: clinical and imaging findings at midterm follow-up, Am. J. Sports Med. 46 (2018) 314–321.
[146] A. Sessa, L. Andriolo, A. Di Martino, I. Romandini, R. De Filippis, S. Zaffagnini, G. Filardo, Cell-free osteochondral scaffold for the treatment of focal articular cartilage defects in early knee OA: 5 years' follow-up results, J. Clin. Med. 8 (2019) 1978.
[147] A. Sessa, I. Romandini, L. Andriolo, A. Di Martino, M. Busacca, S. Zaffagnini, G. Filardo, Treatment of juvenile knee osteochondritis dissecans with a cell-free biomimetic osteochondral scaffold: clinical and MRI results at mid-term follow-up, Cartilage 13 (2021) 1137S, 47S.
[148] P. Verdonk, A. Dhollander, K.F. Almqvist, R. Verdonk, J. Victor, Treatment of osteochonral lesions in the knee using a cell-free scaffold, Bone Joint Lett. J 97-B (2015) 318–323.
[149] E. Di Cave, P. Versari, F. Sciarretta, D. Luzon, L. Marcellini, Biphasic bioresorbable scaffold (TruFit Plug®) for the treatment of osteochondral lesions of talus: 6- to 8-year follow-up, Foot 33 (2017) 48–52.

[150] A. Dhollander, P. Verdonk, K.F. Almqvist, R. Verdonk, J. Victor, Clinical and MRI outcome of an osteochondral scaffold plug for the treatment of cartilage lesions in the knee, Acta Orthop. Belg. 81 (2015) 629–638.
[151] G. Dell'Osso, V. Bottai, G. Bugelli, T. Manisco, N. Cazzella, F. Celli, G. Guido, S. Giannotti, The biphasic bioresorbable scaffold (Trufit®) in the osteochondral knee lesions: long-term clinical and MRI assessment in 30 patients, Musculoskelet. Surg. 100 (2016) 93–96.
[152] A.J. Krych, D.H. Nawabi, N.A. Farshad-Amacker, K.J. Jones, T.G. Maak, H. G. Potter, R.J. Williams 3rd, Bone marrow concentrate improves early cartilage phase maturation of a scaffold plug in the knee: a comparative magnetic resonance imaging analysis to platelet-rich plasma and control, Am. J. Sports Med. 44 (2016) 91–98.
[153] F.S. Shivji, A. Mumith, S. Yasen, J.T.K. Melton, A.J. Wilson, Treatment of focal chondral lesions in the knee using a synthetic scaffold plug: long-term clinical and radiological results, J. Orthop. 20 (2020) 12–16.
[154] D. Wang, D.H. Nawabi, A.J. Krych, K.J. Jones, J. Nguyen, A.M. Elbuluk, N. A. Farshad-Amacker, H.G. Potter, R.J. Williams 3rd, Synthetic biphasic scaffolds versus microfracture for articular cartilage defects of the knee: a retrospective comparative study, Cartilage 13 (2021) 1002S, 13S.
[155] E. Kon, D. Robinson, P. Verdonk, M. Drobnic, J.M. Patrascu, O. Dulic, G. Gavrilovic, G. Filardo, A novel aragonite-based scaffold for osteochondral regeneration: early experience on human implants and technical developments, Injury 47 (2016) S27–S32.
[156] E. Kon, B. Di Matteo, P. Verdonk, M. Drobnic, O. Dulic, G. Gavrilovic, J. M. Patrascu, K. Zaslav, G. Kwiatkowski, N. Altschuler, D. Robinson, Aragonite-based scaffold for the treatment of joint surface lesions in mild to moderate osteoarthritic knees: results of a 2-year multicenter prospective study, Am. J. Sports Med. 49 (2021) 588–598.
[157] U. Kanatli, A. Eren, T.K. Eren, A. Vural, D.E. Geylan, A.Y. Oner, Single-step arthroscopic repair with cell-free polymer-based scaffold in osteochondral lesions of the talus: clinical and radiological results, Arthroscopy 33 (2017) 1718–1726.
[158] R. D'Ambrosi, F. Valli, P. De Luca, N. Ursino, F.G. Usuelli, MaioRegen osteochondral substitute for the treatment of knee defects: a systematic review of the literature, J. Clin. Med. 8 (2019) 783.
[159] A. Boffa, L. Solaro, A. Poggi, L. Andriolo, D. Reale, A. Di Martino, Multi-layer cell-free scaffolds for osteochondral defects of the knee: a systematic review and meta-analysis of clinical evidence, J. Exp. Orthop. 8 (2021) 56.
[160] X. Zhou, T. Esworthy, S.-J. Lee, S. Miao, H. Cui, M. Plesiniak, H. Fenniri, T. Webster, R.D. Rao, L.G. Zhang, 3D Printed scaffolds with hierarchical biomimetic structure for osteochondral regeneration, Nanomedicine 19 (2019) 58–70.
[161] D. Kilian, P. Sembdner, H. Bretschneider, T. Ahlfeld, L. Mika, J. Lützner, S. Holtzhausen, A. Lode, R. Stelzer, M. Gelinsky, 3D printing of patient-specific implants for osteochondral defects: workflow for an MRI-guided zonal design, Bio-Des. Manuf. 4 (2021) 818–832.
[162] R. Choe, E. Devoy, E. Jabari, J.D. Packer, J.P. Fisher, Biomechanical aspects of osteochondral regeneration: implications and strategies for three-dimensional bioprinting, Tissue Eng, Part B Rev 28 (2022) 766–788.
[163] J. Wei, P. Ran, Q. Li, J. Lu, L. Zhao, Y. Liu, X. Li, Hierarchically structured injectable hydrogels with loaded cell spheroids for cartilage repairing and osteoarthritis treatment, Chem. Eng. J. 430 (2022), 132211.
[164] G. Baek, H. Choi, Y. Kim, H.C. Lee, C. Choi, Mesenchymal stem cell-derived extracellular vesicles as therapeutics and as a drug delivery platform, Stem Cells Transl. Med. 8 (2019) 880–886.
[165] S.T. Ryan, E. Hosseini-Beheshti, D. Afrose, X. Ding, B. Xia, G.E. Grau, C.B. Little, L. McClements, J.J. Li, Extracellular vesicles from mesenchymal stromal cells for the treatment of inflammation-related conditions, Int. J. Mol. Sci. 22 (2021) 3023.
[166] J.J. Li, E. Hosseini-Beheshti, G.E. Grau, H. Zreiqat, C.B. Little, Stem cell-derived extracellular vesicles for treating joint injury and osteoarthritis, Nanomaterials 9 (2019) 261.
[167] L.A. Vonk, S.F.J. van Dooremalen, N. Liv, J. Klumperman, P.J. Coffer, D.B.F. Saris, M.J. Lorenowicz, Mesenchymal stromal/stem cell-derived extracellular vesicles promote human cartilage regeneration in vitro, Theranostics 8 (2018) 906–920.
[168] R. Wang, B. Xu, H. Xu, TGF-β1 promoted chondrocyte proliferation by regulating Sp1 through MSC-exosomes derived miR-135b, Cell Cycle 17 (2018) 2756–2765.
[169] G. Won Lee, M. Thangavelu, M. Joung Choi, E. Yeong Shin, H. Sol Kim, J. Seon Baek, Y. Woon Jeong, J. Eun Song, C. Carlomagno, J. Miguel Oliveira, R. Luis Reis, G. Khang, Exosome mediated transfer of miRNA-140 promotes enhanced chondrogenic differentiation of bone marrow stem cells for enhanced cartilage repair and regeneration, J. Cell. Biochem. 121 (2020) 3642–3652.
[170] H.P. Bei, P.M. Hung, H.L. Yeung, S. Wang, X. Zhao, Bone-a-Petite: engineering exosomes towards bone, osteochondral, and cartilage repair, Small 17 (2021), 2101741.
[171] S. Duchi, S. Doyle, T. Eekel, C.D. O'Connell, C. Augustine, P. Choong, C. Onofrillo, C. Di Bella, Protocols for culturing and imaging a human ex vivo osteochondral model for cartilage biomanufacturing applications, Materials 12 (2019) 640.
[172] G.N. Hall, W.L. Tam, K.S. Andrikopoulos, L. Casas-Fraile, G.A. Voyiatzis, L. Geris, F.P. Luyten, I. Papantoniou, Patterned, organoid-based cartilaginous implants exhibit zone specific functionality forming osteochondral-like tissues in vivo, Biomaterials 273 (2021), 120820.
[173] S.K. O'Connor, D.B. Katz, S.J. Oswald, L. Groneck, F. Guilak, Formation of osteochondral organoids from murine induced pluripotent stem cells, Tissue Eng. 27 (2021) 1099–1109.
[174] L. Banh, K.K. Cheung, M.W.Y. Chan, E.W.K. Young, S. Viswanathan, Advances in organ-on-a-chip systems for modelling joint tissue and osteoarthritic diseases, Osteoarthritis Cartilage 30 (2022) 1050–1061.